Journal of Statistical Physics, Vol. 84, Nos. 5/6, 1996

Exact Ground-State Correlation Functions of One-Dimensional Strongly Correlated Electron Models with Resonating-Valence-Bond Ground State

Masanori Yamanaka,[1,3] Shinsuke Honjo,[1] Yasuhiro Hatsugai,[2] and Mahito Kohmoto[1]

Received September 18, 1995; final February 27, 1996

We investigate one-dimensional strongly correlated electron models which have the resonating-valence-bond state as the exact ground state. The correlation functions are evaluated exactly using the transfer matrix method for the geometric representations of the valence-bond states. In this method, we only treat matrices with small dimensions. This enables us to give analytical results. It is shown that the correlation functions decay exponentially with distance. The result suggests that there is a finite excitation gap, and that the ground state is insulating. Since the corresponding noninteracting systems may be insulating or metallic, we can say that the gap originates from strong correlation. The persistent currents of the present models are also investigated and found to be exactly vanishing.

KEY WORDS: Strongly correlated electron systems; solvable model; correlation function; Kondo insulator; resonating-valence-bond state; transfer matrix; persistent current.

1. INTRODUCTION

Strongly interacting electron systems have been one of the most important subjects in condensed matter physics. Although rigorous results and exact solutions are useful, they are rare. Recently, Brandt and Giesekus[1] introduced a model of strongly interacting electrons on d-dimensional ($d \geqslant 2$)

[1] Institute for Solid State Physics, University of Tokyo, 7-22-1, Roppongi, Minato-ku, Tokyo 106 Japan; e-mail: yamanaka@kodama.issp.u-tokyo.ac.jp, honjo@kodama.issp.u-tokyo.ac.jp, kohmoto@issp.u-tokyo.ac.jp.

[2] Department of Applied Physics, University of Tokyo, 7-3-1, Hongo, Bunkyo-ku, Tokyo 113 Japan; e-mail: hatsugai@tansei.cc.u-tokyo.ac.jp.

[3] Present address: Department of Applied Physics, University of Tokyo, 7-3-1, Hongo, Bunkyo-ku, Tokyo 113 Japan.

822/84/5-6-17

perovskite-like lattices in which the exact ground-state wave functions were obtained for a certain range of the parameters. Mielke[2] showed that the exact ground state can be obtained in similar models on a general class of line graphs. Following the work of Brandt and Giesekus, models in which the exact ground state can be obtained were constructed by several authors.[3–5] These models are conveniently described by the cell construction of Tasaki,[4] which will be reviewed in Section 2 (also see Appendix A and ref. 5). Tasaki[5] proved the uniqueness of the ground states in this class of models. Not only the ground state, but also the singlet-pair correlation function in a model on a tree was obtained.[4] Bares and Lee[6] performed a detailed analysis for one of the models of Strack.[3] They proved the uniqueness of the ground state and exactly evaluated the equal-time correlation functions by a transfer matrix method.

It was pointed out [refs. 4 and 6] that the exact ground states have the resonating-valence-bond (RVB) structure.[7,8] It is the so-called hopping-dominated RVB states[9] which are different from the tunneling-dominated RVB states. The latter have been studied intensively in connection with high-T_c superconductivity.[10–16] Tasaki and Kohmoto[9] studied the difference of the mechanism that causes the resonance in the hopping-dominated RVB states and the tunneling-dominated RVB states.

In this paper we shall exactly evaluate the equal-time correlation functions of one-dimensional models (Models A, B, and C) which will be defined in Section 4. One of Strack's models which was studied by Bares and Lee is called Model B in this paper. We shall use the transfer matrix method for the geometric representations of the valence-bond states,[13,16–18] which is different from that of Bares and Lee. In one dimension, the extension of the formalism to other models which will not be included in this paper is cumbersome but essentially straightforward. It is crucial that we do not have to treat large matrices as needed in the method of Bares and Lee. (In one of the models by Strack, for example, we only treat 3×3 transfer matrices, while Bares and Lee needed those of 16×16.) This enables us to give a completely analytical solution with a finite amount of effort.

It is shown that all the correlation functions decay exponentially with distance. The result suggests the existence of a finite excitation gap. It is expected that the excitation gap originates from the structure of the ground state which is described by a collection of local spin singlets. The filling factor of the ground state corresponds to that of a band insulating state or metallic one in the noninteracting system. The properties of the ground state and the gap are completely different from those in the noninteracting system. The existence of the excitation gap is expected to be a general feature of this cass of models. In a certain range of parameters, Model B includes one of the models by Strack,[3,6] where we reproduce the results

of Bares and Lee. In a limit of parameters, it corresponds to a kind of Kondo lattice regime in the sense that there are one localized electron and one conduction electron per unit cell, where the ground state is described by a collection of a local singlet between them. The persistent currents[19–23] are also calculated and turn out to be vanishing.

The plan of this paper is as follows: In Section 2 we review the cell construction of the models. In Section 3 we describe the geometric representation of the correlation functions in arbitrary dimensions. In Section 4 we perform a detailed analysis of the one-dimensional models using the method of Section 3. In Section 5 the absence of the persistent currents is shown. Section 6 is a summary. The reader interested only in the physical results may look at Sections 2 and 6 for general properties of systems in one dimension, and then read Sections 4.1.1, 4.1.6, 4.3.1, 4.3.4, 4.4.1, and 4.4.4 as examples. The results for the correlation functions are shown at the end of each subsubsection in Section 4.

2. CELL CONSTRUCTION AND THE GROUND STATE

Let us first introduce the solvable models in arbitrary dimension by following the construction in refs. 4 and 5. In the present paper, we only consider the translation-invariant lattices.[4] The lattice is constructed from identical cells C_n with $n = 1, 2, \ldots, N$, where N is the number of cells. The cell C_n is a finite set of sites, where each site $r \in C_n$ ($r = 1, 2, \ldots, R$, where[5] $R = |C_n|$) is either a site with infinitely large on-site Coulomb repulsion (a $U = \infty$ site or a d-site), which can have at most one electron, or a $U = 0$ site (or a p-site), which can have at most two electrons with opposite spins. The full lattice Λ_N ($= \bigcup_{n=1}^{N} C_n$) is constructed by starting from the lattice $\Lambda_1 = C_1$ and adding cells $C_2, C_3, \ldots, C_N$ successively. When we add a new cell C_{n+1} to the lattice Λ_n ($= \bigcup_{i=1}^{n} C_i$), we identify some of the sites in C_{n+1} with sites in Λ_n in a one-to-one manner. We note that a cell is not a unit cell in the sense of crystallography. We denote sites in the full lattice Λ_N by x ($x = 1, 2, \ldots, |\Lambda_N|$). A site x may belong to several different cells. The correspondence between x ($\in \Lambda_N$) and r ($\in C_n$) is given by

$$x = f(n, r) \tag{2.1}$$

where $f(n, r)$ depends on the model under consideration. See Fig. 1 for the correspondence.

[4] We can construct more generalized models whose lattices are not translation invariant. See ref. 5 for such models.

[5] Throughout the present paper, $|S|$ denotes the number of elements in a set S.

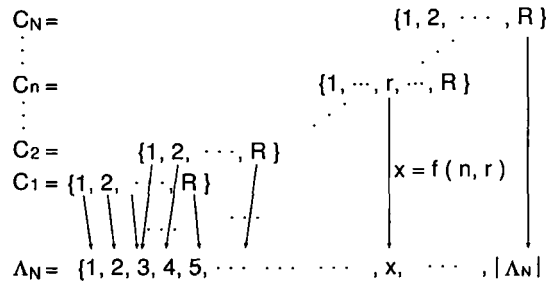

Fig. 1. The correspondence between the sites x ($\in \Lambda_N$) and r ($\in C_n$).

For a cell C_n, we associate a cell Hamiltonian

$$H_n = \sum_{\sigma=\uparrow,\downarrow} \alpha_{n,\sigma} \mathscr{P}_n \alpha_{n,\sigma}^{\dagger} \tag{2.2}$$

with

$$\alpha_{n,\sigma} = \sum_{r=1}^{R} \lambda_r^{(n)} c_{r,\sigma} \tag{2.3}$$

where $\lambda_r^{(n)}$ are nonvanishing complex coefficients[6] and are chosen independently in each cell.[7] (In Section 5 we impose the twisted boundary condition by making use of this property. In Sections 3 and 4 we only consider cases where all the cells have the same λ_r. Thus we have translationally invariant systems and we drop the index n in $\lambda_r^{(n)}$ there.) Here $c_{r,\sigma}$ and $c_{r,\sigma}^{\dagger}$ are the annihilation and the creation operators, respectively, of an electron at site r with spin $\sigma = \uparrow, \downarrow$. They satisfy the standard anticommutation relations $\{c_{r,\sigma}^{\dagger}, c_{s,\tau}\} = \delta_{r,s}\delta_{\sigma,\tau}$ and $\{c_{r,\sigma}^{\dagger}, c_{s,\tau}^{\dagger}\} = \{c_{r,\sigma}, c_{s,\tau}\} = 0$. The projection operator which eliminates a double occupancy on d-sites is

$$\mathscr{P}_n = \prod_{r \in C_{n;\, U=\infty}} (1 - n_{r,\uparrow} n_{r,\downarrow}) \tag{2.4}$$

where $C_{n;\, U=\infty}$ is the set of $U=\infty$ sites in C_n and $n_{r,\sigma} = c_{r,\sigma}^{\dagger} c_{r,\sigma}$ is the number operator. This represents the infinitely large on-site Coulomb repulsion. The full Hamiltonian is

$$H = \sum_{n=1}^{N} H_n \tag{2.5}$$

[6] When a magnetic field is applied, $\lambda_r^{(n)}$ are complex. The proof of the uniqueness of the ground state in ref. 5 holds also in this case.

[7] When a site size x belongs to more than one cell, $\lambda_x^{(n)}$ can be chosen independently in each cell.

We rewrite this Hamiltonian into the standard form. From the identities[1, 5]

$$\begin{aligned} c_{r,\sigma}\mathscr{P}_n c^\dagger_{s,\sigma} &= -\mathscr{P}_n c^\dagger_{s,\sigma} c_{r,\sigma}\mathscr{P}_n && \text{for} \quad r \neq s \\ c_{r,\sigma}\mathscr{P}_n c^\dagger_{r,\sigma} &= \mathscr{P}_n(1-n_{r,\uparrow}-n_{r,\downarrow})\,\mathscr{P}_n && \text{for} \quad r \in C_{n;\,U=\infty} \\ c_{r,\sigma}\mathscr{P}_n c^\dagger_{r,\sigma} &= \mathscr{P}_n(1-n_{r,\sigma})\,\mathscr{P}_n && \text{for} \quad r \in C_{n;\,U=0} \end{aligned} \tag{2.6}$$

where $C_{n;\,U=0}$ is the set of $U=0$ sites in C_n, the cell Hamiltonian (2.2) is

$$\begin{aligned} H_n &= \sum_{\sigma=\uparrow,\downarrow} \sum_{r,s\in C_n} \lambda_s^{(n)} (\lambda_r^{(n)})^* \, c_{s,\sigma}\mathscr{P}_n c^\dagger_{r,\sigma} \\ &= \mathscr{P}_n \Bigg\{ \sum_{r\in C_n} 2\,|\lambda_r^{(n)}|^2 - \Bigg[\sum_{\sigma=\uparrow,\downarrow} \sum_{r\neq s(\in C_n)} (\lambda_r^{(n)})^* \lambda_s^{(n)} c^\dagger_{r,\sigma} c_{s,\sigma} \\ &\qquad + \sum_{\sigma=\uparrow,\downarrow} \sum_{r\in C_{n;\,U=\infty}} 2\,|\lambda_r^{(n)}|^2 c^\dagger_{r,\sigma} c_{r,\sigma} \\ &\qquad + \sum_{\sigma=\uparrow,\downarrow} \sum_{r\in C_{n;\,U=\infty}} |\lambda_r^{(n)}|^2 c^\dagger_{r,\sigma} c_{r,\sigma} \Bigg] \Bigg\} \mathscr{P}_n \\ &= \mathscr{P}_n \left\{ E_n - \sum_{\sigma=\uparrow,\downarrow} \sum_{r,s\in C_n} t_{r,s}^{(n)} c^\dagger_{r,\sigma} c_{s,\sigma} \right\} \mathscr{P}_n \end{aligned} \tag{2.7}$$

where

$$t_{r,s}^{(n)} = \begin{cases} (\lambda_r^{(n)})^* \lambda_s^{(n)} & \text{for} \quad r \neq s \\ 2\,|\lambda_r^{(n)}|^2 & \text{for} \quad r = s \text{ and } r, s \in C_{n;\,U=\infty} \\ |\lambda_r^{(n)}|^2 & \text{for} \quad r = s \text{ and } r, s \in C_{n;\,U=0} \end{cases} \tag{2.8}$$

$$E_n = \sum_{r\in C_n} 2\,|\lambda_r^{(n)}|^2 \tag{2.9}$$

From (2.5), we have

$$H = -E_0 - \mathscr{P} \left\{ \sum_{\sigma=\uparrow,\downarrow} \sum_{x,y\in\Lambda_N} t_{x,y} c^\dagger_{x,\sigma} c_{y,\sigma} \right\} \mathscr{P} \tag{2.10}$$

where

$$t_{x,y} = \sum_{n=1}^{N} t_{r,s}^{(n)} \qquad \text{for} \quad x = f(n,r), \quad y = f(n,s) \tag{2.11}$$

$$E_0 = -\sum_{n=1}^{N} E_n \tag{2.12}$$

and

$$\mathscr{P} = \prod_{n=1}^{N} \mathscr{P}_n \tag{2.13}$$

It was shown in refs. 4 and 5 that for the electron number $2N$ the unique ground state of the Hamiltonian (2.5) or (2.10) has zero energy and is given by

$$|\Phi_{\text{G.S.}}\rangle = \mathscr{P} \prod_{\sigma=\uparrow,\downarrow} \prod_{n=1}^{N} \alpha_{n,\sigma}^{\dagger} |0\rangle \tag{2.14}$$

where $|0\rangle$ is the vacuum state. As we will see in (3.3), we have a single valence bond in each cell. Therefore, the filling of the ground state is $1/N_a$, where N_a is the number of sites in the unit cell. In Sections 4 and 5 we use the second term in (2.10) as the Hamiltonian and denote it by H_S. The unique ground state of the Hamiltonian H_S is given by (2.14) with the energy E_0 in (2.12).

3. GEOMETRIC REPRESENTATION OF THE CORRELATION FUNCTIONS

We describe the geometric representation of the norm of the ground state and the correlation functions which was formulated by Tasaki[24] in arbitrary dimensions. The geometric representation of the norm is described in refs. 4, 9, and 25 for the lattice composed of d-sites only. Here, we have the lattice with both p- and d-sites. The ground state (2.14) can be written

$$|\Phi_{\text{G.S.}}\rangle = \mathscr{P} \prod_{n=1}^{N} \sum_{r,s \in C_n} \lambda_r^* \lambda_s^* c_{r,\uparrow}^{\dagger} c_{s,\downarrow}^{\dagger} |0\rangle = \mathscr{P} \prod_{n=1}^{N} \sum_{r \leqslant s \in C_n} \lambda_{rs}^* b_{r,s}^{\dagger} |0\rangle \tag{3.1}$$

where

$$b_{r,s}^{\dagger} = \begin{cases} c_{r,\uparrow}^{\dagger} c_{s,\downarrow}^{\dagger} + c_{s,\uparrow}^{\dagger} c_{r,\downarrow}^{\dagger} & \text{for} \quad r \neq s \\ c_{r,\uparrow}^{\dagger} c_{s,\downarrow}^{\dagger} & \text{for} \quad r = s \end{cases}$$

and

$$\lambda_{r,s}^* = \lambda_r^* \lambda_s^*$$

The operator $b^{\dagger}_{r,s}$ is the creation operator of the valence bond (i.e., a singlet pair) between sites r and s if $r \neq s$. It creates a doubly occupied site if $r = s$. They obey the commutation relations

$$[b_{r,s}, b_{t,u}] = [b^{\dagger}_{r,s}, b^{\dagger}_{t,u}] = [b^{\dagger}_{r,s}, b_{t,u}] = 0 \tag{3.2}$$

where r, s, t, and u are different sites. This operator satisfies the relation $b^{\dagger}_{r,s} = b^{\dagger}_{s,r}$ and the ground state (3.1) is a hopping-dominated RVB state according to the terminology of ref. 9. It is different from the tunneling-dominated RVB states.[9-16]

Now we rewrite the ground state (3.1) in a convenient form for diagrammatic evaluations of the norm and the correlation functions. The diagrammatic method was first introduced by Rumer[26] and Pauling.[27] We denote a valence bond by $\{x, y\}$ and a doubly occupied site by $\{x, x\}$, which is regarded as a self-closed bond (Fig. 2). Since a self-closed bond is actually a doubly occupied site, it is allowed only at p-sites. Let a valence-bond configuration V be a set of N bonds constructed by choosing a single bond from each cell. We show examples in Figs. 3a and 3b. The bonds do not share a d-site, since it can have at most one electron. A p-site is shared by at most two bonds. In this way, the projection $\mathscr{P}$ defined by (2.4) and (2.13) is automatically taken into account. We denote by $\mathscr{V}$ the set of all the possible valence-bond configurations. The ground state (3.1) is rearranged, and written as

$$|\Phi_{\text{G.S.}}\rangle = \sum_{V \in \mathscr{V}} \prod_{\{x,y\} \in V} \lambda^{*}_{x,y} b^{\dagger}_{x,y} |0\rangle \tag{3.3}$$

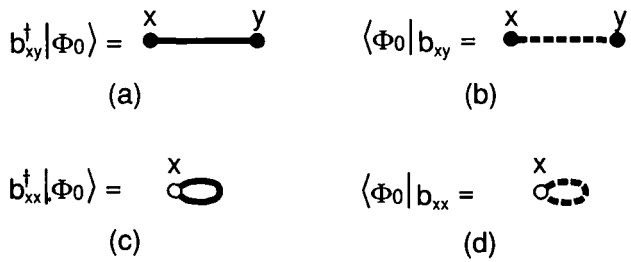

Fig. 2. Diagrammatic representation of the valence bonds. The solid (broken) line represents a valence bond in the ket (bra). We distinguish four kinds of bonds and call them (a) a non-closed ket-bond, (b) a nonclosed bra-bond, (c) a self-closed ket-bond, and (d) a self-closed bra-bond. A d-site with $U = \infty$ is denoted by a solid circle, and a p-site with $U = 0$ is denoted by an open circle.

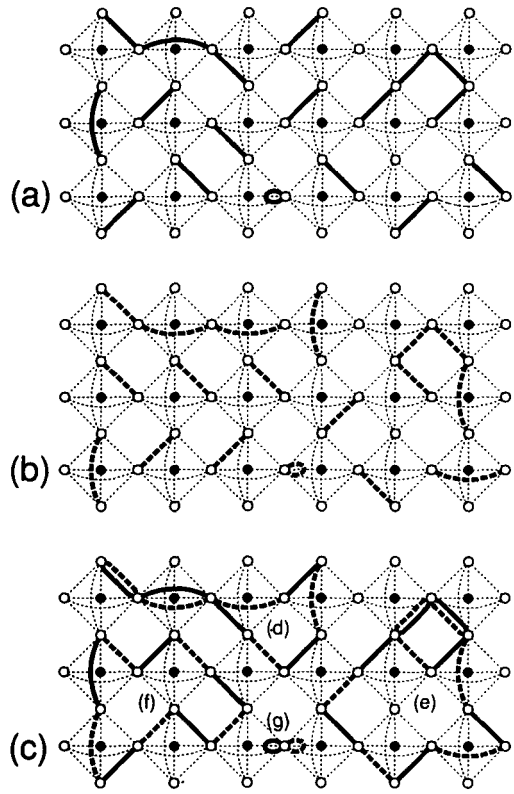

Fig. 3. Examples of valence-bond configurations (a) V, (b) V', and (c) their overlap $V \cup V'$. The lattice is constructed from a cell with one d-site and four p-sites. The p-sites in adjacent cells actually comprise a single p-site. The thin broken lines represent hoppings of electrons. The graph $V \cup V'$ is factorized into four connected subgraphs (d)–(g).

3.1. Norm of the Ground State

From (3.3), the norm of the ground state is

$$\langle \Phi_{\mathrm{G.S.}} | \Phi_{\mathrm{G.S.}} \rangle = \sum_{V \in \mathcal{V}} \sum_{V' \in \mathcal{V}} \lambda(V')\, \lambda^*(V) \langle 0 | \prod_{\{x', y'\} \in V'} b_{x', y'} \prod_{\{x, y\} \in V} b^{\dagger}_{x, y} | 0 \rangle \tag{3.4}$$

where $\lambda(V) = \prod_{\{x, y\} \in V} \lambda_{x, y}$. Let us consider a graph $V \cup V'$ in the expectation value. We call a bond which belongs to V' a bra-bond and one which belongs to V a ket-bond (Fig. 2). We only consider graphs $V \cup V'$ in

which the numbers of bra-bonds and ket-bonds are equal at every site. (An example is shown in Fig. 3c.) Otherwise, the expectation value is vanishing, since the numbers of the creation and annihilation operators are different at the site.

The graph $V \cup V'$ can be decomposed into connected subgraphs, since the operators $b_{x',y'}$ and $b^\dagger_{x,y}$ commute [see (3.2)]. An example is shown in Figs. 3d–3g. We denote the number of the subgraphs by $n(V \cup V')$. This decomposition is written

$$V \cup V' = \sum_{i=1}^{n(V \cup V')} U_i \cup U'_i \tag{3.5}$$

where $U_i \subset V$ and $U'_i \subset V'$.

By noting that $b_{x',y'}$ and $b^\dagger_{x,y}$ commute with each other for distinct x, y, x', and y' [see (3.2)], we find that the expectation value in (3.4) can be factorized into parts corresponding to connected subgraphs. Thus, we have

$$\langle \Phi_{\text{G.S.}} | \Phi_{\text{G.S.}} \rangle = \sum_{V, V' \in \mathcal{V}} \left\{ \prod_{i=1}^{n(V \cup V')} \lambda(U'_i)\, \lambda^*(U_i) \times \langle 0 | \prod_{\{x',y'\} \in U'_i} b_{x',y'} \prod_{\{x,y\} \in U_i} b^\dagger_{x,y} | 0 \rangle \right\} \tag{3.6}$$

We note that each U_i, U'_i in (3.6) depends on the whole of configurations V, V', and $V \cup V'$.

It sometimes happens that two bra-bonds and two ket-bonds are connected to a single p-site in a connected subgraph $U_i \cup U'_i$. For our calculations, it is convenient to eliminate such sites. This is done by using the identity $b^\dagger_{x,y} b^\dagger_{y,z} = -b^\dagger_{y,y} b^\dagger_{x,z}$ (see Fig. 4a). Examples of eliminations of such sites are shown diagrammatically in Figs. 4b–4d. The procedure in Fig. 4b generates a minus sign. We assign the sign to the nonclosed bond. We shall always apply this procedure hereafter and it should be understood implicitly. After this procedure, the subgraph $U_i \cup U'_i$ may be decomposed into several graphs. We denote the number of the graphs by $n(U_i \cup U'_i)$. The decomposition is unique and is written

$$U_i \cup U'_i \to \sum_{j=1}^{n(U_i \cup U'_i)} W_j \cup W'_j \tag{3.7}$$

The arrow indicates that W_j, W'_j are not necessarily subsets of $U_i \cup U'_i$. We only have three kinds of graphs $W_j \cup W'_j$: self-closed bonds (Fig. 4e),

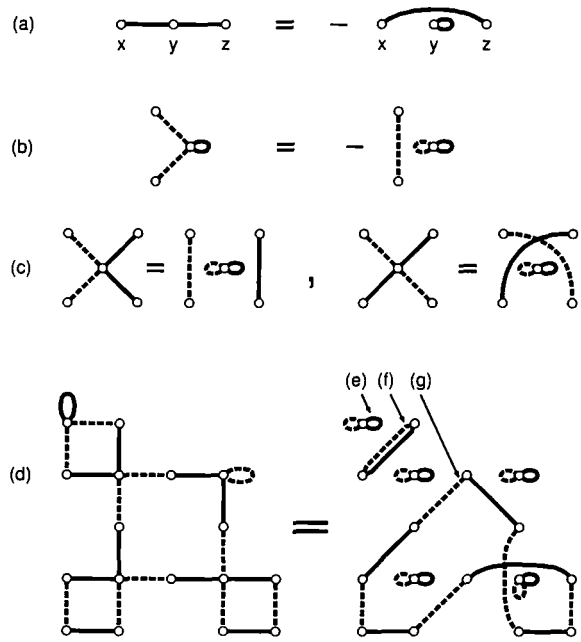

Fig. 4. (a) Diagrammatic representation of the identity $b^{\dagger}_{x,y}b^{\dagger}_{y,z} = -b^{\dagger}_{y,y}b^{\dagger}_{x,z}$. Examples of the elimination of a p-site with four bonds (b) and (c), which exhaust all the cases. For (b), we apply the identity (a) once. For (c), we apply it two times. (d) Example of the decomposition of a connected graph to subgraphs. We have self-closed bonds (e), a degenerate loop (f), and a nondegenerate loop (g) after the procedure.

degenerate loops, which consist of a pair of bonds (Fig. 4f), and non-degenerate loops, which consist of an even number of distinct bonds (Fig. 4g). We call the graph $W_j \cup W'_j$ a loop. From the decomposition (3.7), we have

$$\langle 0| \prod_{\{x',y'\} \in U'_i} b_{x',y'} \prod_{\{x,y\} \in U_i} b^{\dagger}_{x,y} |0\rangle = \prod_{j=1}^{n(U_i \cup U'_i)} (-1)^{m_j} w_j \tag{3.8}$$

where m_j is the number of the procedures shown in Fig. 4b and

$$w_j = \langle 0| \prod_{\{x',y'\} \in W'_j} b_{x',y'} \prod_{\{x,y\} \in W_j} b^{\dagger}_{x,y} |0\rangle \tag{3.9}$$

We call it the weight. The value is classified by

$$w_j = \begin{cases} 1 & \text{if } W_j \cup W_j' \text{ is a pair of the self-closed bonds (Fig. 4e)} \\ 2 & \text{if } W_j \cup W_j' \text{ is a degenerate loop (Fig. 4f)} \\ 2(-1)^{l_j/2-1} & \text{if } W_j \cup W_j' \text{ is a nondegenerate loop (Fig. 4g)} \end{cases} \tag{3.10}$$

where l_j is the number of bonds in the jth nondegenerate loop. These weights are derived in Appendix B. Now the norm of the ground state (3.6) is written

$$\langle \Phi_{\text{G.S.}} | \Phi_{\text{G.S.}} \rangle = \sum_{V, V' \in \gamma} \left\{ \prod_{i=1}^{n(V \cup V')} \left[\prod_{j=1}^{n(U_i \cup U_i')} \lambda(W_j') \lambda^*(W_j)(-1)^{m_j} w_j \right] \right\} \tag{3.11}$$

3.2. Spin Correlation Function

The spin correlation function is given by

$$\langle S_x^z S_y^z \rangle = \frac{\langle \Phi_{\text{G.S.}} | S_x^z S_y^z | \Phi_{\text{G.S.}} \rangle}{\langle \Phi_{\text{G.S.}} | \Phi_{\text{G.S.}} \rangle} \tag{3.12}$$

where $S_x^z = (c_{x,\uparrow}^\dagger c_{x,\uparrow} - c_{x,\downarrow}^\dagger c_{x,\downarrow})/2$ is the z component of the spin operator on site x. From (3.3), the numerator is written

$$\langle \Phi_{\text{G.S.}} | S_x^z S_y^z | \Phi_{\text{G.S.}} \rangle = \sum_{V \in \gamma} \sum_{V' \in \gamma} \lambda(V') \lambda^*(V) \times \langle 0 | \left(\prod_{\{u', v'\} \in V'} b_{u', v'} \right) S_x^z S_y^z \prod_{\{u, v\} \in V} b_{u, v}^\dagger | 0 \rangle \tag{3.13}$$

From the commutation relations (3.2) and $[S_x^z, b_{u,v}] = [S_x^z, b_{u,v}^\dagger] = 0$, where x, u, and v are different sites, we can decompose the graph $V \cup V'$ into connected subgraphs $U_i \cup U_i'$ as we did in Section 3.1. We only need to consider the case where sites x and y belong to a single subgraph denoted as $U^{(x,y)} \cup U'^{(x,y)}$. Otherwise, the expectation value in (3.13) is vanishing. The decomposition is written

$$V \cup V' = U^{(x,y)} \cup U'^{(x,y)} + \sum_{i=1}^{n(V \cup V')-1} U_i \cup U_i' \tag{3.14}$$

After the elimination of p-sites with four nonclosed bonds, we only need to consider the case where sites x and y belong to a single loop (Fig. 5a) denoted as $W^{(x,y)} \cup W'^{(x,y)}$. Otherwise, the expectation value in (3.13) is vanishing. We have

$$V \cup V' \to W^{(x,y)} \cup W'^{(x,y)} + \sum_{j=1}^{n(U^{(x,y)} \cup U'^{(x,y)})-1} W_j \cup W'_j$$

$$+ \sum_{i=1}^{n(V \cup V')-1} \left(\sum_{j=1}^{n(U_i \cup U'_i)} W_j \cup W'_j \right) \tag{3.15}$$

$$= W^{(x,y)} \cup W'^{(x,y)} + \sum_{j=1}^{\mathcal{N}_W} W_j \cup W'_j \tag{3.16}$$

We note that each W_j, W'_j in the second term of (3.15) depends on the graphs $U^{(x,y)}$, $U'^{(x,y)}$, and $U^{(x,y)} \cup U'^{(x,y)}$, and those in the third term depend on the graphs U_i, U'_i, and $U_i \cup U'_i$. We denote the total number of the loops $W_j \cup W'_j$ in the second and the third terms of (3.15) by $\mathcal{N}_W$.

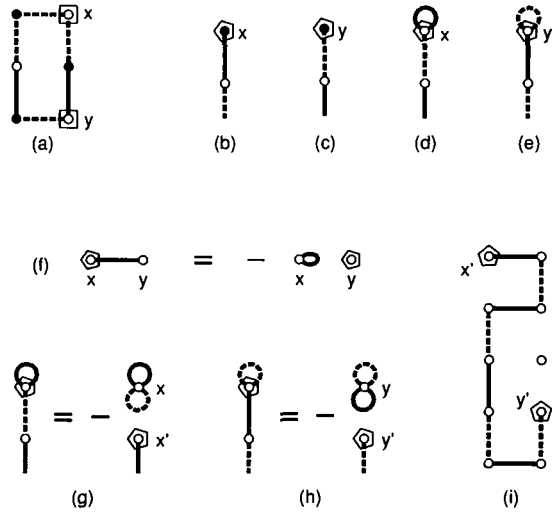

Fig. 5. (a) Example of a graph where sites x and y belong to a single subgraph in the geometric representation of the spin correlation function. A square represents the spin operator S^z. (b, c) Type (i) configurations and (d, e) type (ii) configurations in the geometric representation of the correlation function $\langle c_{i,\sigma} c^\dagger_{j\sigma} \rangle$. A pentagon represents the operator $c^\dagger_{x,\sigma}$. (f) Diagrammatic representation of the identity $c^\dagger_{x,\sigma} b^\dagger_{x,y} = -c^\dagger_{y,\sigma} b^\dagger_{y,y}$. (g, h) Examples of the elimination of the type (ii) configuration. (i) Example of a line.

Their labelings in (3.16) were rearranged. The weight for the loop $W^{(x,y)} \cup W'^{(x,y)}$ is

$$\begin{aligned} w(x, y) &= \langle 0| \left(\prod_{\{z', w'\} \in W'^{(x,y)}} b_{z', w'} \right) S_x^z S_y^z \prod_{\{z, w\} \in W^{(x,y)}} b_{z, w}^\dagger |0\rangle \\ &= (-1)^{d(x,y)} \tfrac{1}{4} \langle 0| \prod_{\{z', w'\} \in W'^{(x,y)}} b_{z', w'} \prod_{\{z, w\} \in W^{(x,y)}} b_{z, w}^\dagger |0\rangle \\ &= (-1)^{d(x,y)} \tfrac{1}{4} w \end{aligned} \tag{3.17}$$

where $d(x, y)$ is the number of bonds between x and y along the loop and w is given by (3.10). A derivation is shown in Appendix C. From (3.8), (3.9), (3.16), and (3.17), we obtain

$$\begin{aligned} \langle \Phi_{\text{G.S.}}| S_x^z S_y^z |\Phi_{\text{G.S.}}\rangle &= \sum_{V, V' \in \mathcal{V}} \left\{ (-1)^{d(x,y)} \tfrac{1}{4} \prod_{i=1}^{n(V \cup V')} \lambda(U_i') \lambda^*(U_i) \right. \\ &\quad \left. \times \langle 0| \prod_{\{x', y'\} \in U_i'} b_{x', y'} \prod_{\{x, y\} \in U_i} b_{x, y}^\dagger |0\rangle \right\} \qquad (3.18) \\ &= \sum_{V, V' \in \mathcal{V}} \left\{ (-1)^{d(x,y)} \tfrac{1}{4} \prod_{i=1}^{n(V \cup V')} \right. \\ &\quad \left. \times \left[\prod_{j=1}^{n(U_j \cup U_j')} \lambda(W_j') \lambda^*(W_j) (-1)^{m_j} w_j \right] \right\} \qquad (3.19) \end{aligned}$$

where the weight for the loop $W^{(x,y)} \cup W'^{(x,y)}$ is included in the product.

3.3. Correlation Function $\langle c_{x,\sigma} c_{y,\sigma}^\dagger \rangle$

We evaluate the correlation function defined by

$$\langle c_{x,\sigma} c_{y,\sigma}^\dagger \rangle = \frac{\langle \Phi_{\text{G.S.}}| c_{x,\sigma} c_{y,\sigma}^\dagger |\Phi_{\text{G.S.}}\rangle}{\langle \Phi_{\text{G.S.}}|\Phi_{\text{G.S.}}\rangle} \tag{3.20}$$

From (3.3), the numerator is written

$$\begin{aligned} \langle \Phi_{\text{G.S.}}| c_{x,\sigma} c_{y,\sigma}^\dagger |\Phi_{\text{G.S.}}\rangle &= \sum_{V \in \mathcal{V}} \sum_{V' \in \mathcal{V}} \lambda(V') \lambda^*(V) \\ &\quad \times \langle 0| \left(\prod_{\{u', v'\} \in V'} b_{u', v'} \right) c_{x,\sigma} c_{y,\sigma}^\dagger \prod_{\{u, v\} \in V} b_{u, v}^\dagger |0\rangle \end{aligned} \tag{3.21}$$

We decompose the graph $V \cup V'$ into connected subgraphs using the commutation relations (3.2) and $[c_{z,\sigma}, b_{x,y}] = [c_{z,\sigma}, b^\dagger_{x,y}] = [c^\dagger_{z,\sigma}, b^\dagger_{x,y}] = 0$, where $z \neq x$ and $z \neq y$, and obtain (3.14). After the elimination of p-sites with four nonclosed bonds, we only need to consider the case where sites x and y belong to a single graph and they satisfy one of the following four conditions: (i) site x (y) with one nonclosed ket (bra)-bond, and (ii) site x (y) with one nonclosed bra (ket)-bond and one self-closed ket (bra)-bond. (See Figs. 5b–5e, where a site with a pentagon represents the operator $c_{x,\sigma}$ or $c^\dagger_{y,\sigma}$.) Otherwise, the expectation value is vanishing. It is convenient to eliminate type (ii) sites using the identity $c^\dagger_{x,\sigma} b^\dagger_{x,y} = -c^\dagger_{y,\sigma} b^\dagger_{x,x}$, which is represented diagrammatically in Fig. 5f. The results are shown in Figs. 4g and 4h. After this procedure, the graph $W^{(x',y')} \cup W'^{(x',y')}$ in (3.14) is a line where bra-bond and ket-bond are placed alternately and x' and y' are always at the end of the line (Fig. 4i). The weight is

$$\begin{aligned} w(x', y') &= \langle 0 | \left(\prod_{\{u', v'\} \in W'^{(x',y')}} b_{u',v'} \right) c_{x',\sigma} c^\dagger_{y',\sigma} \prod_{\{u, v\} \in W^{(x',y')}} b^\dagger_{u,v} | 0 \rangle \\ &= (-1)^{l(x',y')/2} \end{aligned} \tag{3.22}$$

where $l(x', y')$ is the number of the bonds (see Appendix D). Thus we have

$$\begin{aligned} &\langle \Phi_{\mathrm{G.S.}} | \, c_{x,\sigma} c^\dagger_{y,\sigma} \, | \Phi_{\mathrm{G.S.}} \rangle \\ &\quad = \sum_{V, V' \in \gamma} \Bigg\{ \lambda(U'^{(x,y)}) \, \lambda^*(U^{(x,y)}) \\ &\qquad \times \langle 0 | \left(\prod_{\{z', w'\} \in U'^{(x,y)}} b_{z',w'} \right) c_{x,\sigma} c^\dagger_{y,\sigma} \prod_{\{z, w\} \in U^{(x,y)}} b^\dagger_{z,w} | 0 \rangle \\ &\qquad \times \prod_{i=1}^{n(V \cup V')-1} \Bigg[\lambda(U'_i) \, \lambda^*(U_i) \\ &\qquad \times \langle 0 | \prod_{\{u', v'\} \in U'_i} b_{u',v'} \prod_{\{u, v\} \in U_i} b^\dagger_{u,v} | 0 \rangle \Bigg] \Bigg\} \end{aligned} \tag{3.23}$$

$$\begin{aligned} &= \sum_{V, V' \in \gamma} \Bigg\{ \lambda(W'^{(x',y')}) \, \lambda^*(W^{(x',y')}) (-1)^{l(x',y')/2 + m} \\ &\qquad \times \prod_{j=1}^{n(W)} \lambda(W'_j) \, \lambda^*(W_j) (-1)^{m_j} w_j \Bigg\} \end{aligned} \tag{3.24}$$

where m is the number of the procedures shown in Fig. 5f for the subgraph $U^{(x,y)} \cup U'^{(x,y)}$.

3.4. Density Correlation Function

We first evaluate the expectation value of the number operator

$$\langle n_{x,\sigma}\rangle = \frac{\langle \Phi_{\text{G.S.}} | n_{x,\sigma} | \Phi_{\text{G.S.}}\rangle}{\langle \Phi_{\text{G.S.}} | \Phi_{\text{G.S.}}\rangle} \tag{3.25}$$

From (3.3), the numerator is written

$$\langle \Phi_{\text{G.S.}} | n_{x,\sigma} | \Phi_{\text{G.S.}}\rangle = \sum_{V\in\mathcal{V}} \sum_{V'\in\mathcal{V}'} \lambda(V')\,\lambda^*(V) \times \langle 0| \left(\prod_{\{u',v'\}\in V'} b_{u',v'} \right) n_{x,\sigma} \prod_{\{u,v\}\in V} b^\dagger_{u,v} |0\rangle \tag{3.26}$$

We only need to consider the graph $V\cup V'$, which contains the site x. Otherwise, the expectation value is vanishing. A similar calculation to that in Section 3.2 leads to

$$\begin{aligned} V\cup V' &= U^{(x)}\cup U'^{(x)} + \sum_{i=1}^{n(V\cup V')-1} U_i\cup U'_i \\ &\to W^{(x)}\cup W'^{(x)} + \sum_{j=1}^{n(U^{(x)}\cup U'^{(x)})-1} W_j\cup W'_j \\ &\quad + \sum_{i=1}^{n(V\cup V')-1} \left(\sum_{j=1}^{n(U_i\cup U'_i)} W_j\cup W_j \right) \\ &= W^{(x)}\cup W'^{(x)} + \sum_{j=1}^{\cdot\cdot W} W_j\cup W'_j \end{aligned} \tag{3.27}$$

where $U^{(x)}\cup U'^{(x)}$ is a subgraph with the site x, and $W^{(x)}\cup W'^{(x)}$ is a loop with the site x after the elimination of p-sites with four nonclosed bonds. We distinguish two kinds of loops: (i) a site x with self-closed bonds, and (ii) a site x with one nonclosed bra-bond and one nonclosed ket-bond (see Figs. 6a and 6b, where a site with a circle represents the number operator). [We note that a subgraph $U^{(x)}\cup U'^{(x)}$ with four nonclosed bonds at the site x is decomposed into type (ii) graph and loops.] The weight is

$$\begin{aligned} w(x) &= \langle 0| \left(\prod_{\{z',w'\}\in W'^{(x)}} b_{z',w'} \right) n_{x,\sigma} \prod_{\{z,w\}\in W^{(x)}} b^\dagger_{z,w} |0\rangle \\ &= \begin{cases} 1 & \text{for (i)} \\ (-1)^{l(x)/2-1} & \text{for (ii)} \end{cases} \end{aligned} \tag{3.28}$$

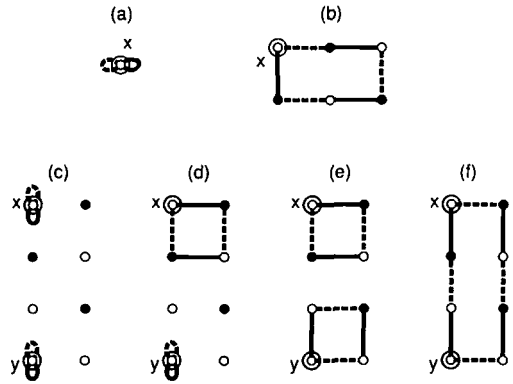

Fig. 6. (a) Type (i) configuration and (b) type (ii) configuration in the expectation value of the number operator. (c) Type (i) configuration, (d) type (ii) configuration, (e) type (iii) configuration, and (f) type (iv) configuration in the geometric representation of the density correlation function.

where $l(x)$ is the number of bonds in the graph. A derivation is given in Appendix E. From (3.8), (3.9), (3.27), and (3.28), we obtain

$$\begin{aligned}
&\langle \Phi_{\text{G.S.}} | \, n_{x,\sigma} \, | \Phi_{\text{G.S.}} \rangle \\
&\quad = \sum_{V,\, V' \in \mathcal{V}} \Bigg\{ \lambda(U'(x))\, \lambda^*(U(x)) \\
&\qquad \times \langle 0 | \Bigg(\prod_{\{z',\, w'\} \in U'(x)} b_{z',\, w'} \Bigg) n_{x,\sigma} \prod_{\{z,\, w\} \in U(x)} b^{\dagger}_{z,\, w} \, | 0 \rangle \\
&\qquad \times \prod_{i=1}^{n(V \cup V') - 1} \Bigg[\lambda(U'_i)\, \lambda^*(U_i) \\
&\qquad \times \langle 0 | \prod_{\{u',\, v'\} \in U'_i} b_{u',\, v'} \prod_{\{u,\, v\} \in U_i} b^{\dagger}_{u,\, v} \, | 0 \rangle \Bigg] \Bigg\} \qquad (3.29) \\
&\quad = \sum_{V,\, V' \in \mathcal{V}} \Bigg\{ \lambda(W'_j(x))\, \lambda^*(W_j(x))(-1)^m \, w(x) \\
&\qquad \times \prod_{j=1}^{l \, W} \lambda(W'_j)\, \lambda^*(W_j)(-1)^{m_j} \, w_j \Bigg\} \qquad (3.30)
\end{aligned}$$

The density correlation function is

$$\begin{aligned}
\langle \delta n_x \, \delta n_y \rangle &= \langle (n_x - \langle n_x \rangle)(n_y - \langle n_y \rangle) \rangle \\
&= \langle n_x n_y \rangle - \langle n_x \rangle \langle n_y \rangle
\end{aligned}$$

$$= \frac{\langle \Phi_{\text{G.S.}} | n_x n_y | \Phi_{\text{G.S.}} \rangle}{\langle \Phi_{\text{G.S.}} | \Phi_{\text{G.S.}} \rangle} - \frac{\langle \Phi_{\text{G.S.}} | n_x | \Phi_{\text{G.S.}} \rangle \langle \Phi_{\text{G.S.}} | n_y | \Phi_{\text{G.S.}} \rangle}{(\langle \Phi_{\text{G.S.}} | \Phi_{\text{G.S.}} \rangle)^2}$$

$$= 4 \left[\frac{D(x, y; \sigma)}{\langle \Phi_{\text{G.S.}} | \Phi_{\text{G.S.}} \rangle} - \langle n_{x,\sigma} \rangle \langle n_{y,\sigma} \rangle \right] \tag{3.31}$$

where

$$D(x, y; \sigma) = \tfrac{1}{2} \langle \Phi_{\text{G.S.}} | c_{x,\sigma} c_{y,\sigma} c^\dagger_{y,\sigma} c^\dagger_{x,\sigma} + c_{x,\sigma} c_{y,-\sigma} c^\dagger_{y,-\sigma} c^\dagger_{x,\sigma} | \Phi_{\text{G.S.}} \rangle \tag{3.32}$$

From (3.3), we have

$$\begin{aligned} D(x, y; \sigma) = \sum_{V \in \mathcal{V}} \sum_{V' \in \mathcal{V}} \lambda(V') \lambda^*(V) \langle 0 | \left(\prod_{\{u', v'\} \in V'} b_{u', v'} \right) \\ \times \tfrac{1}{2} (c_{x,\sigma} c_{y,\sigma} c^\dagger_{y,\sigma} c^\dagger_{x,\sigma} + c_{x,\sigma} c_{y,-\sigma} c^\dagger_{y,-\sigma} c^\dagger_{x,\sigma}) \\ \times \prod_{\{u, v\} \in V} b^\dagger_{u,v} | 0 \rangle \end{aligned} \tag{3.33}$$

We only need to consider the graph $V \cup V'$ which contains the sites x and y. Otherwise, the expectation value is vanishing. A similar calculation to that in Section 3.2 leads to (3.16), where $W^{(x,y)} \cup W'^{(x,y)}$ is a loop (or two loops) which contain(s) the sites x and y. We classify the loops $W^{(x,y)} \cup W'^{(x,y)}$ as (i) sites x and y each belongs to two distinct self-closed bonds, (ii) site x (y) belongs to the loop and site y (x) belongs to the self-closed bonds, (iii) sites x and y each belongs to two distinct loops, and (iv) sites x and y belong to a single graph (see Figs. 6c–6f). Otherwise, the expectation value is vanishing. The weight is

$$\begin{aligned} & w(x, y; \sigma) \\ & = \langle 0 | \left(\prod_{\{u', v'\} \in W'^{(x,y)}} b_{u', v'} \right) \\ & \quad \times \tfrac{1}{2} (c_{x,\sigma} c_{y,\sigma} c^\dagger_{y,\sigma} c^\dagger_{x,\sigma} + c_{x,\sigma} c_{y,-\sigma} c^\dagger_{y,-\sigma} c^\dagger_{x,\sigma}) \prod_{\{u, v\} \in W^{(x,y)}} b^\dagger_{u,v} | 0 \rangle \end{aligned} \tag{3.34}$$

$$= \begin{cases} 1 & \text{for (i)} \\ (-1)^{l(x)/2 - 1} & \text{for (ii) when the site} \\ & \quad x \text{ belongs to the loop} \\ (-1)^{l(x)/2 - 1} \times (-1)^{l_i(y)/2 - 1} & \text{for (iii)} \\ (-1)^{l(x,y)/2 - 1}/2 & \text{for (iv)} \end{cases} \tag{3.35}$$

where $l(x)$ and $l(x, y)$ are the numbers of bonds. A derivation is given in Appendix F. From (3.8), (3.9), and (3.35), we obtain

$$
\begin{aligned}
&D(x, y; \sigma) \\
&= \sum_{V, V' \in \mathcal{Y}'} \Bigg\{ \lambda(U'^{(x,y)})\, \lambda^*(U^{(x,y)}) \langle 0 | \Bigg(\prod_{\{z', w'\} \in U'^{(x,y)}} b_{z', w'} \Bigg) \\
&\quad \times \tfrac{1}{2} (c_{x,\sigma} c_{y,\sigma} c^\dagger_{y,\sigma} c^\dagger_{x,\sigma} + c_{x,\sigma} c_{y,-\sigma} c^\dagger_{y,-\sigma} c^\dagger_{x,\sigma}) \prod_{\{z, w\} \in U^{(x,y)}} b^\dagger_{z,w} |0\rangle \\
&\quad \times \prod_{i=1}^{n(V \cup V')-1} \Bigg[\lambda(U'_i)\, \lambda^*(U_i) \\
&\quad \times \langle 0 | \prod_{\{u', v'\} \in W'_i} b_{u', v'} \prod_{\{u, v\} \in W_i} b^\dagger_{u,v} |0\rangle \Bigg] \Bigg\} \qquad (3.36) \\
&= \sum_{V, V' \in \mathcal{Y}'} \Bigg\{ \lambda(W'^{(x,y)})\, \lambda^*(W^{(x,y)}) (-1)^m w(x, y; \sigma) \\
&\quad \times \prod_{j=1}^{N_W} \lambda(W'_j)\, \lambda^*(W_j) (-1)^{m_j} w_j \Bigg\} \qquad (3.37)
\end{aligned}
$$

3.5. Singlet-Pair Correlation Function

The singlet-pair correlation function is given by

$$
\langle b^\dagger_{x,y} b_{u,v} \rangle = \frac{\langle \Phi_{\text{G.S.}} | b^\dagger_{x,y} b_{u,v} | \Phi_{\text{G.S.}} \rangle}{\langle \Phi_{\text{G.S.}} | \Phi_{\text{G.S.}} \rangle} \qquad (3.38)
$$

From (3.3), we obtain

$$
\begin{aligned}
&\langle \Phi_{\text{G.S.}} | b^\dagger_{x,y} b_{u,v} | \Phi_{\text{G.S.}} \rangle \\
&\quad = \sum_{V \in \mathcal{Y}'} \sum_{V' \in \mathcal{Y}'} \lambda(V')\, \lambda^*(V) \\
&\qquad \times \langle 0 | \Bigg(\prod_{\{x', y'\} \in V'} b_{x', y'} \Bigg) b^\dagger_{x,y} b_{u,v} \prod_{\{x, y\} \in V} b^\dagger_{x,y} |0\rangle \\
&\quad = \sum_{V, V' \in \mathcal{Y}'} \Bigg\{ \prod_{i=1}^{n(V \cup V' \cup \{x,y\} \cup \{u,v\})} \lambda(U'_j)\, \lambda^*(U_j) \\
&\qquad \times \langle 0 | \Bigg(\prod_{\{x', y'\} \in U'} b_{x', y'} \Bigg) b^\dagger_{x,y} b_{u,v} \prod_{\{x, y\} \in U} b^\dagger_{x,y} |0\rangle \Bigg\} \qquad (3.39)
\end{aligned}
$$

$$= \sum_{V,\, V' \in \gamma} \left\{ \prod_{i=1}^{n(V \cup V' \cup \{x,\, y\} \cup \{u,\, v\})} \times \left[\prod_{j=1}^{n(U_i \cup U_i')} \lambda(W_j')\, \lambda^*(W_j)(-1)^{m_j} w_j \right] \right\} \tag{3.40}$$

where V and V' satisfy the condition that the graph $V \cup V' \cup \{x, y\} \cup \{u, v\}$ consists of connected subgraphs.

4. EXPLICIT CALCULATIONS OF THE CORRELATION FUNCTIONS

The results of Sections 2 and 3 are valid in any dimensions. At the moment, however, their practical use is limited to models in one dimension in which the transfer matrix method can be applied. In this section, the equal-time correlation functions are evaluated exactly for one-dimensional models. We shall show the analytical procedures for obtaining them for Model A defined below in Section 4.1, illustrating the method in detail. The results are shown for a system size N and in the thermodynamic limit. For Models B and C, we only show the results in the thermodynamic limit.[28]

4.1. Model A

4.1.1. Hamiltonian. Let us consider a lattice constructed from cells with three sites. We have two lattices which satisfy the uniqueness condition of ref. 5. One of them, which we call Model A (the other is called Model B; see Section 4.3), is constructed from a cell with two d-sites and one p-site (Fig. 7a). Note that a cell is not a unit cell. A unit cell is composed of a d-site and a p-site. In the models constructed by the cell construction, Model A is the simplest one for the following two reasons. The structure of the lattice is the simplest. (We can construct lattices from cells with two sites. The exact ground state, however, contains two electrons per site and is fully filled.) The calculation of the correlation function is easier than that of Model B.

The cell Hamiltonian (2.2) is obtained by choosing

$$\alpha_{n,\sigma}^{(A)} = \sum_{r=1}^{3} \lambda_r c_{r,\sigma} \equiv \lambda_1 c_{1,\sigma}^d + \lambda_2 c_{2,\sigma}^d + \lambda_3 c_{3,\sigma}^p$$

in (2.3) and setting $\lambda_3 = 1$ without loss of generality (see Fig. 7a for the intracell index). Here $c_{r,\sigma}^d$ ($c_{r,\sigma}^p$) is the annihilation operator on a d (p)-site.

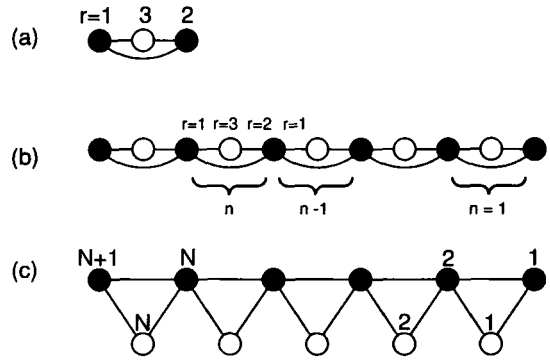

Fig. 7. Model A. (a) A cell composed of two d-sites ($U=\infty$) and one p-site ($U=0$). (b) The lattice constructed from the cell with cell labelings. (c) The same lattice as (b) drawn differently with unit cell labelings.

The full Hamiltonian is obtained by identifying site 1 in the $(n-1)$th cell with site 2 in the nth cell (Fig. 7b). The Hamiltonian is

$$H_S=\mathscr{P}\sum_{\sigma=\uparrow,\downarrow}\left\{\sum_{n=1}^{N}\left[(-\lambda_1\lambda_2 c^{d\dagger}_{n+1,\sigma}c^{d}_{n,\sigma}-\lambda_1 c^{d\dagger}_{n+1,\sigma}c^{p}_{n,\sigma}-\lambda_2 c^{d\dagger}_{n,\sigma}c^{p}_{n,\sigma}+\text{h.c.})\right.\right.$$
$$\left.\left.+\varepsilon^{d}_{n}c^{d\dagger}_{n,\sigma}c^{d}_{n,\sigma}+\varepsilon^{p}c^{p\dagger}_{n,\sigma}c^{p}_{n,\sigma}\right]+\varepsilon^{d}_{N+1}c^{d\dagger}_{N+1,\sigma}c^{d}_{N+1,\sigma}\right\}\mathscr{P} \tag{4.1}$$

where the on-site potentials are $\varepsilon^{d}_{1}=-2\lambda_2^2$, $\varepsilon^{d}_{n}=-2(\lambda_1^2+\lambda_2^2)$ $(2\leqslant n\leqslant N)$, $\varepsilon^{d}_{N+1}=-2\lambda_1^2$, and $\varepsilon^{p}=-1$. A unit cell is labeled by n. The ground state is

$$|\Phi^{A}_{\text{G.S.}}\rangle=\mathscr{P}\prod_{n=1}^{N}\prod_{\sigma=\uparrow,\downarrow}\alpha^{(A)\dagger}_{n,\sigma}|0\rangle \tag{4.2}$$

$$=\mathscr{P}\prod_{n=1}^{N}\prod_{\sigma=\uparrow,\downarrow}(\lambda_1 c^{d\dagger}_{n,\sigma}+\lambda_2 c^{d\dagger}_{n+1,\sigma}+c^{p\dagger}_{n,\sigma})|0\rangle \tag{4.3}$$

which is a half-filled state.

4.1.2. Band Structure in the Single-Electron Problem. Before studying the ground state (4.3), we investigate the corresponding noninteracting system. We consider the system with an even number of

unit cells under the periodic boundary condition $c^d_{N+1} = c^d_1$. A one-particle state can be written

$$|\Phi_F\rangle = \sum_n \sum_{\alpha=p,d} \varphi^\alpha_n c^{\alpha\dagger}_{n,\uparrow} |0\rangle \tag{4.4}$$

where φ^α_n are complex coefficients. The single-electron Schrödinger equation $H|\Phi_F\rangle = E|\Phi_F\rangle$, where E is the energy eigenvalue, corresponding to the Hamiltonian (4.1) is

$$\begin{aligned} E\varphi^d_n &= -\lambda_1\lambda_2(\varphi^d_{n-1} + \varphi^d_{n+1}) - 2(\lambda_1^2 + \lambda_2^2)\,\varphi^d_n - \lambda_1\varphi^p_{n-1} - \lambda_2\varphi^p_{n+1} \\ E\varphi^p_n &= -\lambda_1\varphi^d_{n-1} - \lambda_2\varphi^d_{n+1} - \varphi^p_n \end{aligned} \tag{4.5}$$

From the Fourier transformation $\varphi^\alpha_n = (1/\sqrt{N})\sum_k e^{ikn}\varphi^\alpha_k$, where

$$k = 0,\ \pm\frac{2\pi}{N},\ \pm\frac{4\pi}{N},\ldots,\ \pm 2\pi\frac{N/2-1}{N},\ \pi \tag{4.6}$$

the Schrödinger equation in the momentum space is

$$\begin{aligned} E\varphi^d_k &= -2(\lambda_1\lambda_2\cos k + \lambda_1^2 + \lambda_2^2)\,\varphi^d_k - (\lambda_1 + \lambda_2 e^{-ik})\,\varphi^p_k \\ E\varphi^p_k &= -(\lambda_1 + \lambda_2 e^{ik})\,\varphi^d_k - \varphi^p_k \end{aligned} \tag{4.7}$$

The eigenenergies are

$$\begin{aligned} E_\pm = -\tfrac{1}{2}\{&2\lambda_1\lambda_2\cos k + 2\lambda_1^2 + \lambda_2^2 + 1 \\ &\mp [(2\lambda_1\lambda_2\cos k + 2\lambda_1^2 + 2\lambda_2^2)^2 - 4(\lambda_1^2 + \lambda_2^2)]^{1/2}\} \end{aligned} \tag{4.8}$$

where $-$, $+$ are the band indexes with $-$ (resp. $+$) corresponding to the $+$ (resp. $-$) sign. The energy gap between two bands is $\Delta = [(2\lambda_1\lambda_2 - 1)(1 + 4\lambda_1^2 - 2\lambda_1\lambda_2 + 4\lambda_2^2)]^{1/2}$. When $2\lambda_1\lambda_2 - 1 = 0$, the gap closes at $k = \pi$. (See Fig. 8.)

In the ground state (4.3) there are $2N$ electrons. Since there are $2N$ sites in the lattice, the electron number corresponds to fullfilling of the lower band. Therefore, the ground state of the noninteracting system is insulating for $2\lambda_1\lambda_2 - 1 \neq 0$. It is metallic when $2\lambda_1\lambda_2 - 1 = 0$.

4.1.3. Norm of the Ground State. Before calculating the correlation functions, we evaluate the norm of the ground state (4.3), since the state is not normalized. For the sake of convenience, we draw the lattice shown in Fig. 7b and Fig. 7c. The ground state admits the geometric

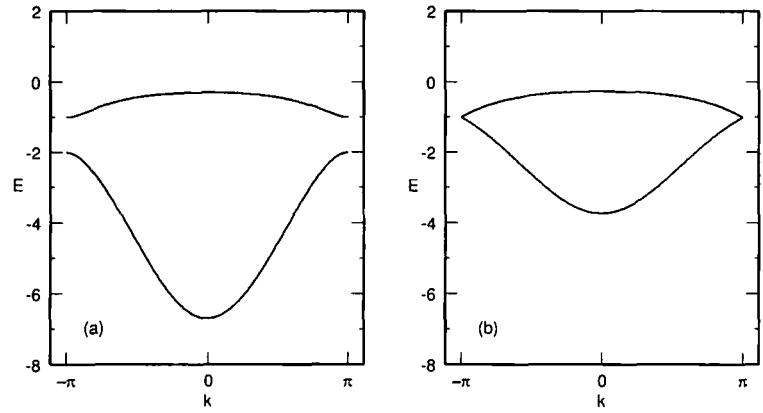

Fig. 8. The dispersion relations E_+ and E_-. (a) The parameters are $\lambda_1 = \lambda_2 = 1$. (b) The parameters are $\lambda_1 = \lambda_2 = 1/\sqrt{2}$.

representation (3.3), where an example of the valence-bond configuration V is shown in Fig. 9a. The geometric representation of the norm is (3.6), where an example of the graph $V \cup V'$ is shown in Fig. 9b. We first evaluate the contribution from a graph $V \cup V'$. It can be decomposed into the subgraphs $U_i \cup U_i'$ $[i = 1, 2, ..., n(V \cup V')]$. No loop extends over more than two cells and there is no p-site with four bonds, since the sites which are identified in the cell construction are d-sites. We do not need the procedures shown in Fig. 4. Therefore, the graph $U_i \cup U_i'$ cannot be decomposed further and we find $n(U_i \cup U_i') = 1$ in (3.7) and $m_j = 0$ in (3.11). The cells with the graph are classified into four kinds (Figs. 9g–9j). Consider the graph shown in Fig. 9g. From (3.10), the weight for the degenerate loop is 2 and the contribution from $\lambda(U_i')\,\lambda^*(U_i)$ in (3.11) is λ_2^2. Therefore, the contribution from the graph is $2\lambda_2^2$. For other graphs see the caption of Figs. 9g–9j.

The sum over the graph $V \cup V'$ in (3.6) is equivalent to that over all the combinations of the above four kinds of cells under the restriction that a d-site has at most two valence bonds. (The restriction means, for example, that the identification of the right d-site in Fig. 9g with the left d-site in Fig. 9i is forbidden.) Hereafter we shall always take into account the restriction and it should be understood implicitly. To evaluate the sum we use the transfer matrix method. We have to distinguish two cases due to the restriction. Let A_n and B_n be the quantity defined by the right-hand side of (3.6) on the lattice A_n. For A_n, the sum is taken over all the combination of the cells shown in Figs. 9g–9j with the restriction that the nth cell is represented by Fig. 9g or 9h. For B_n, the sum is taken as for A_n with

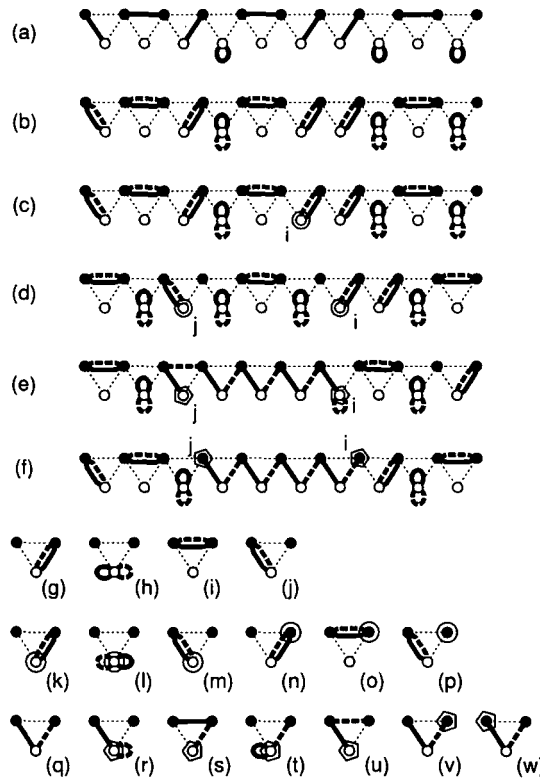

Fig. 9. Examples of configurations of valence bonds in the geometric representation for (a) the ground state, (b) the norm of the ground state, (c) the expectation value of the number operator $n^p_{i,\sigma}$, (d) the density correlation function for p-sites, (e) the correlation functions $\langle c^p_{i,\sigma} c^{p\dagger}_{j\sigma} \rangle$, and (f) the correlation function $\langle c^d_{i,\sigma} c^{d\dagger}_{j\sigma} \rangle$. (g)–(j) Configurations of the valence bonds on a cell in the geometric representation of the norm. The weights including the contributions from $\lambda(U)\,\lambda(U')$ are (g) $2\lambda_2^2$, (h) 1, (i) $2\lambda_1^2\lambda_2^2$, and (j) $2\lambda_1^2$. Configurations of the valence bonds on the ith cell in the geometric representation for (k–m) $\langle n^p_{i,\sigma} \rangle$ and (n–p) $\langle n^d_{i,\sigma} \rangle$. The weights including the contributions from $\lambda(U)\,\lambda(U')$ are (k) λ_2^2, (l) 1, (m) λ_1^2, (n) λ_2^2, (o) $\lambda_1^2\lambda_2^2$, and (p) λ_1^2. Configurations of the valence bonds on (q) the nth cell $(i+1 \leqslant n \leqslant j-1)$ in the geometric representation for $\langle c^\alpha_{i,\sigma} c^{\alpha\dagger}_{j,\sigma} \rangle$, and those on (r, s) the ith cell and (t, u) the jth cell for $\alpha = p$, and on (v) the ith cell and (w) the $(j-1)$th cell for $\alpha = d$. The contributions from $\lambda(U)\,\lambda(U')$ are (q) $\lambda_1\lambda_2$, (r) λ_1, (s) $\lambda_1\lambda_2^2$, (t) λ_2, (u) $\lambda_1^2\lambda_2$, (v) $\lambda_1\lambda_2$, and (w) $\lambda_1\lambda_2$.

the restriction that the nth cell is represented by Fig. 9c or 9d. They are represented diagrammatically as

$A_n =$ 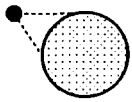 (4.9)

$B_n =$ 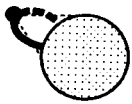 (4.10)

We note that the norm in the system size N is

$$\langle \Phi_{\text{G.S.}} | \Phi_{\text{G.S.}} \rangle = A_N + B_N \tag{4.11}$$

Given A_{n-1} and B_{n-1}, we can form A_n and B_n by attaching them to the nth cell. Let us consider A_n first. When the nth cell is represented by Fig. 9g, we can attach A_{n-1} and cannot attach B_{n-1}. When the nth cell is represented by Fig. 9h, we can attach A_{n-1} or B_{n-1} to it. Thus we have the recursion relation

$A_n =$ 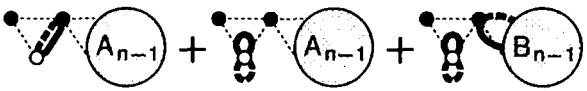

$$= 2\lambda_2^2 A_{n-1} + A_{n-1} + B_{n-1} \tag{4.12}$$

For B_n a similar calculation leads to

$B_n =$ 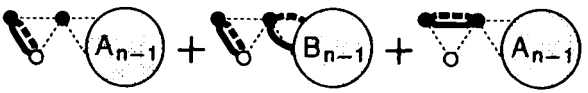

$$= 2\lambda_1^2 A_{n-1} + 2\lambda_1^2 B_{n-1} + 2\lambda_1^2 \lambda_2^2 A_{n-1} \tag{4.13}$$

They are conveniently written in matrix form as

$$\begin{pmatrix} A_n \\ B_n \end{pmatrix} = \mathsf{T}_n \begin{pmatrix} A_{n-1} \\ B_{n-1} \end{pmatrix}, \qquad \mathsf{T}_n = \begin{pmatrix} 1 + 2\lambda_2^2 & 1 \\ 2\lambda_1^2 + 2\lambda_1^2\lambda_2^2 & 2\lambda_1^2 \end{pmatrix} \tag{4.14}$$

The initial vector is $\mathbf{I} \equiv (A_0, B_0)^T = (1, 0)^T$, since any cell in Fig. 9g–9j is allowed as the first cell. To obtain the quantity (4.11), we choose the final vector $\mathbf{F} \equiv (A_N, B_N)^T = (1, 1)^T$. Since the transfer matrix is not symmetric,

it is convenient to diagonalize it using the right and left eigenvectors. The matrix can be diagonalized as

$$\mathsf{T}_n = \mathsf{R}\mathsf{D}\mathsf{R}^{-1} = \mathsf{L}^{-1}\mathsf{D}\mathsf{L} \tag{4.15}$$

where

$$\mathsf{D} = \begin{pmatrix} e_1 & 0 \\ 0 & e_2 \end{pmatrix}, \qquad \mathsf{R} = \begin{pmatrix} R_{11} & R_{12} \\ R_{21} & R_{22} \end{pmatrix}, \qquad \mathsf{L} = \begin{pmatrix} L_{11} & L_{12} \\ L_{21} & L_{22} \end{pmatrix} \tag{4.16}$$

where e_i are the eigenvalues of T_n, $e_1 = (2\lambda_1^2 + 2\lambda_2^2 + 1 + \omega_1)/2$, and $e_2 = (2\lambda_1^2 + 2\lambda_2^2 + 1 - \omega_1)/2$, with $\omega_1 = (4\lambda_1^4 + 4\lambda_2^4 + 4\lambda_1^2 + 4\lambda_2^2 + 1)^{1/2}$. They satisfy $e_1 > e_2 > 0$ for $\lambda_1 \neq 0$ and $\lambda_2 \neq 0$. We choose the left eigenvectors $\mathbf{L}_1 = (L_{11}, L_{12})^T$ and $\mathbf{L}_2 = (L_{21}, L_{22})^T$ corresponding to the eigenvalues e_1 and e_2, respectively, and the right eigenvectors $\mathbf{R}_1 = (R_{11}, R_{21})^T$ and $\mathbf{R}_2 = (R_{12}, R_{22})^T$. Using the diagonal matrix $\mathsf{C} = \mathsf{L}\mathsf{R}$, we obtain

$$\mathsf{T}_n = \mathsf{R}\mathsf{D}\mathsf{L}\mathsf{C}^{-1} \tag{4.17}$$

where

$$\mathsf{C} = \begin{pmatrix} c_1 & 0 \\ 0 & c_2 \end{pmatrix} \tag{4.18}$$

From these quantities, the norm of the ground state in the system size N is found to be

$$\begin{aligned} \langle \Phi^A_{\text{G.S.}} | \Phi^A_{\text{G.S.}} \rangle &= \mathbf{F}^T \mathsf{T}_N \cdots \mathsf{T}_2 \mathsf{T}_1 \mathbf{I} \\ &= \mathbf{F}^T \mathsf{R} \mathsf{D}^N \mathsf{L} \mathsf{C}^{-1} \mathbf{I} \\ &= \frac{1 + 2\lambda_1^2 + 2\lambda_2^2 + 4\lambda_1^2\lambda_2^2 + \omega_1}{2\omega_1} e_1^N \\ &\quad - \frac{1 + 2\lambda_1^2 + 2\lambda_2^2 + 4\lambda_1^2\lambda_2^2 - \omega_1}{2\omega_1} e_2^N \end{aligned} \tag{4.19}$$

where we used the relation $\mathsf{L}\mathsf{C}^{-1}\mathsf{R} = \mathsf{I}$, where I is the identity matrix. In the thermodynamic limit, the eigenvalue e_1 dominates and we have

$$\langle \Phi^A_{\text{G.S.}} | \Phi^A_{\text{G.S.}} \rangle = \frac{1 + 2\lambda_1^2 + 2\lambda_2^2 + 4\lambda_1^2\lambda_2^2 + \omega_1}{2\omega_1} \tag{4.20}$$

4.1.4. Expectation Value of the Number Operator. We calculate the occupation on a p-site $\langle n^p_{i,\sigma} \rangle$. The geometric representation of the expectation value is (3.29), where an example of the graph $V \cup V'$ is shown in Fig. 9c. We do not need the procedures shown in Fig. 4, because there is no site with four bonds. Therefore, we find $n(U_i \cup U_i') = 1$ in (3.27) and $m_j = 0$ in (3.30). In the representation, the operator $n^p_{i,\sigma}$ modifies the weight associated with the graph which contains the ith cell. Therefore, we replace the transfer matrix T_i by $\mathsf{N}_i^{(p)}$, which is a matrix associated with the operator $n^p_{i,\sigma}$. The expectation value can be written

$$\langle \Phi^A_{\text{G.S.}} | \, n^p_{i,\sigma} \, | \Phi^A_{\text{G.S.}} \rangle = \mathbf{F}^T \mathsf{T}_N \cdots \mathsf{T}_{i+1} \mathsf{N}_i^{(p)} \mathsf{T}_{i-1} \cdots \mathsf{T}_1 \mathbf{I} \tag{4.21}$$

We derive the matrix $\mathsf{N}_i^{(p)}$. We have three kinds of graphs on the ith cell (Figs. 9k–9m). Let $A_i^{(p)}$ and $B_i^{(p)}$ be the quantity defined by the right-hand side of (3.29) on the lattice Λ_i. The restriction for the sum is that the ith cell is represented either by Fig. 9k or (l) for $A_i^{(p)}$ and by (m) for $B_i^{(p)}$. They are represented diagrammatically as

$A_i^{(p)} =$ 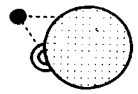 (4.22)

$B_i^{(p)} =$ 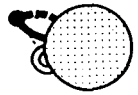 (4.23)

and the recursion relations are

$A_i^{(p)} =$ 

$$= \lambda_2^2 A_{i-1} + A_{i-1} + B_{i-1} \tag{4.24}$$

$B_i^{(p)} =$ 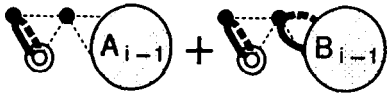

$$= \lambda_1^2 A_{i-1} + \lambda_1^2 B_{i-1} \tag{4.25}$$

From (3.28) the loop with operator $n_{i,\sigma}$ has weight 1. It is written as

$$\begin{pmatrix} A_i^{(p)} \\ B_i^{(p)} \end{pmatrix} = \mathsf{N}_i^{(p)} \begin{pmatrix} A_{i-1} \\ B_{i-1} \end{pmatrix}, \qquad \mathsf{N}_i^{(p)} = \begin{pmatrix} 1+\lambda_2^2 & 1 \\ \lambda_1^2 & \lambda_1^2 \end{pmatrix} \tag{4.26}$$

From (4.51), (4.52), (4.19), and (4.26), we have

$$\begin{aligned}\langle n^p_{i,\sigma}\rangle &= \frac{\mathbf{F}^T\mathsf{T}^{N-i}\mathsf{N}_i^{(p)}\mathsf{T}^{i-1}\mathbf{I}}{\mathbf{F}^T\mathsf{T}^N\mathbf{I}} \\ &= \frac{\mathbf{F}^T\mathsf{R}\mathsf{D}^{N-i}\mathsf{L}\mathsf{C}^{-1}\mathsf{N}_i^{(p)}\mathsf{R}\mathsf{D}^{i-1}\mathsf{L}\mathsf{C}^{-1}\mathbf{I}}{\mathbf{F}^T\mathsf{R}\mathsf{D}^N\mathsf{C}^{-1}\mathsf{L}\mathbf{I}} \\ &= \frac{C_1 - C_2(e_2/e_1)^i - C_3(e_2/e_1)^{N-i} + C_4(e_2/e_1)^N}{\frac{1}{2}\omega_1\{[(1+2\lambda_1^2)(1+2\lambda_2^2)+\omega_1] \\ &\qquad -[(1+2\lambda_1^2)(1+2\lambda_2^2)-\omega_1](e_2/e_1)^N\}}\end{aligned} \tag{4.27}$$

where

$$\begin{aligned}C_1 &= (e_1-2\lambda_1^2)(e_1-2\lambda_2^2)(e_1-\lambda_1^2-\lambda_2^2) \\ C_2 &= (e_1-2\lambda_2^2)(e_2-2\lambda_1^2)(e_1e_2-\lambda_2^2e_1-\lambda_1^2e_2)/e_2 \\ C_3 &= (e_1-2\lambda_1^2)(e_2-2\lambda_2^2)(e_1e_2-\lambda_2^1e_1-\lambda_1^2e_2)/e_1 \\ C_4 &= (e_2-2\lambda_1^2)(e_2-2\lambda_2^2)(e_2-2\lambda_1^2-2\lambda_2^2)\end{aligned}$$

in the system size N. In the thermodynamic limit, N, i, $N-i\to\infty$, we obtain

$$\langle n^p_{i,\sigma}\rangle = \frac{1}{2}\left(1+\frac{1}{\omega_1}\right) \tag{4.28}$$

Since there are two electrons in a unit cell, from (4.28) we have the occupation on a d-site

$$\langle n^d_{i,\sigma}\rangle = \frac{1}{2}\left(1-\frac{1}{\omega_1}\right) \tag{4.29}$$

We can also obtain the same quantity from the geometric representation of the expectation value. From the graphs shown in Figs. 9n–9p we have the matrix associated with the operator $n^d_{i,\sigma}$:

$$\mathsf{N}_i^{(d)} = \begin{pmatrix} \lambda_2^2 & 0 \\ \lambda_1^2\lambda_2^2 & \lambda_1^2 \end{pmatrix} \tag{4.30}$$

which will be used to obtain the density correlation function.

The results are shown in Figs. 10a and 10b for $\alpha = p$ and d, respectively. We consider the following cases: (i) $\lambda_1, \lambda_2 \gg 1$ $(\lambda_1 = \lambda_2)$; (ii) $|\lambda_1|$,

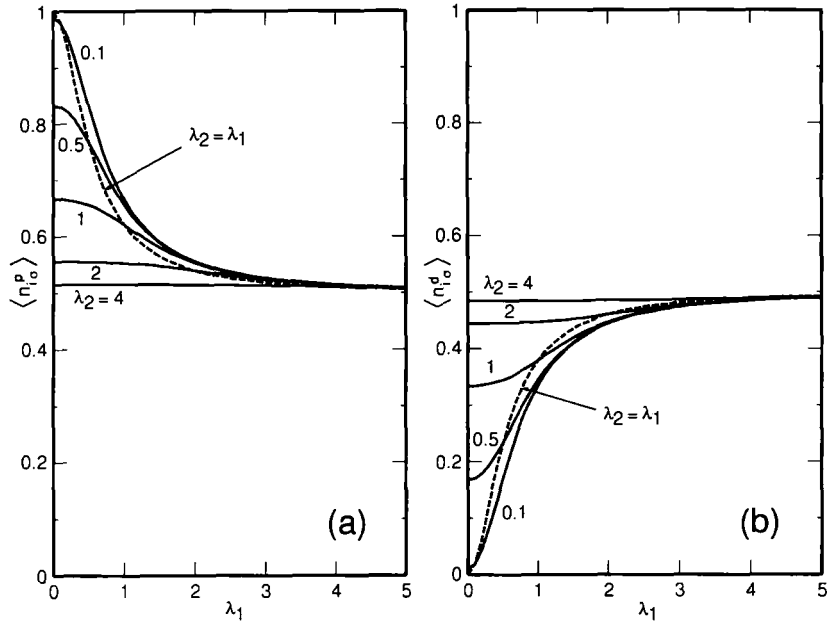

Fig. 10. Occupation on (a) the p-site and (b) the d-site for $\lambda_2=0.1$, 0.5, 1, 2, and 4 (solid lines) and $\lambda_2=\lambda_1$ (broken line).

$|\lambda_2| \ll 1$ ($\lambda_1=\lambda_2$); and (iii) $|\lambda_1| \ll 1$, $\lambda_2 \gg 1$. For (i), on-site potentials satisfy the relation $\varepsilon_d \ll \varepsilon_p$. There is almost one electron per site. For (ii), on-site potentials satisfy the relation $\varepsilon_p < \varepsilon_d$, $\varepsilon_d - \varepsilon_p \gg \lambda_1\lambda_2$. The d-sites are almost empty. The p-sites are almost doubly occupied. For (iii), the system decouples to a collection of pairs of p- and d-sites.

4.1.5. Two-Point Correlation Functions. We calculate the density correlation function for the p-site. We first evaluate the first term in (3.31). The geometric representation of the expectation value is (3.36), where an example of the graph $V \cup V'$ is shown in Fig. 9d. We do not need the procedures shown in Fig. 4, because there is no site with four bonds. Therefore, we find $n(U_i \cup U_i')=1$ in (3.15) and $m_j=0$ in (3.37). In the representation, the operators modify the weight associated with the graph which contains cells between the cells i and j. From the derivation of the matrix $\mathsf{N}_i^{(p)}$, the expectation value is

$$D(x, y; \sigma) = \mathbf{F}^T \mathsf{T}_N \cdots \mathsf{T}_{j+1} \mathsf{N}_j^{(p)} \mathsf{T}_{j-1} \cdots \mathsf{T}_{i+1} \mathsf{N}_i^{(p)} \mathsf{T}_{i-1} \cdots \mathsf{T}_1 \mathbf{I} \quad (4.31)$$

From (4.26) and (4.31), the first term in the right-hand side of (3.31) is

$$\begin{aligned}
&\frac{D(x, y; \sigma)}{\langle \Phi_{\text{G.S.}} | \Phi_{\text{G.S.}} \rangle} \\
&\quad = \frac{\mathbf{F}^T \mathsf{T}_N \mathsf{T}_{N-1} \cdots \mathsf{T}_{j+1} \mathsf{N}_j^{(p)} \mathsf{T}_{j-1} \cdots \mathsf{T}_{i+1} \mathsf{N}_i^{(p)} \mathsf{T}_{i-1} \cdots \mathsf{T}_1 \mathbf{I}}{\mathbf{F}^T \mathsf{T}^N \mathbf{I}} \\
&\quad = \left[C_1 - C_2 \left(\frac{e_2}{e_1}\right)^i + C_3 \left(\frac{e_2}{e_1}\right)^j - C_4 \left(\frac{e_2}{e_1}\right)^{j-i} \right. \\
&\qquad \left. + C_5 \left(\frac{e_2}{e_1}\right)^{N-j+i} - C_6 \left(\frac{e_2}{e_1}\right)^{N-j} + C_7 \left(\frac{e_2}{e_1}\right)^{N-i} - C_8 \left(\frac{e_2}{e_1}\right)^N \right] \\
&\qquad \times \left(\frac{\omega_1^2}{2} \left\{ [(1+2\lambda_1^2)(1+2\lambda_2^2) + \omega_1] \right. \right. \\
&\qquad \left. \left. - [(1+2\lambda_1^2)(1+2\lambda_2^2) - \omega_1] \left(\frac{e_2}{e_1}\right)^N \right\} \right)^{-1}
\end{aligned} \tag{4.32}$$

where

$$\begin{aligned}
C_1 &= (e_1 - 2\lambda_1^2)(e_1 - 2\lambda_2^2)(\lambda_1^2 + \lambda_2^2 - e_1) \\
C_2 &= (e_1 - 2\lambda_2^2)(e_2 - 2\lambda_1^2)(\lambda_1^2 + \lambda_2^2 - e_1)(\lambda_2^2 e_1 + \lambda_1^2 e_2 - e_1 e_2)/e_2 \\
C_3 &= (e_1 - 2\lambda_1^2)(e_2 - 2\lambda_2^2)(\lambda_1^2 + \lambda_2^2 - e_2)(\lambda_2^2 e_1 + \lambda_1^2 e_2 - e_1 e_2)/e_2 \\
C_4 &= (e_1 - 2\lambda_1^2)(e_1 - 2\lambda_2^2)(\lambda_1^2 e_1 + \lambda_2^2 e_2 - e_1 e_2) \\
&\qquad \times (e_1 e_2 - \lambda_2^2 e_1 - \lambda_1^2 e_2)/(e_1 e_2) \\
C_5 &= (e_2 - 2\lambda_1^2)(e_2 - 2\lambda_2^2)(\lambda_2^2 e_1 + \lambda_1^2 e_2 - e_1 e_2) \\
&\qquad \times (e_1 e_2 - \lambda_1^2 e_1 - \lambda_2^2 e_2)/(e_1 e_2) \\
C_6 &= (e_1 - 2\lambda_1^2)(e_2 - 2\lambda_2^2)(\lambda_1^2 + \lambda_2^2 - e_1)(\lambda_1^2 e_1 + \lambda_2^2 e_2 - e_1 e_2)/e_1 \\
C_7 &= (e_1 - 2\lambda_1^2)(e_2 - 2\lambda_2^2)(\lambda_1^2 + \lambda_2^2 - e_2)(\lambda_1^2 e_1 + \lambda_2^2 e_2 - e_1 e_2)/e_1 \\
C_8 &= (e_2 - 2\lambda_1^2)(e_2 - 2\lambda_2^2)(\lambda_1^2 + \lambda_2^2 - e_2)
\end{aligned}$$

in the system size N. In the thermodynamic limit $N-j,\ i \to \infty$ keeping $|j-i|$ finite, we have

$$\begin{aligned}
\frac{D(x, y; \sigma)}{\langle \Phi_{\text{G.S.}} | \Phi_{\text{G.S.}} \rangle} &= \left[\frac{1}{2} \left(\frac{1}{\omega_1} + 1 \right) \right]^2 \\
&\quad - \left(\frac{e_2}{e_1}\right)^{-|i-j|} \frac{\lambda_1^2 \lambda_2^2 [1 + 2(\lambda_1^2 + \lambda_2^2 + \lambda_1^4 + \lambda_2^4)]}{e_1^2 \omega_1^2}
\end{aligned} \tag{4.33}$$

From (4.28), the first term in the right-hand side cancels out with the last term in (3.31). We obtain

$$\langle n_i^p n_j^p \rangle - \langle n_i^p \rangle \langle n_j^p \rangle = -\left(\frac{e_2}{e_1}\right)^{-|i-j|} \frac{4\lambda_1^2 \lambda_2^2 [1 + 2(\lambda_1^2 + \lambda_2^2 + \lambda_1^4 + \lambda_2^4)]}{e_1^2 \omega_1^2} \tag{4.34}$$

For the d-site, a similar calculation leads to

$$\langle n_i^d n_j^d \rangle - \langle n_i^d \rangle \langle n_j^d \rangle = -\left(\frac{e_2}{e_1}\right)^{-|i-j|} \frac{4\lambda_1^2 \lambda_2^2}{(e_1 + e_2)\omega_1} \tag{4.35}$$

The density correlation functions take negative values and decay exponentially with distance. We show the results in Figs. 11a and 11b. For the parameter region (i) identified at the end of Section 4.1.4, the density correlation between p-sites is enhanced and that between d-sites is suppressed. For (ii) and (iii), they are suppressed.

Since we have no nondegenerate loop, the spin correlation functions $\langle S_i^z S_j^z \rangle$ are vanishing for $|j-i| \geqslant 2$. Since we have no self-closed bond at the sites where the adjacent cells are identified, $\langle b_{i,j}^\dagger b_{k,l} \rangle$ is vanishing for $|k-i| \geqslant 1$.

We evaluate the correlation function $\langle c_{i,\sigma}^p c_{j,\sigma}^{p\dagger} \rangle$. The geometric representation of the expectation value is (3.23), where an example of the graph $V \cup V'$ is shown in Fig. 9e. We do not need the procedures shown in Fig. 4, because there is no site with four bonds. Therefore, we find $n(U_i \cup U_i') = 1$ in (3.15) and $m_j = 0$ in (3.24). In the representation, the operators modify the weight associated with the graph(s) which contains the cells between i and j. Let the transfer matrix associated with the operator $c_{i,\sigma}^p$ ($c_{j,\sigma}^{p\dagger}$) be $\mathsf{G}_i^{R,(p)}$ ($\mathsf{G}_j^{L,(p)}$). We need a new matrix G_n for the nth cell ($i+1 \leqslant n \leqslant j-1$). From these matrices the expectation value can be written

$$\langle c_{i,\sigma}^p c_{j,\sigma}^{p\dagger} \rangle = \mathbf{F}^T \mathsf{T}_N \cdots \mathsf{T}_{j+1} \mathsf{G}_j^{L,(p)} \mathsf{G}_{j-1} \cdots \mathsf{G}_{i+1} \mathsf{G}_i^{R,(p)} \mathsf{T}_{i-1} \cdots \mathsf{T}_1 \mathbf{I} \tag{4.36}$$

We derive the matrices. We first consider the matrix G_n. It is reduced to a number, because we have only one kind of graph (a line) on the nth cell ($i+1 \leqslant n \leqslant j-1$) (Fig. 9q). Let G_n be the quantity defined by a sum. The sum is taken over $V \cup V'$ on the lattice Λ_n such that the graph consists of loops shown in Figs. 9g–9j on the kth cell ($1 \leqslant k \leqslant i-1$) and the line shown in Fig. 9q on the nth cell ($i \leqslant n \leqslant j$). A line with $2n$ bonds is on n cells, since a cell has two valence bonds. The weight for the line is $(-1)^n$.

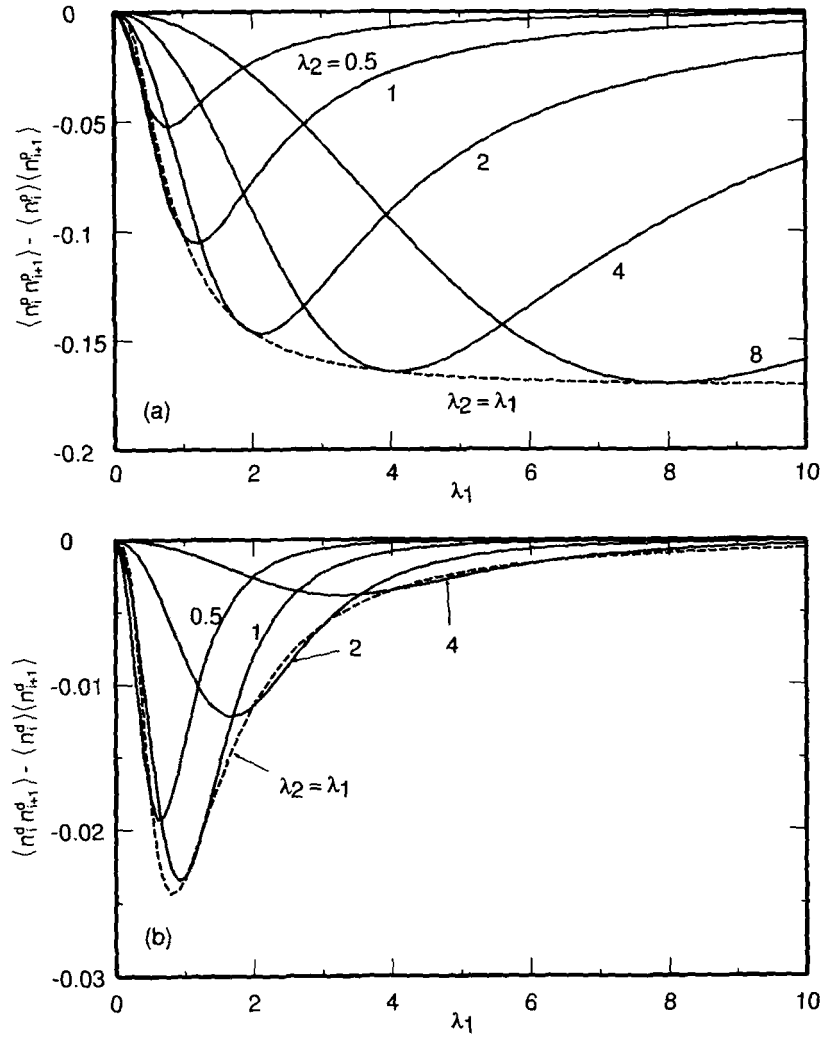

Fig. 11. (a) Density correlation function for the nearest neighbor p-sites for $\lambda_2 = 0.5$, 1, 2, 4, and 8 (solid lines) and $\lambda_2 = \lambda_1$ (broken line). (b) That for the nearest neighbor d-sites for $\lambda_2 = 0.5$, 1, 2, and 4 (solid lines) and $\lambda_2 = \lambda_1$ (broken line).

We assign -1 to each n cells. In this way, the weight (3.22) is automatically taken into account. They are represented diagrammatically as

$G_n =$ 

$=$ 

$$= -\lambda_1 \lambda_2 G_{n-1} \tag{4.37}$$

We have

$$G_n = -\lambda_1 \lambda_2 \tag{4.38}$$

For the matrix $G_i^{(p)}$, let $G_i^{R,(p)}$ be the quantity defined by a sum. The sum is taken over $V \cup V'$ on the lattice Λ_i such that the graph consists of loops shown in Figs. 9g–9j on the kth cell $(1 \leqslant k \leqslant i-1)$ and the graph shown in Fig. 9r or 9s on the ith cell. The recursion relation is

$G_i^{(p)} =$ 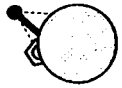

$=$ 

$$= \lambda_1 A_{i-1} + \lambda_1 B_{i-1} + \lambda_1 \lambda_2^2 A_{i-1} \tag{4.39}$$

and is written

$$G_i^{(p)} = \mathsf{G}_i^{R,(p)} \begin{pmatrix} A_{j-1} \\ B_{j-1} \end{pmatrix}, \qquad \mathsf{G}_i^{R,(p)} = (\lambda_1 + \lambda_1 \lambda_2^2, \lambda_1) \tag{4.40}$$

For $\mathsf{G}_j^{L,(p)}$, let $A_j^{(p)}$ and $B_j^{(p)}$ be the quantity defined by the right-hand side of (3.23) on the lattice Λ_j. The sum is taken over the graph $V \cup V'$ such that the graph consists of loops shown in Figs. 9g–9j on the kth cell $(1 \leqslant k \leqslant i-1)$ and the graph shown in Fig. 9q on the lth cell $(i \leqslant l \leqslant j)$. The

restriction for the sum is that the jth cell is represented by either Fig. 9t for $A_j^{(p)}$ or 9u for $B_j^{(p)}$. The recursion relations are

$A_j^{(p)} =$ 

$$= \lambda_2 G_{j-1} \tag{4.41}$$

$B_j^{(p)} =$ 

$$= \lambda_1^2 \lambda_2 G_{j-1} \tag{4.42}$$

and are written

$$\begin{pmatrix} A_j^{(p)} \\ B_j^{(p)} \end{pmatrix} = \mathsf{G}_j^{L,(p)} G_{j-1}, \qquad \mathsf{G}_j^{L,(p)} = \begin{pmatrix} \lambda_2 \\ \lambda_1^2 \lambda_2 \end{pmatrix} \tag{4.43}$$

From (4.19), (4.36), (4.38), (4.40), and (4.43) we obtain

$$\begin{aligned} &\langle c_{i,\sigma}^p c_{j,\sigma}^{p\dagger} \rangle \\ &\quad = \frac{\mathbf{F}^T \mathsf{T}^{N-j} \mathsf{G}_j^{L,(p)} \mathsf{G}^{j-i-1} \mathsf{G}_i^{R,(p)} \mathsf{T}^{i-1} \mathbf{I}}{\mathbf{F}^T \mathsf{T}^N \mathbf{I}} \\ &\quad = -(-\lambda_1 \lambda_2)^{j-i} \\ &\qquad \times \frac{C_1 (1/e_1)^{j-i-1} - C_2 (e_2/e_1)^{i-1} - C_3 (e_2/e_1)^{N-j} + C_4 (e_2/e_1)^N}{\omega_1 \{ [(1+2\lambda_1^2)(1+2\lambda_2^2) + \omega_1] \\ &\qquad\qquad - [(1+2\lambda_1^2)(1+2\lambda_2^2) - \omega_1](e_2/e_1)^N \}} \end{aligned} \tag{4.44}$$

where

$$\begin{aligned} C_1 &= (e_1 - 2\lambda_1^2)(e_1 - \lambda_1^2)(e_1 - 2\lambda_2^2)(e_1 - \lambda_2^2)/e_1 \\ C_2 &= (e_1 - \lambda_1^2)(e_1 - 2\lambda_2^2)(e_2 - 2\lambda_1^2)(e_2 - \lambda_2^2)/e_1^{j-i+1} \\ C_3 &= (e_1 - 2\lambda_1^2)(e_1 - \lambda_2^2)(e_2 - \lambda_1^2)(e_2 - 2\lambda_2^2)/e_1^{j-i+1} \\ C_4 &= (e_1 - 2\lambda_1^2)(e_1 - \lambda_1^2)(e_1 - 2\lambda_2^2)(e_1 - \lambda_2^2)/e_2^{j-i+1} \end{aligned}$$

in the system size N. In the thermodynamic limit $N-j,\ i \to \infty$ keeping $|j-i|$ finite, we obtain

$$\langle c_{i,\sigma}^p c_{j,\sigma}^{p\dagger} \rangle = -\left(-\frac{\lambda_1 \lambda_2}{e_1} \right)^{-|i-j|} \frac{(2\lambda_1^2 + 1 + \omega_1)(2\lambda_2^2 + 1 + \omega_1)}{4 e_1 \omega_1} \tag{4.45}$$

Next, we evaluate the correlation function $\langle c^d_{i,\sigma} c^{d\dagger}_{j,\sigma} \rangle$. We show an example of the graph $V \cup V'$ in Fig. 9f. (We have only one kind of line.) Using the graph of the ends of the line (Figs. 9v and 9w), we find for the matrices in (4.36)

$$\mathsf{G}_i^{R,(d)} = (-\lambda_1 \lambda_2, 0), \qquad \mathsf{G}_j^{L,(d)} = \begin{pmatrix} 1 \\ 2\lambda_1^2 \end{pmatrix} \tag{4.46}$$

From these matrices we obtain

$$\langle c^d_{i,\sigma} c^{d\dagger}_{j,\sigma} \rangle = \frac{1}{\omega_1} \left(-\frac{\lambda_1 \lambda_2}{e_1} \right)^{-|i-j|} \tag{4.47}$$

The correlation functions decay exponentially with the oscillating sign.

For a finite lattice under open boundary condition, the system is not translational invariant. In the thermodynamic limit, however, by the Fourier transformation of the correlation function $\langle c_{i,\sigma} c^\dagger_{j,\sigma} \rangle$, we obtain the momentum distribution function[6] for $\alpha = p, d$

$$\langle n^\alpha_{k,\sigma} \rangle = f^{(\alpha)} F(k, r) + f_0^{(\alpha)} \tag{4.48}$$

where $f_0^{(\alpha)} = \langle n^\alpha_{i,\sigma} \rangle$ and

$$F(k, r) = \frac{2r[\cos k - r]}{1 + r^2 - 2r \cos k} \tag{4.49}$$

where

$$f^{(p)} = -(2\lambda_1^2 + 1 + \omega_1)(2\lambda_2^2 + 1 + \omega_1)/4 e_1 \omega_1$$
$$f^{(d)} = 1/\omega_1, \qquad r = -\lambda_1 \lambda_2 / e_1$$

The results are shown in Figs. 12. There is no singularity in $\langle n^\alpha_{k,\sigma} \rangle$. For the parameter range (i) in Section 4.1.4, the momentum distribution for the d-site is completely flat, while that for the p-site has a broad peak around $k = 0$. For (ii), the momentum distribution for the p-site is almost unity for every k and is completely flat, while that for the d-site is almost zero. For (iii), both of them are completely flat.

4.1.6. Discussion. All the correlation functions under consideration decay exponentially with distance. These results suggest the existence of a finite excitation gap. Therefore, it is expected that the state is not metallic but rather insulating. The correlation lengths are given by $\xi_{nn} = [\ln(e_2/e_1)]^{-1}$

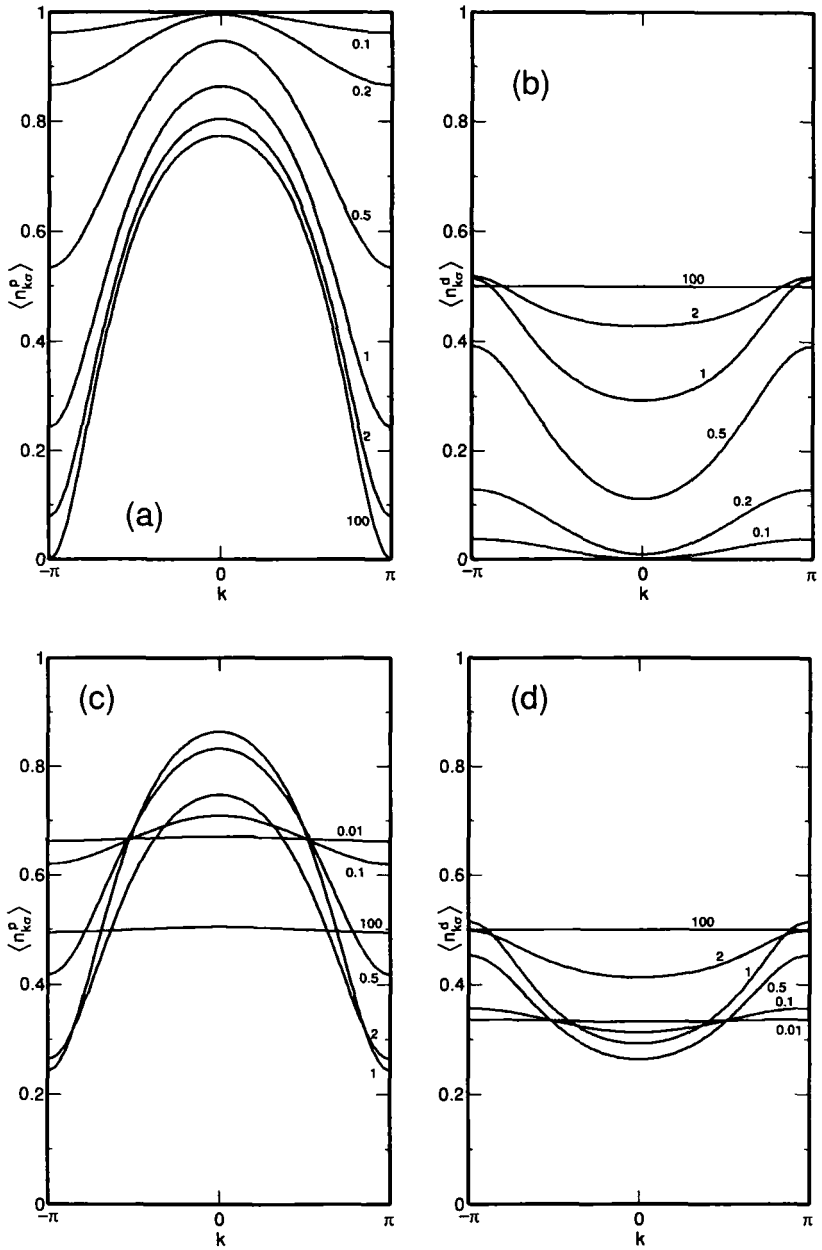

Fig. 12. Momentum distribution functions for (a) the p-site and (b) the d-site for $\lambda_1 = \lambda_2 = 0.1$, 0.2, 0.5, 1, 2, and 100, and those for (c) the p-site and (d) the d-site for $\lambda_2 = 0.01$, 0.1, 0.5, 1, 2, and 100 with $\lambda_1 = 1$.

for the density correlation functions and $\xi_{cc}=[\ln(\lambda_1\lambda_2/e_1)]^{-1}$ for the correlation functions $\langle c^{\alpha}_{i,\sigma}c^{\beta\dagger}_{j,\sigma}\rangle$ (Fig. 13). The correlation lengths of the correlation between p-sites and that between d-sites are the same. The spin correlation functions vanish for $|j-i|\geqslant 2$. The singlet-pair correlation functions vanish for any $|j-i|$.

We consider the limit $|\lambda_1|, |\lambda_2|\ll 1$ $(\lambda_1=\lambda_2)$. We obtain $\xi_{nn}, \xi_{cc}=0$. The density correlation functions for the nearest neighbor sites vanish. The ground state is described by a collection of the decoupled p-sites which are doubly occupied.

We consider the limit $\lambda_1, \lambda_2\gg 1$ $(\lambda_1=\lambda_2)$. The correlation length converges to a finite value:

$$\xi_{nn}=\left[\ln\left(\frac{2-\sqrt{2}}{2+\sqrt{2}}\right)\right]^{-1} \quad \text{and} \quad \xi_{cc}=\left[\ln\left(\frac{1}{4+2\sqrt{2}}\right)\right]^{-1}$$

The density correlation function for the nearest neighbor p-sites remains finite, while that for the nearest neighbor d-sites vanishes. Since there is almost one electron per site, the correlation between d-sites is suppressed and that between p-sites is enhanced.

For $|\lambda_1|\ll 1$ and $\lambda_2\gg 1$ the correlations are suppressed. This is because the system decouples to a collection of pairs of p- and d-sites.

The ground state (4.3) is a half-filling state. In the noninteracting system, the filling factor corresponds to that of a metallic state at $2\lambda_1\lambda_2-1=0$ and that of a band insulator for $2\lambda_1\lambda_2-1\neq 0$. Therefore, we

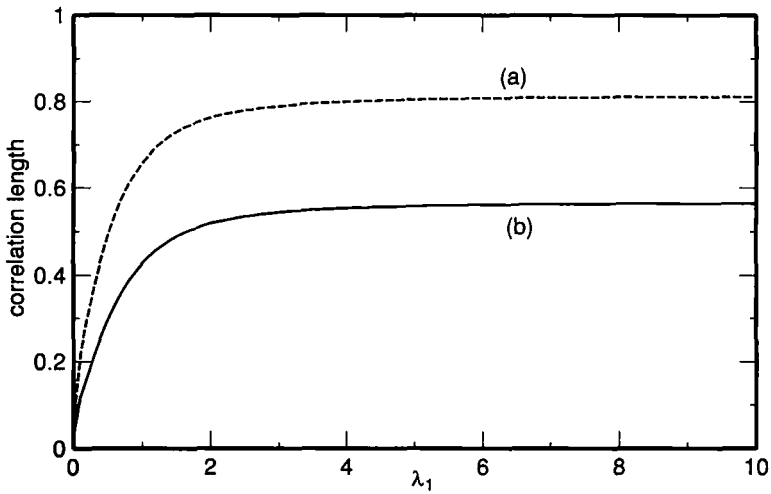

Fig. 13. Correlation length of (a) the correlation function $\langle c_{i,\sigma}c^{\dagger}_{j,\sigma}\rangle$ and (b) the density correlation function for $\lambda_1=\lambda_2$.

have a metal–insulator transition when λ_1, λ_2 are fixed to satisfy $2\lambda_1\lambda_2 - 1 = 0$, and the on-site Coulomb interaction U on d-sites is varied from 0 to ∞. In the noninteracting system, the correlation length, which is proportional to the inverse of the energy gap, takes a finite value for $|\lambda_1|$, $|\lambda_2| \ll 1$, it diverges when $2\lambda_1\lambda_2 - 1 = 0$, and it goes to zero for $\lambda_1, \lambda_2 \gg 1$. These properties are completely different from those of the ground state (4.3).

4.2. Notation of the Transfer Matrices

In order to present the calculations in latter models efficiently, we fix some notations. From the derivation in Section (4.1.3), the norm of the ground state can be generally written

$$\langle \Phi_{\text{G.S.}} | \Phi_{\text{G.S.}} \rangle = \mathbf{F}^T \mathsf{T}_N \cdots \mathsf{T}_2 \mathsf{T}_1 \mathbf{I} \tag{4.50}$$

where the matrices depend on the model under consideration.

We describe the expectation value of a local operator $\mathcal{O}_i$ by using the transfer matrices. In the geometric representation, when there is an operator $\mathcal{O}_i$ the weight associated with the graph which contains the ith cell is modified. Therefore, we replace the transfer matrix T_i by O_i, which is a matrix associated with the operator $\mathcal{O}_i$. The expectation value is written

$$\langle \Phi_{\text{G.S.}} | \mathcal{O}_i | \Phi_{\text{G.S.}} \rangle = \mathbf{F}^T \mathsf{T}_N \cdots \mathsf{T}_{i+1} \mathsf{O}_i \mathsf{T}_{i-1} \cdots \mathsf{T}_1 \mathbf{I} \tag{4.51}$$

When $\mathcal{O}_i$ is the number operator $n^{\alpha}_{i,\sigma}$, where $\alpha = d$ (p) for a p (d)-site, let the corresponding matrix be

$$\mathsf{O}_i = \mathsf{N}_i^{(\alpha)} \tag{4.52}$$

For the two-point correlation function $\langle \mathcal{O}_i^R \mathcal{O}_j^L \rangle$, the weight associated with the graph which contains the cells between i and j is modified. Let P_k be the transfer matrix between the sites $i+1$ and $j-1$, and O_i^R (O_j^L) be the matrix associated with the operator $\mathcal{O}_i^R$ ($\mathcal{O}_j^L$). We have

$$\langle \Phi_{\text{G.S.}} | \mathcal{O}_i^R \mathcal{O}_j^L | \Phi_{\text{G.S.}} \rangle = \mathbf{F}^T \mathsf{T}_N \mathsf{T}_{N-1} \cdots \mathsf{T}_{j+1} \mathsf{O}_j^L \mathsf{P}_{j-1} \cdots \mathsf{P}_{i+1} \mathsf{O}_i^R \mathsf{T}_{i-1} \cdots \mathsf{T}_1 \mathbf{I} \tag{4.53}$$

We use the following notations:

$\mathsf{P}_k = \mathsf{T}_k$,	$\mathsf{O}_i^R = \mathsf{N}_i^{(\alpha)}$,	$\mathsf{O}_j^L = \mathsf{N}_j^{(\alpha)}$	for $D(i, j; \sigma)$ in (3.32)
$\mathsf{P}_k = \mathsf{S}_k$,	$\mathsf{O}_i^R = \mathsf{S}_i^{R,(\alpha)}$,	$\mathsf{O}_j^L = \mathsf{S}_j^{L,(\alpha)}$	for spin correlation function

$$\mathsf{P}_k = \mathsf{H}_k, \quad \mathsf{O}_i^R = \mathsf{H}_i^{R,(\gamma)}, \quad \mathsf{O}_j^L = \mathsf{H}_j^{L,(\gamma)} \quad \text{for singlet-pair correlation function}$$

$$\mathsf{P}_k = \mathsf{G}_k, \quad \mathsf{O}_i^R = \mathsf{G}_i^{R,(\alpha)}, \quad \mathsf{O}_j^L = \mathsf{G}_j^{L,(\alpha)} \quad \text{for correlation function } \langle c_{i,\sigma} c_{j,\sigma}^\dagger \rangle \tag{4.54}$$

For the singlet-pair correlation function $\langle b_{i,j}^\dagger b_{k,l} \rangle$, we distinguish the following four cases by γ:

$$\begin{aligned} &\text{(i)} \quad \gamma = p \qquad \text{sites } i \text{ an d } j \text{ are } p\text{-sites and } i = j \\ &\text{(ii)} \quad \gamma = pp \qquad \text{sites } i \text{ and } j \text{ are } p\text{-sites and } i \neq j \\ &\text{(iii)} \quad \gamma = pd \qquad \text{site } i \text{ is } p\text{-site and site } j \text{ is } d\text{-site} \\ &\text{(iv)} \quad \gamma = dd \qquad \text{sites } i \text{ and } j \text{ are } d\text{-sites} \end{aligned} \tag{4.55}$$

We can evaluate multipoint correlation functions for operators which are constructed from fermion operators. The numerator of the correlation function is obtained by the insertion of the transfer matrices which are associated with the operators.

4.3. Model B

4.3.1. Hamiltonian. Model B is constructed from a cell with two p-sites and one d-site (Fig. 14a). This is one of the models of Strack[3] which was studied by Bares and Lee.[6] The cell Hamiltonian (2.2) is obtained by choosing

$$\alpha_{n,\sigma}^{(B)} = \sum_{r=1}^{3} \lambda_r c_{r,\sigma} \equiv \lambda_1 c_{1,\sigma}^p + \lambda_2 c_{2,\sigma}^p + \lambda_3 c_{3,\sigma}^d$$

in (2.3) and setting $\lambda_3 = 1$ without loss of generality (see Fig. 14a for the intracell index). The full Hamiltonian is obtained by identifying site 1 in the $(n-1)$th cell with site 2 in the nth cell (Fig. 14b). The Hamiltonian is

$$H_S = \mathscr{P} \sum_{\sigma=\uparrow,\downarrow} \left\{ \sum_{n=1}^{N} [(-\lambda_1 \lambda_2 c_{n+1,\sigma}^{p\dagger} c_{n,\sigma}^p - \lambda_1 c_{n+1,\sigma}^{p\dagger} c_{n,\sigma}^d - \lambda_2 c_{n,\sigma}^{p\dagger} c_{n,\sigma}^d + \text{h.c.}) + \varepsilon_n^p c_{n,\sigma}^{p\dagger} c_{n,\sigma}^p + \varepsilon^d c_{n,\sigma}^{d\dagger} c_{n,\sigma}^d] + \varepsilon_{N+1}^p c_{N+1,\sigma}^{p\dagger} c_{N+1,\sigma}^p \right\} \mathscr{P} \tag{4.56}$$

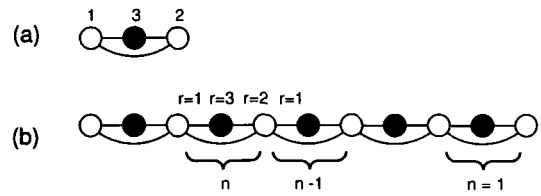

Fig. 14. Model B. (a) A cell composed of two p-sites ($U=0$) and one d-site ($U=\infty$). (b) The lattice constructed from the cell with cell labelings.

where the on-site potentials are $\varepsilon_1^p = -\lambda_2^2$, $\varepsilon_n^p = -(\lambda_1^2+\lambda_2^2)$ $(2 \leqslant n \leqslant N)$, $\varepsilon_{N+1}^p = -\lambda_1^2$, and $\varepsilon^d = -2$. A unit cell is labeled by n. The ground state is

$$|\Phi_{\text{G.S.}}^B\rangle = \mathscr{P} \prod_{n=1}^{N} \prod_{\sigma=\uparrow,\downarrow} \alpha_{n,\sigma}^{(B)\dagger} |0\rangle$$

$$= \mathscr{P} \prod_{n=1}^{N} \prod_{\sigma=\uparrow,\downarrow} (\lambda_1 c_{n,\sigma}^{p\dagger} + \lambda_2 c_{n+1,\sigma}^{p\dagger} + c_{n,\sigma}^{d\dagger}) |0\rangle \qquad (4.57)$$

which is a half-filled state. In the parameter space $\lambda_2 = -\lambda_1$, this model reduces to one of the models in ref. 3. The model in ref. 6 is recovered by setting $\lambda_1 = -\lambda_2 = \tilde{V}^{-1}$.

4.3.2. Band Structure in the Single-Electron Problem. We investigate the single-electron problem for the Hamiltonian (4.56). We consider the system with an even number of unit cells under the periodic boundary condition. A similar calculation to that in Section 4.1.2 leads to the dispersion relation

$$E_{\pm} = -\tfrac{1}{2}\{2\lambda_1\lambda_2 \cos k + \lambda_1^2 + \lambda_2^2 + 2 \mp [(2\lambda_1\lambda_2 \cos k + \lambda_1^2 + \lambda_2^2)^2 + 4]^{1/2}\} \qquad (4.58)$$

where $-$, $+$ are the band index with $-$ (resp. $+$) corresponding to the $+$ (resp. $-$) sign, and k is the wave vector with (4.6). The energy gap between two bands is

$$\Delta = \tfrac{1}{2}[(\lambda_1+\lambda_2)^4 + 4]^{1/2} + \tfrac{1}{2}[(\lambda_1-\lambda_2)^4 + 4]^{1/2} - 2\lambda_1\lambda_2$$

which is nonvanishing for any finite λ_1, λ_2. (See Fig. 15.)

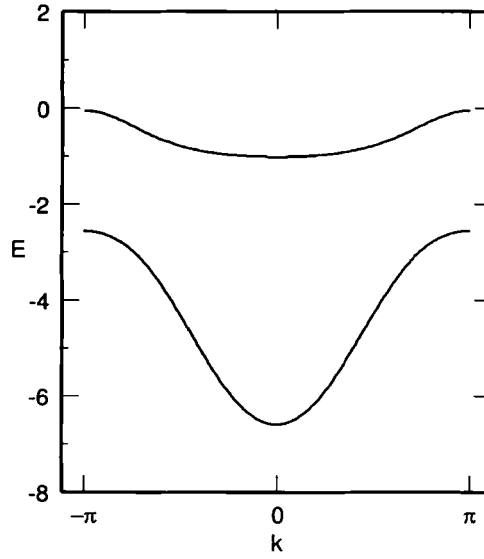

Fig. 15. The dispersion relations E_+ and E_-. The parameters are $\lambda_1 = \lambda_2 = 1$.

The electron number in the ground state (4.57) corresponds to fullfilling of the lower band. Therefore, the ground state of the noninteracting system is insulating.

4.3.3. Correlation Functions. From (4.50), the norm of the ground state is

$$\langle \Phi^B_{\text{G.S.}} | \Phi^B_{\text{G.S.}} \rangle = \frac{e_1^N}{c_1}(R_{11}L_{11} + 2R_{21}L_{21} + R_{31}L_{31}) \tag{4.59}$$

where the corresponding matrices in (4.14), (4.16), and (4.18) are[8]

$$\mathsf{T}_n = \begin{pmatrix} 2\lambda_2^2 + \lambda_2^4 & 2\lambda_2^2 & 0 \\ \lambda_1^2 + \lambda_1^2\lambda_2^2 & 2\lambda_1^2 + \lambda_1^2\lambda_2^2 & \lambda_1^2 \\ \lambda_1^4 & 2\lambda_1^4 & \lambda_1^4 \end{pmatrix}, \qquad \mathsf{I} = \begin{pmatrix} 1 \\ 0 \\ 0 \end{pmatrix}, \qquad \mathsf{F} = \begin{pmatrix} 1 \\ 2 \\ 1 \end{pmatrix}$$

$$\mathsf{D} = \begin{pmatrix} e_1 & 0 & 0 \\ 0 & e_2 & 0 \\ 0 & 0 & e_3 \end{pmatrix}, \qquad \mathsf{C} = \begin{pmatrix} c_1 & 0 & 0 \\ 0 & c_2 & 0 \\ 0 & 0 & c_3 \end{pmatrix} \tag{4.60}$$

[8] The derivation of the transfer matrices for Models B and C is available on request.

Here e_i ($i=1$, 2, and 3) are the eigenvalues of T_n,

$$e_1=\frac{s}{3}+\frac{1}{3}(p^{1/3}-tp^{1/3})$$

$$e_2=\frac{s}{3}-\frac{1}{6}[(p^{1/3}-tp^{1/3})+i\sqrt{3}\,(p^{1/3}+tp^{1/3})]$$

$$e_3=\frac{s}{3}-\frac{1}{6}[(p^{1/3}-tp^{1/3})-i\sqrt{3}\,(p^{1/3}+tp^{1/3})]$$

where

$$s=2\lambda_1+2\lambda_2+\lambda_1^2+\lambda_1\lambda_2+\lambda_2^2$$

$$t=-4\lambda_1^2-2\lambda_1\lambda_2-4\lambda_2^2-4\lambda_1^3-2\lambda_1^2\lambda_2-2\lambda_1\lambda_2^2$$
$$-4\lambda_2^3-\lambda_1^4+\lambda_1^3\lambda_2+\lambda_1\lambda_2^3-\lambda_2^4$$

$$p=(p_1+3^{3/2}\sqrt{p_2})/2$$

Here

$$p_1=16\lambda_1^3+12\lambda_1^2\lambda_2+12\lambda_1\lambda_2^2+16\lambda_2^3+24\lambda_1^4$$
$$+18\lambda_1^3\lambda_2+6\lambda_1^2\lambda_2^2+18\lambda_1\lambda_2^3+24\lambda_2^4+12\lambda_1^5-12\lambda_1^3\lambda_2^2$$
$$-12\lambda_1^2\lambda_2^3+12\lambda_2^5+2\lambda_1^6-3\lambda_1^5\lambda_2+14\lambda_1^3\lambda_2^3-3\lambda_1\lambda_2^5+2\lambda_2^6$$

$$p_2=\lambda_1^2\lambda_2^2(-16\lambda_1^2-16\lambda_2^2-48\lambda_1^3-32\lambda_1^2\lambda_2-32\lambda_1\lambda_2^2$$
$$-48\lambda_2^3-68\lambda_1^4-72\lambda_1^3\lambda_2-60\lambda_1^2\lambda_2^2-72\lambda_1\lambda_2^3$$
$$-68\lambda_2^4-56\lambda_1^5-40\lambda_1^4\lambda_2-32\lambda_1^3\lambda_2^2-32\lambda_1^2\lambda_2^3-40\lambda_1\lambda_2^4$$
$$-56\lambda_2^5-28\lambda_1^6+12\lambda_1^5\lambda_2+12\lambda_1^4\lambda_2^2+8\lambda_1^3\lambda_2^3$$
$$+12\lambda_1^2\lambda_2^4+12\lambda_1\lambda_2^5-28\lambda_2^6-8\lambda_1^7+16\lambda_1^6\lambda_2-8\lambda_1^4\lambda_2^3-8\lambda_1^3\lambda_2^4$$
$$+16\lambda_1\lambda_2^6-8\lambda_2^7-\lambda_1^8+4\lambda_1^7\lambda_2-4\lambda_1^6\lambda_2^2-4\lambda_1^5\lambda_2^3$$
$$+10\lambda_1^4\lambda_2^4-4\lambda_1^3\lambda_2^5-4\lambda_1^2\lambda_2^6+4\lambda_1\lambda_2^7-\lambda_2^8)$$

They satisfy $e_1>e_2>e_3>0$ for $\lambda_1\neq 0$ and $\lambda_2\neq 0$. The matrix $\mathsf{L}=(L_{ij})$ [$\mathsf{R}=(R_{ij})$] is constructed from the left (right) eigenvectors. We choose the left eigenvectors $\mathbf{L}_1=(L_{11}, L_{12}, L_{13})^T$, $\mathbf{L}_2=(L_{21}, L_{22}, L_{23})^T$, and $\mathbf{L}_3=(L_{31}, L_{32}, L_{33})^T$ corresponding to the eigenvalues e_1, e, and e_3, respectively, where $L_{j1}=\lambda_1^2(\lambda_1^4-e_j)(1+\lambda_2^2)-\lambda_1^6$, $L_{j2}=(\lambda_1^4-e_j)(2\lambda_2^2-\lambda_2^4-e_j)$, and $L_{j3}=\lambda_1^2(2\lambda_2^2-\lambda_2^4-e_j)$. We choose the right eigenvectors $\mathbf{R}_1=(R_{11},$

$R_{21}, R_{31})^T$, $\mathbf{R}_2=(R_{12}, R_{22}, R_{32})^T$, and $\mathbf{R}_3=(R_{13}, R_{23}, R_{33})^T$, where $R_{1j}=2\lambda_2^2(\lambda_1^4-e_j)$, $R_{2j}=(\lambda_1^4-e_j)(e_j-2\lambda_2^2-\lambda_2^4)$, and $R_{3j}=2\lambda_1^4(\lambda_2^2+\lambda_2^4-e_j)$.

We evaluate the expectation value of the number operator $\langle n_{i,\sigma}^{\alpha}\rangle$. The transfer matrices associated with $n_{i,\sigma}^{\alpha}$ are

$$\mathsf{N}_i^{(p)}=\begin{pmatrix}\lambda_2^2+\lambda_2^4 & 2\lambda_2^2 & 0\\ \frac{1}{2}\lambda_1^2\lambda_2^2 & \lambda_1^2+\lambda_1^2\lambda_2^2 & \lambda_1^2\\ 0 & \lambda_1^4 & 0\end{pmatrix},\qquad \mathsf{N}_i^{(d)}=\begin{pmatrix}\lambda_2^2 & \lambda_2^2 & 0\\ \frac{1}{2}\lambda_1^2 & \lambda_1^2 & \frac{1}{2}\lambda_1^2\\ 0 & 0 & 0\end{pmatrix} \tag{4.61}$$

From (4.27) and (4.59)–(4.61), we obtain

$$\langle n_{i,\sigma}^{\alpha}\rangle=\begin{cases}(L_{11}-\frac{1}{2}\lambda_1 L_{12})\,\lambda_2 R_{11}+(L_{12}-L_{13})\,R_{21}+L_{13}R_{31}\\ \quad \text{for}\quad \alpha=p\\ (\lambda_2 L_{11}+\frac{1}{2}\lambda_1 L_{12})\,R_{11}+(\lambda_2 L_{11}+\lambda_1 L_{12})\,R_{21}+\frac{1}{2}\lambda_1 L_{12}R_{31}\\ \quad \text{for}\quad \alpha=d\end{cases} \tag{4.62}$$

in the thermodynamic limit $N, i, N-i\to\infty$. It can be verified that there are two electrons per unit cell, as $\langle n_i^p\rangle+\langle n_i^d\rangle=2$. The results are shown in Fig. 16. The case $\lambda_2=|\lambda_1|$ was discussed in ref. 6. We consider the case

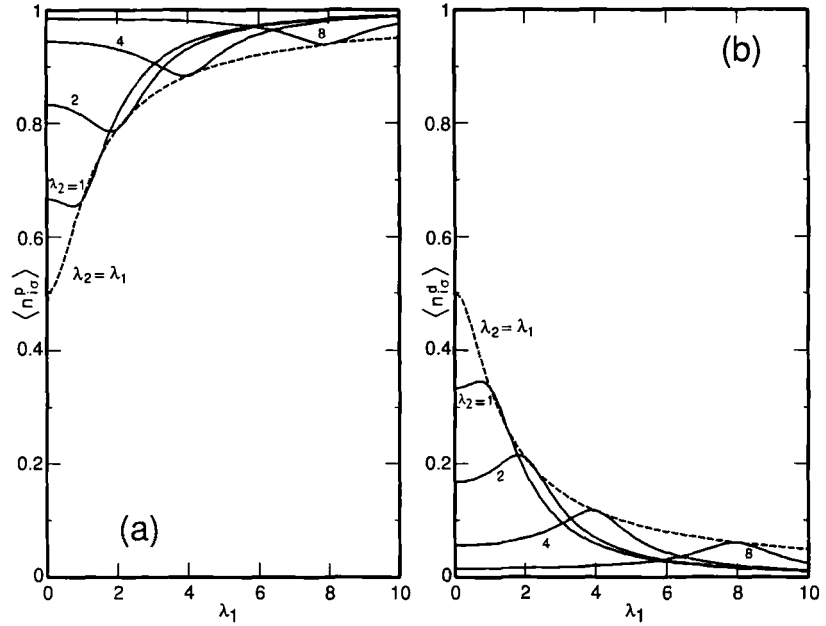

Fig. 16. Occupation on (a) the p-site and (b) the d-site for $\lambda_2=1$, 2, 4, and 8 (solid lines) and $\lambda_2=\lambda_1$ (broken line).

$|\lambda_1| \ll 1$, $\lambda_2 \gg 1$. The occupation on a p (d)-site has a minimum (maximum) at an intermediate value of λ_1.

From (3.31), (4.27), (4.32), and (4.59)–(4.61), the density correlation functions are

$$\langle n_i^\alpha n_j^\alpha \rangle - \langle n_i^\alpha \rangle \langle n_j^\alpha \rangle = \left(\frac{e_2}{e_1}\right)^{-|i-j|} \frac{1}{e_1 e_2 c_1 c_2} R_2^{(\alpha)} L_2^{(\alpha)} + \left(\frac{e_3}{e_1}\right)^{-|i-j|} \frac{1}{e_1 e_3 c_1 c_3} R_3^{(\alpha)} L_3^{(\alpha)} \tag{4.63}$$

where

$$R_j^{(p)} = (L_{11} - L_{12}/2)\, R_{1j} + (L_{12} - L_{13})\, R_{2j} + L_{13} R_{3j}$$

$$L_j^{(p)} = R_{11} L_{j1} + (-R_{11}/2 + R_{21})\, L_{j2} + (-R_{21} + R_{31})\, L_{j3}$$

$$R_j^{(d)} = (\lambda_2 L_{11} + \lambda_1 L_{12}/2)\, R_{1j} + (\lambda_2 L_{11} + \lambda_1 L_{12})\, R_{2j} + \lambda_1 L_{12} R_{3j}/2$$

$$L_j^{(d)} = \lambda_2 (R_{11} + R_{21})\, L_{21} + \lambda_1 (R_{11}/2 + R_{21} + 2R_{31})\, L_{22}$$

in the thermodynamic limit $N - j$, $i \to \infty$ keeping $|j - i|$ finite. The density correlation functions take negative values and decay exponentially with distance. We show the results in Fig. 17. For $|\lambda_1| \ll 1$ and $\lambda_2 \gg 1$ the density correlations are suppressed. They have a minimum at an intermediate value of λ_1.

We evaluate the spin correlation function. The transfer matrices are

$$\mathsf{S}_n = \lambda_1^2 \lambda_2^2$$

$$\mathsf{S}_i^{R,(p)} = (\tfrac{1}{2}\lambda_1^2 \lambda_2^2, 0, 0), \qquad \mathsf{S}_j^{L,(p)} = \begin{pmatrix} 0 \\ -\lambda_1^2 \\ -\lambda_1^4 \end{pmatrix} \tag{4.64}$$

$$\mathsf{S}_i^{R,(d)} = (\tfrac{1}{2}\lambda_1^2, \lambda_1^2, \tfrac{1}{2}\lambda_1^2), \qquad \mathsf{S}_j^{L,(d)} = \begin{pmatrix} -\lambda_2^2 \\ 0 \\ 0 \end{pmatrix}$$

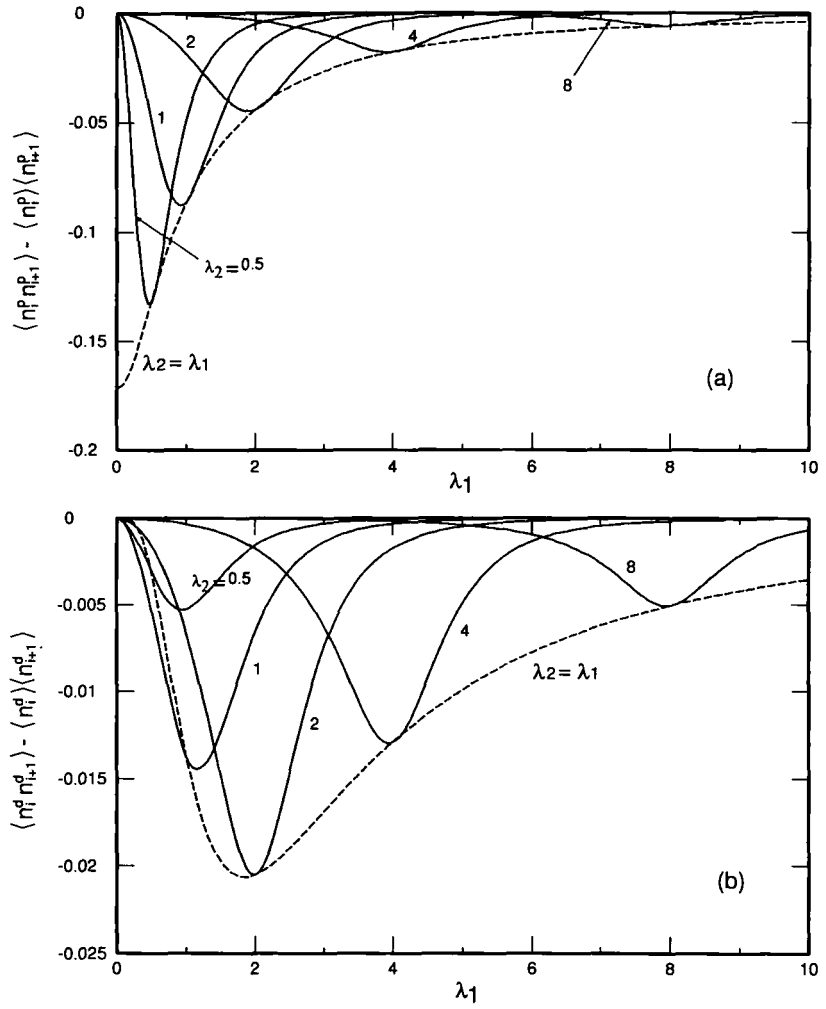

Fig. 17. Density correlation functions for (a) the nearest neighbor p-sites and (b) for d-sites for $\lambda_2 = 0.5$, 1, 2, 4, and 8 (solid lines) and $\lambda_2 = \lambda_1$ (broken line).

From (4.53), (4.54), (4.59), and (4.64) we have

$$\begin{aligned}
&\langle S_i^z S_j^z \rangle \\
&\quad = \frac{\mathbf{F}^T \mathsf{T}^{N-j} \mathsf{S}_j^{L,(\alpha)} \mathsf{S}^{j-i-1} \mathsf{S}_i^{R,(\beta)} \mathsf{T}^{i-1} \mathbf{I}}{\mathbf{F}^T \mathsf{T}^N \mathbf{I}} \qquad (4.65) \\
&\quad = \left(\frac{\lambda_1^2 \lambda_2^2}{e_1}\right)^{-|i-j|} \\
&\qquad \times \begin{cases}
-\dfrac{\lambda_1^2}{2e_1 c_1}(L_{12} + \lambda_1^2 L_{13})\, R_{11} \\
\quad \text{for } \beta = p \text{ and } \alpha = p \\
-\dfrac{1}{2e_1 c_1} L_{11}(R_{11} + 2R_{21} + R_{31}) \\
\quad \text{for } \beta = d \text{ and } \alpha = d \\
-\dfrac{\lambda_1^2}{2\lambda_2^2 e_1 c_1}(L_{12} + \lambda_1^2 L_{13})(R_{11} + 2R_{21} + R_{31}) \\
\quad \text{for } \beta = p \text{ and } \alpha = d \\
-\dfrac{\lambda_2^2}{2e_1 c_1}(L_{11} R_{11}) \\
\quad \text{for } \beta = d \text{ and } \alpha = p
\end{cases} \qquad (4.66)
\end{aligned}$$

We note that $\langle S_{x+1}^{z,p} S_x^{z,d} \rangle \neq \langle S_x^{z,p} S_x^{z,d} \rangle$, because the Hamiltonian is not invariant under the reflection of the lattice. All the spin correlation functions take negative values and decay exponentially with distance. We show the results in Fig. 18. For $|\lambda_1| \ll 1$ and $\lambda_2 \gg 1$ the spin correlations are suppressed.

We evaluate the singlet-pair correlation function (3.38) where i and j (k and l) are in the same cell. For (4.55), case (ii), the correlation function is vanishing. We evaluate them for (4.55), cases (i) and (iii). The transfer matrices are

$$\mathsf{H}_n = 2$$

$$\mathsf{H}_i^{R,(pp)} = \lambda_1^2 \lambda_2^2 (1, 0, 0), \qquad \mathsf{H}_k^{L,(pp)} = \begin{pmatrix} 0 \\ 2\lambda_1^2 \\ 2\lambda_1^4 \end{pmatrix} \qquad (4.67)$$

$$\mathsf{H}_i^{R,(dp)} = 2\lambda_1^2 \lambda_2 (1, 1, 0), \qquad \mathsf{H}_k^{L,(dp)} = \begin{pmatrix} 0 \\ 2\lambda_1 \lambda_2^2 \\ \cdot\ 0 \end{pmatrix}$$

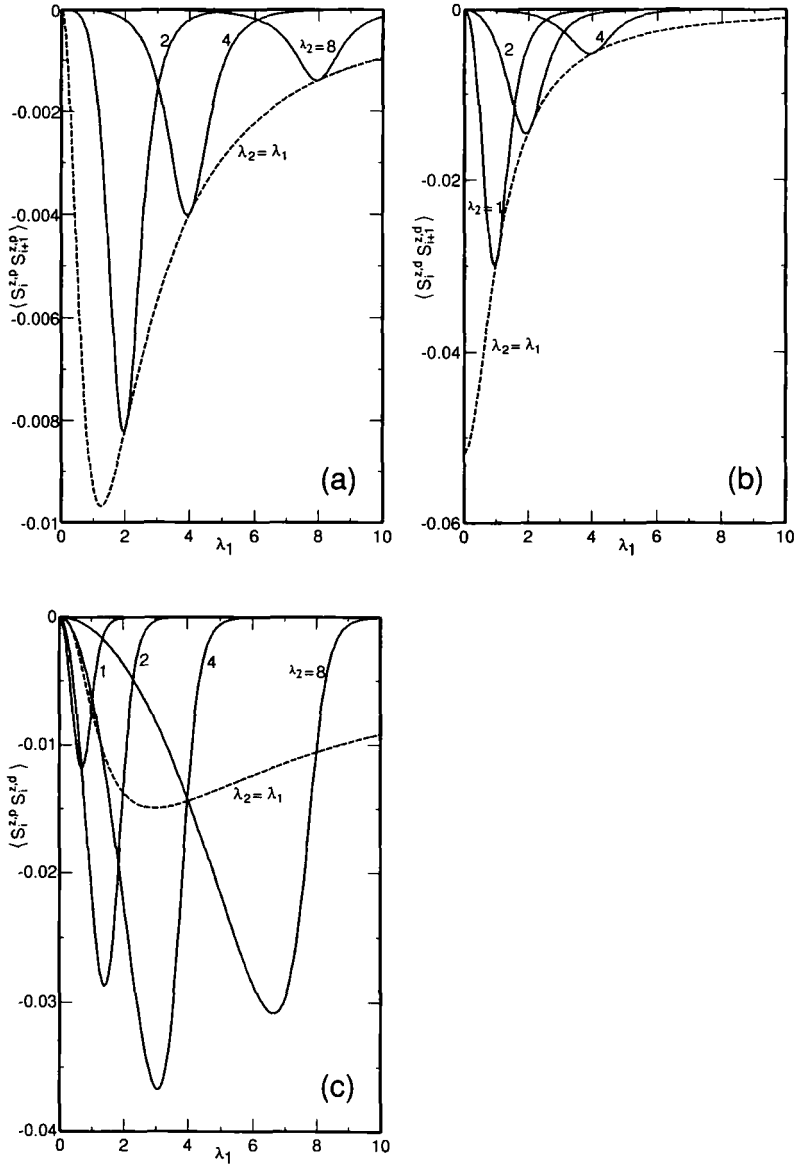

Fig. 18. Spin correlation functions for (a) the nearest neighbor p-sites for $\lambda_2=2$, 4, and 8 (solid lines), (b) d-sites for $\lambda_2=1$, 2, and 4 (solid lines), and (c) p- and d-sites for $\lambda_2=1$, 2, 4, and 8 (solid lines). The broken lines are for $\lambda_2=\lambda_1$.

From (4.53), (4.54), (4.59), and (4.67) we obtain

$$\langle b^{\dagger}_{i,j} b_{k,l} \rangle = \frac{\mathbf{F}^T \mathsf{T}^{N-k} \mathsf{H}_k^{L,(\gamma)} \mathsf{H}^{k-i-1} \mathsf{H}_i^{R,(\gamma)} \mathsf{T}^{i-1} \mathbf{I}}{\mathbf{F}^T \mathsf{T}^N \mathbf{I}} \tag{4.68}$$

$$= \left(\frac{\lambda_1^2 \lambda_2^2}{e_1}\right)^{-|i-k|} \begin{cases} L_{13} R_{11} & \text{for} \quad \gamma = p \\ \dfrac{4\lambda_1 \lambda_2}{e_1 c_1} L_{12}(R_{11} + R_{21}) & \text{for} \quad \gamma = dp \end{cases} \tag{4.69}$$

The singlet-pair correlation function decays exponentially with distance. The results are shown in Fig. 19 for $\gamma = p$. For $|\lambda_1| \ll 1$ and $\lambda_2 \gg 1$ the singlet-pair correlations are suppressed.

We evaluate the correlation function $\langle c^{\alpha}_{i,\sigma} c^{\alpha\dagger}_{j,\sigma} \rangle$. The transfer matrices are

$$\mathsf{G}_n = -\lambda_1 \lambda_2 \begin{pmatrix} 1+\lambda_2^2 & 1 \\ \lambda_1^2 & \lambda_1^2 \end{pmatrix}$$

$$\mathsf{G}_i^{R,(p)} = -\lambda_1 \lambda_2 \begin{pmatrix} 1+\lambda_2^2 & 1 & 0 \\ \lambda_1^2 & \lambda_1^2 & 0 \end{pmatrix}, \qquad \mathsf{G}_j^{L,(p)} = \begin{pmatrix} \lambda_2^2 & 0 \\ \lambda_1^2 + \frac{1}{2}\lambda_1^2 \lambda_2^2 & \lambda_1^2 \\ \lambda_1^4 & \lambda_1^4 \end{pmatrix} \tag{4.70}$$

$$\mathsf{G}_i^{R,(d)} = -\lambda_1 \begin{pmatrix} \lambda_2^2 & \lambda_2^2 & 0 \\ \lambda_1^2 & 2\lambda_1^2 & \lambda_1^2 \end{pmatrix}, \qquad \mathsf{G}_j^{L,(d)} = -\lambda_2 \begin{pmatrix} \lambda_2^2 & 0 \\ \frac{1}{2}\lambda_1^2 & \frac{1}{2}\lambda_1^2 \\ 0 & 0 \end{pmatrix}$$

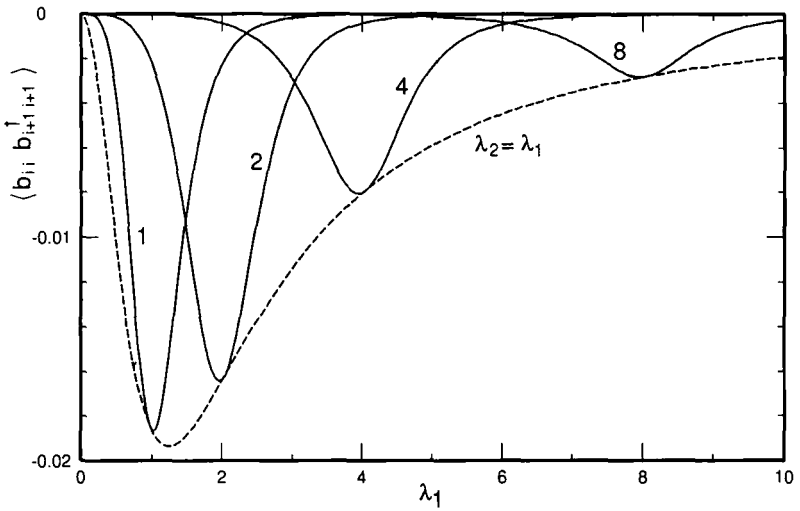

Fig. 19. Singlet-pair correlation function for the nearest neighbor p-sites for $\lambda_2 = 1, 2, 4,$ and 8 (solid lines) and $\lambda_2 = \lambda_1$ (broken line).

The matrix G_n is diagonalized

$$\mathsf{G}_n = -\lambda_1\lambda_2\tilde{\mathsf{R}}\tilde{\mathsf{D}}\tilde{\mathsf{C}}^{-1}\tilde{\mathsf{L}} \tag{4.71}$$

where

$$\tilde{\mathsf{D}} = \begin{pmatrix} g_1 & 0 \\ 0 & g_2 \end{pmatrix}, \quad \tilde{\mathsf{R}} = \begin{pmatrix} \tilde{R}_{11} & \tilde{R}_{12} \\ \tilde{R}_{21} & \tilde{R}_{22} \end{pmatrix}, \quad \tilde{\mathsf{L}} = \begin{pmatrix} \tilde{L}_{11} & \tilde{L}_{12} \\ \tilde{L}_{21} & \tilde{L}_{22} \end{pmatrix}, \quad \tilde{\mathsf{C}} = \begin{pmatrix} \tilde{c}_1 & 0 \\ 0 & \tilde{c}_2 \end{pmatrix} \tag{4.72}$$

Here g_k are the eigenvalues of G_n, $g_1 = (1+\lambda_1+\lambda_2+\omega_2)/2$ and $g_2 = (1+\lambda_1+\lambda_2-\omega_2)/2$, with $\omega_2 = [1+2(\lambda_1+\lambda_2)+(\lambda_1-\lambda_2)^2]^{1/2}$. They satisfy $g_1 > g_2 > 0$ for $\lambda_1 \neq 0$ and $\lambda_2 \neq 0$. We choose the left eigenvectors $\tilde{L}_1 = (\tilde{L}_{11}, \tilde{L}_{12})^T$ and $\tilde{L}_2 = (\tilde{L}_{21}, \tilde{L}_{22})^T$ corresponding to the eigenvalues g_1 and g_2, respectively, where $\tilde{L}_{j1} = g_j - \lambda_1^2$ and $\tilde{L}_{j2} = 1$, and the right eigenvectors $\tilde{R}_1 = (\tilde{R}_{11}, \tilde{R}_{21})^T$ and $\tilde{R}_2 = (\tilde{R}_{12}, \tilde{R}_{22})^T$, where $\tilde{R}_{1j} = g_j - \lambda_1^2$ and $\tilde{R}_{2j} = \lambda_1^2$. Here $\tilde{\mathsf{C}} = \tilde{\mathsf{L}}\tilde{\mathsf{R}}$.

From these matrices and (4.44), we obtain

$$\langle c_{i,\sigma} c_{j,\sigma}^{\dagger} \rangle = \left(-\lambda_1\lambda_2 \frac{g_1}{e_1}\right)^{-|i-j|} f_1^{(\alpha)} + \left(-\lambda_1\lambda_2 \frac{g_2}{e_1}\right)^{-|i-j|} f_2^{(\alpha)} \tag{4.73}$$

where

$$f_m^{(p)} = \frac{1}{c_1 \tilde{c}_m}\left[\frac{1}{2}(g_m - \lambda_1^2) L_{12} + \lambda_1^2 L_{13}\right][(g_m - \lambda_1^2) R_{11} + R_{21}] \tag{4.74}$$

$$f_m^{(d)} = \frac{1}{e_1 g_m c_1 \tilde{c}_m}\left[\lambda_2^2(g_m - \lambda_1^2) L_{11} + \frac{1}{2} g_m \lambda_1^2 L_{12}\right]$$
$$\times [\lambda_2^2(g_m - \lambda_1^2)(R_{11} + R_{21}) + \lambda_1^2(R_{11} + 2R_{21} + R_{31})] \tag{4.75}$$

The correlation functions decay exponentially.

By the Fourier transformation of the correlation function $\langle c_{i,\sigma} c_{j,\sigma}^{\dagger} \rangle$ we obtain the momentum distribution function for $\alpha = p$ and d,

$$\langle n_{k,\sigma}^{\alpha} \rangle = f_1^{(\alpha)} F_1(k, r_1) + f_2^{(\alpha)} F_2(k, r_2) + f_0^{(\alpha)} \tag{4.76}$$

where $f_0^{(\alpha)} = \langle n_{i,\sigma}^{\alpha} \rangle$ and

$$F_i(k, r_i) = \frac{2r_i[\cos k - r_i]}{1 + r_i^2 - 2r_i \cos k} \tag{4.77}$$

where $r_i = -\lambda_1 \lambda_2 g_i/e_1$. The results are shown in Fig. 20. There is no singularity in $\langle n^{\alpha}_{k,\sigma} \rangle$. For $|\lambda_1| \ll 1$ and $\lambda_2 \gg 1$ the momentum distributions for the p- and d-sites are flat.

4.3.4. Discussion. All the correlation functions under consideration decay exponentially with distance. These results suggest the existence of a finite excitation gap. The existence of the energy gap is numerically confirmed in ref. 28. Therefore, it is expected that the state is insulating. The correlation lengths are given by $\xi_{nn} = [\ln(e_2/e_1)]^{-1}$ and $\xi_{ss} = \xi_{bb} = [\ln(\lambda_1^2 \lambda_2^2/e_1)]^{-1}$ for the spin and singlet-pair correlation functions, respectively, and $\xi_{cc} = [\ln(\lambda_1^2 \lambda_2^2 g_1/e_1)]^{-1}$ (Fig. 21). (They satisfy the relation $\xi_{cc} > \xi_{nn} > \xi_{ss} = \xi_{bb}$.) The correlation lengths of the correlation between p-sites and that between d-sites are the same. We note that the spin correlation is ferromagnetic.

We consider the region $\lambda_1, \lambda_2 \gg 1$. The d-sites are almost empty and the p-sites are almost doubly occupied. The correlation lengths behave like $\xi_{cc} \sim \lambda_1$ and $\xi_{nn}, \xi_{ss}, \xi_{bb} \sim \lambda_1/2$ (for $\lambda_1 = \lambda_2$). The correlation functions for the nearest neighbor sites are suppressed.

For $|\lambda_1|, |\lambda_2| \ll 1$, there is almost one electron per site. The density correlation functions for the nearest neighbor p-sites are enhanced, while those for d-sites are suppressed. The spin correlation functions for the nearest neighbor p-sites are suppressed, and those for d-sites are enhanced. Therefore, the electrons on the d-sites have a tendency to behave like a localized spin. This corresponds to a kind of Kondo lattice regime[6] in the sense that there are one localized electron and one conduction electron per unit cell. The ground state is described by a collection of local singlets between them. The effective exchange coupling between the p- and d-sites $J \sim \lambda_1 \lambda_2/(\varepsilon^p - \varepsilon^d)$ is comparable to the hopping amplitude between p-sites.

For $|\lambda_1| \ll 1$ and $\lambda_2 \gg 1$ the correlations are suppressed. This is because the system decouples to a collection of pairs of p- and d-sites.

The ground state (4.57) is a half-filling state. The filling factor corresponds to that of a band insulator in the noninteracting system where the excitation gap satisfies the relation $1 < \Delta < 2$. Therefore, the correlation length is finite and is almost independent of the parameters λ_1 and λ_2, which is a different situation from that of the ground state (4.57). The properties of the ground state (4.57) are completely different from those of the noninteracting system.

4.4. Model C

4.4.1. Hamiltonian. The lattice of Model C is constructed from a cell with four d-sites and one p-site (Fig. 22a). The model has four free

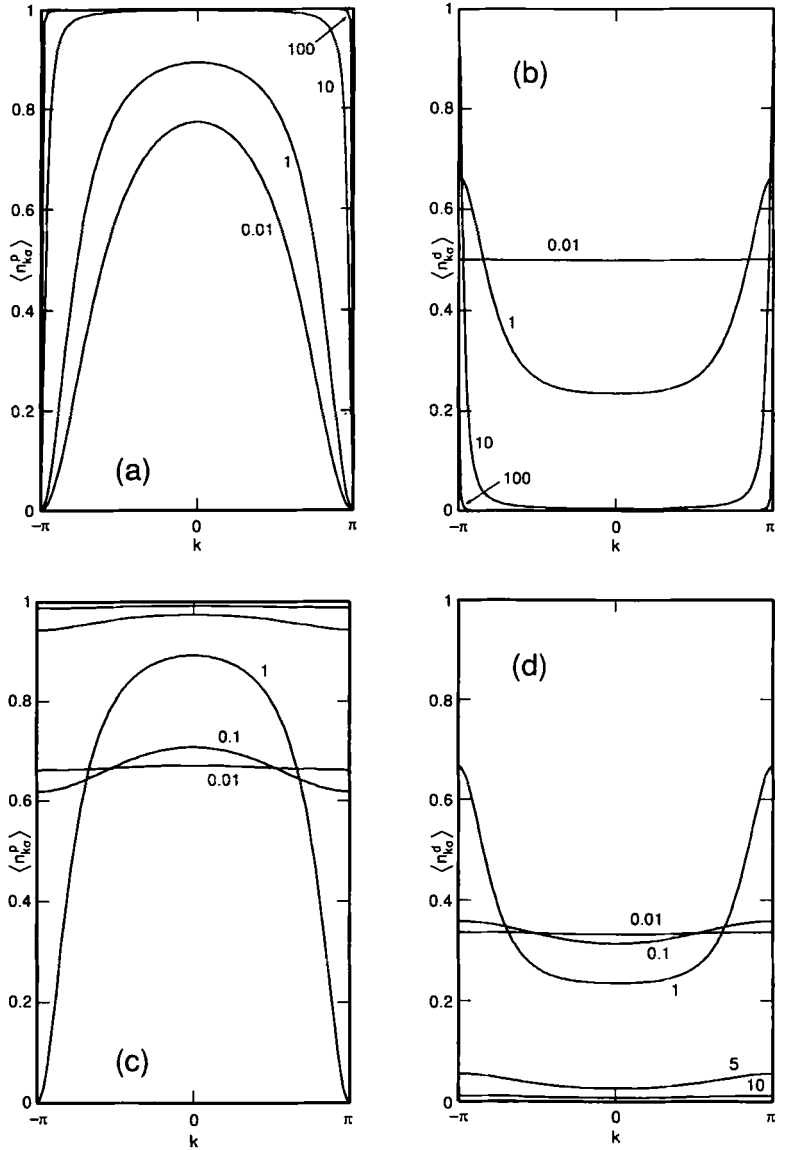

Fig. 20. Momentum distribution functions for (a) the p-site and (b) the d-site for $\lambda_1 = \lambda_2 = 0.01$, 1, 10, and 100, and those for (c) the p-site and (d) the d-site for $\lambda_2 = 0.01$, 0.1, 1, 5, and 10 with $\lambda_1 = 1$.

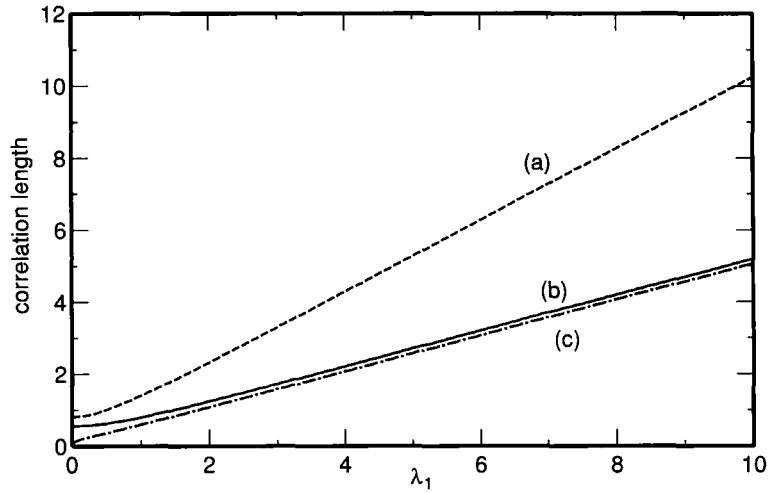

Fig. 21. Correlation length of (a) the correlation function $\langle c_{i,\sigma} c^{\dagger}_{j,\sigma} \rangle$, (b) the density correlation function, and (c) the spin and the singlet-pair correlation functions for $\lambda_1 = \lambda_2$.

parameters. We investigate the simplest model with one parameter. The cell Hamiltonian is obtained by choosing

$$\alpha^{(C)}_{n,\sigma} = \sum_{r=1}^{5} \lambda_r c_{r,\sigma} \equiv \lambda_1 c^{d}_{1,\sigma} + \lambda_2 c^{d}_{2,\sigma} + \lambda_3 c^{d}_{3,\sigma} + \lambda_4 c^{d}_{4,\sigma} + \lambda_5 c^{p}_{5,\sigma}$$

and setting $\lambda_r = 1$ ($r = 1, 2, 3, 4$) and $\lambda_5 = \lambda$ (see Fig. 22a for the intracell index). The full Hamiltonian is obtained by identifying sites 1 and 2 in the $(n-1)$th cell with sites 3 and 4 in the nth cell, respectively (Fig. 22b). The Hamiltonian is

$$\begin{aligned} H_S = \mathscr{P} \sum_{\sigma=\uparrow,\downarrow} \Bigg\{ \sum_{n=1}^{N} \big[& (-\lambda c^{d1\dagger}_{n,\sigma} c^{p}_{n,\sigma} - \lambda c^{d2\dagger}_{n,\sigma} c^{p}_{n,\sigma} - \lambda c^{d1\dagger}_{n+1,\sigma} c^{p}_{n,\sigma} - \lambda c^{d2\dagger}_{n+1,\sigma} c^{p}_{n,\sigma} \\ & - c^{d1\dagger}_{n,\sigma} c^{d2}_{n,\sigma} - c^{d1\dagger}_{n+1,\sigma} c^{d1}_{n,\sigma} - c^{d2\dagger}_{n+1,\sigma} c^{d2}_{n,\sigma} - c^{d1\dagger}_{n+1,\sigma} c^{d2}_{n,\sigma} - c^{d2\dagger}_{n+1,\sigma} c^{d1}_{n,\sigma} + \text{h.c.}) \\ & + \varepsilon^{p} c^{p\dagger}_{n,\sigma} c^{p}_{n,\sigma} + \varepsilon^{d}_{n} c^{d1\dagger}_{n,\sigma} c^{d1}_{n,\sigma} + \varepsilon^{d}_{n} c^{d2\dagger}_{n,\sigma} c^{d2}_{n,\sigma} \big] \\ & + \varepsilon^{d}_{N+1} c^{d1\dagger}_{N+1,\sigma} c^{d1}_{N+1,\sigma} + \varepsilon^{d}_{N+1} c^{d2\dagger}_{N+1,\sigma} c^{d2}_{N+1,\sigma} \Bigg\} \mathscr{P} \end{aligned} \tag{4.78}$$

where the on-site potentials are $\varepsilon^{p} = -\lambda^2$, $\varepsilon^{d}_{n} = -4$ $(2 \leqslant n \leqslant N)$, and $\varepsilon^{d}_{1} = \varepsilon^{d}_{N+1} = -2$. A unit cell is labeled by n. Here $c^{d1}_{n,\sigma}$ ($c^{d2}_{n,\sigma}$) is the

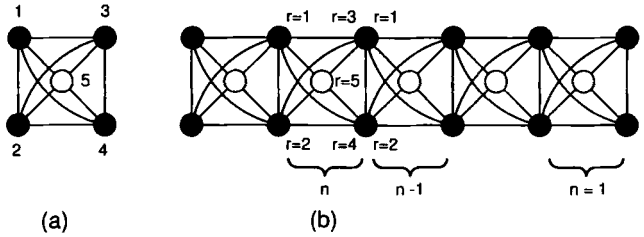

Fig. 22. Model C. (a) A cell composed of one p-site ($U=0$) and four d-sites ($U=\infty$). (b) The lattice constructed from the cell with cell labelings.

annihilation operator on a d-site for $r=3$ (4) in the nth cell. The ground state is

$$|\Phi^{C}_{\text{G.S.}}\rangle = \mathscr{P}\prod_{i=1}^{N}\prod_{\sigma=\uparrow,\downarrow}\alpha^{(C)}_{n,\sigma}|0\rangle$$

$$= \mathscr{P}\prod_{n=1}^{N}\prod_{\sigma=\uparrow,\downarrow}(c^{d1\dagger}_{n,\sigma}+c^{d2\dagger}_{n,\sigma}+c^{d1\dagger}_{n+1,\sigma}+c^{d2\dagger}_{n+1,\sigma}+\lambda c^{p\dagger}_{n,\sigma})|0\rangle \qquad (4.79)$$

which is a 1/3-filling state.

4.4.2. Band Structure in the Single-Electron Problem. We investigate the single-electron problem for the Hamiltonian (4.78). We consider the system with an even number of cells under periodic boundary conditions. A similar calculation to that in Section 4.1.2 leads to the dispersion relations

$$E_1 = -\tfrac{1}{2}\{6+\lambda^2+4\cos k+[(6+\lambda^2+4\cos k)^2-8\lambda^2]^{1/2}\}$$

$$E_2 = -2 \qquad (4.80)$$

$$E_3 = -\tfrac{1}{2}\{6+\lambda^2+4\cos k-[(6+\lambda^2+4\cos k)^2-8\lambda^2]^{1/2}\}$$

where 1, 2, and 3 are the band indexes and k is the wave vector with (4.6). The energy gap between the lowest two bands is $\Delta=0$ for $0<\lambda<\sqrt{2}$ and $\Delta=\lambda^2$ for $\lambda>\sqrt{2}$. (See Fig. 23.)

The electron number in the ground state (4.79) corresponds to full-filling of the lowest band. Therefore, the ground state of the noninteracting system is metallic for $0<\lambda<\sqrt{2}$ and is insulating for $\lambda>\sqrt{2}$.

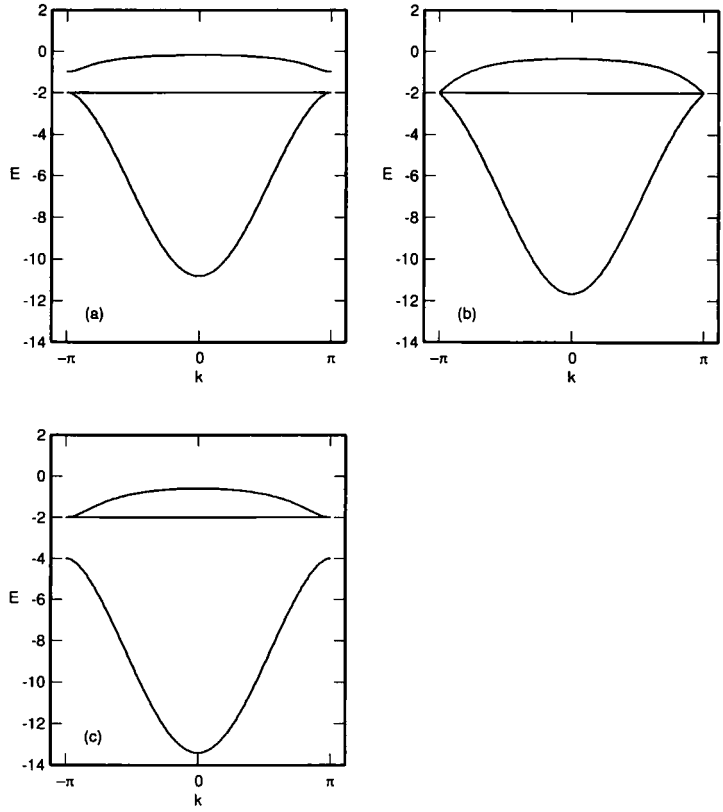

Fig. 23. The dispersion relations E_1, E_2, and E_3. The parameters are (a) $\lambda = 1$, (b) $\lambda = \sqrt{2}$, and (c) $\lambda = 2$.

4.4.3. Correlation Functions. From (4.50), the norm of the ground state is

$$\langle \Phi^C_{\text{G.S.}} | \Phi^C_{\text{G.S.}} \rangle = \frac{e_1^N}{c_1} (R_{11} L_{11} + 4R_{21} L_{21} + R_{31} L_{31}) \tag{4.81}$$

where the corresponding matrices in (4.60) are

$$\mathsf{T}_n = \begin{pmatrix} 2+4\lambda^2+\lambda^4 & 4\lambda^2+4\lambda^4 & \lambda^4 \\ 2+\lambda^2 & 2+4\lambda^2 & \lambda^2 \\ 2 & 8 & 2 \end{pmatrix}, \qquad \mathsf{I} = \begin{pmatrix} 1 \\ 0 \\ 0 \end{pmatrix}, \qquad \mathsf{F} = \begin{pmatrix} 1 \\ 4 \\ 1 \end{pmatrix}$$

$$\mathsf{D}=\begin{pmatrix} e_1 & 0 & 0 \\ 0 & e_2 & 0 \\ 0 & 0 & e_3 \end{pmatrix}, \qquad \mathsf{C}=\begin{pmatrix} c_1 & 0 & 0 \\ 0 & c_2 & 0 \\ 0 & 0 & c_3 \end{pmatrix} \tag{4.82}$$

Here e_i ($i=1$, 2, and 3) are the eigenvalues of T_n,

$$e_1=\frac{1}{3}\left(s+\frac{t}{q}\right)$$

$$e_2=\frac{s}{3}+\frac{i}{12}\left[(1+2\sqrt{3})\frac{t}{q}+(1-2\sqrt{3})\,q\right]$$

$$e_3=\frac{s}{3}-\frac{i}{12}\left[(1+2\sqrt{3})\frac{t}{q}+(1-2\sqrt{3})\,q\right]$$

where $s=6+8\lambda^2+\lambda^4$, $t=\lambda^2(48+58\lambda^2+16\lambda^4+\lambda^6)$, and $q=(p_1+3^{3/2}p_2 i)^{1/3}$ with

$$p_1=468\lambda^4+512\lambda^6+183\lambda^8+24\lambda^{10}+\lambda^{12}$$

$$p_2=\lambda^6(4096+6736\lambda^2+4288\lambda^4+1328\lambda^6+192\lambda^8+9\lambda^{10})$$

They satisfy $e_1>e_2>e_3>0$ for $\lambda\neq 0$. The matrix $\mathsf{L}=(L_{ij})$ [$\mathsf{R}=(R_{ij})$] is constructed from the left (right) eigenvectors. We choose them as we did in Section 4.3, where $L_{j1}=(e_j-2)^2-4e_j\lambda^2$, $L_{j2}=4\lambda^2(e_j\lambda^2+e_j-2)$, $L_{j3}=\lambda^4(e_j+2)$, $R_{1j}=(e_j-2)^2-4e_j\lambda^2$, $R_{2j}=(2+\lambda^2)\,e_j-4$, and $R_{3j}=2(e_j+6)$.

We evaluate the expectation value of the number operator $\langle n^{\alpha}_{i,\sigma}\rangle$. The transfer matrices associated with $n^{\alpha}_{i,\sigma}$ are

$$\mathsf{N}_i^{(p)}=\begin{pmatrix} 2\lambda^2+\lambda^4 & 2\lambda^2+4\lambda^4 & \lambda^4 \\ \frac{1}{2}\lambda^2 & 2\lambda^2 & \frac{1}{2}\lambda^2 \\ 0 & 0 & 0 \end{pmatrix}, \qquad \mathsf{N}_i^{(d)}=\begin{pmatrix} 1+\lambda^2 & 2\lambda^2+\lambda^4 & \frac{1}{2}\lambda^4 \\ \frac{1}{2} & 1+\lambda^2 & \frac{1}{2}\lambda^2 \\ 0 & 2 & 1 \end{pmatrix} \tag{4.83}$$

From (4.27) and (4.81)–(4.83), we obtain

$$\langle n^{\alpha}_{i,\sigma}\rangle=\begin{cases} \dfrac{\lambda^2}{4c_1}(4L_{11}R_{21}+L_{12}R_{31}) \\ \qquad \text{for} \quad \alpha=p \\ \dfrac{1}{4c_1}[(2L_{11}-L_{12}+2L_{13})\,R_{11}+(2L_{12}-4L_{13})\,R_{21}+2L_{13}R_{31}] \\ \qquad \text{for} \quad \alpha=d \end{cases} \tag{4.84}$$

It can be verified that there are two electrons per unit cell, as $\langle n_i^p \rangle + 2\langle n_i^d \rangle = 2$. The results are shown in Fig. 24a. For $|\lambda| \ll 1$, on-site potentials satisfy the relations $\varepsilon_d < \varepsilon_p$ and $|\varepsilon_p - \varepsilon_d| \gg |\lambda|$ (the hybridization). There is almost one electron per d-site. The p-sites are almost empty. For $\lambda \gg 1$, on-site potentials satisfy the relations $\varepsilon_p \ll \varepsilon_d$ and $\varepsilon_d - \varepsilon_p \gg \lambda$. The p-sites are almoust doubly occupied. The d-sites are almost empty.

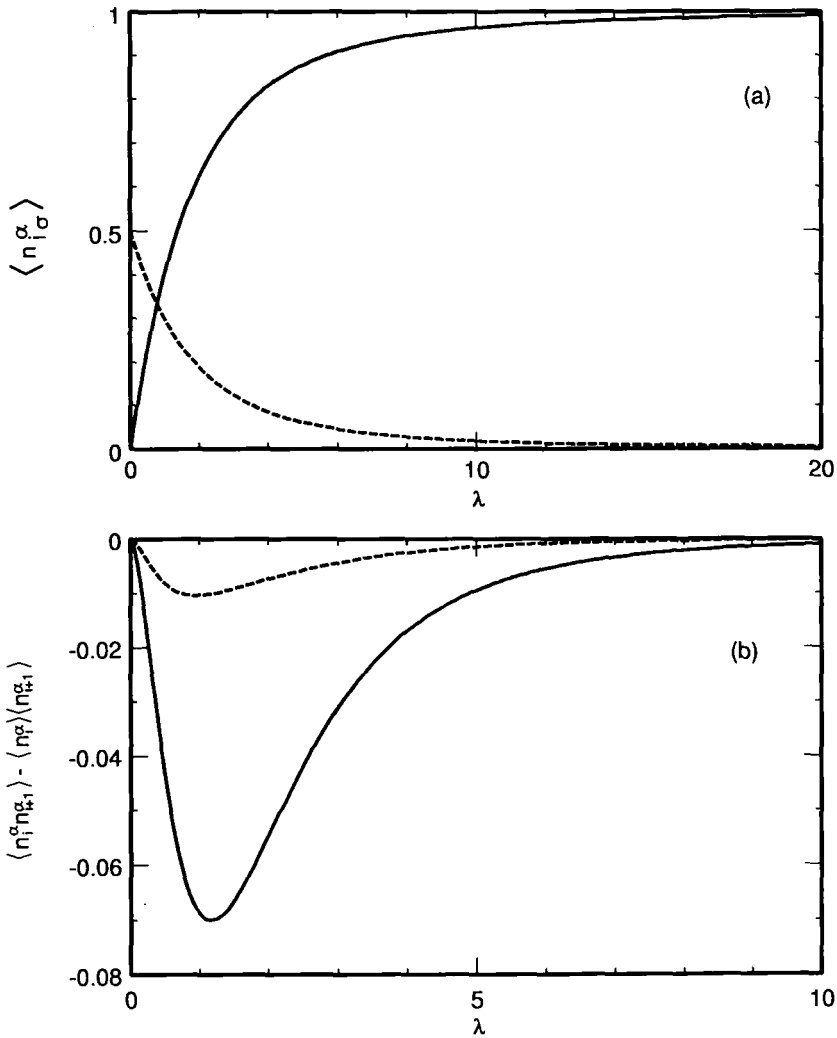

Fig. 24. (a) Occupation on the p-site (solid line) and the d-site (broken line). (b) Density correlation function for the nearest neighbor p-sites (solid line) and d-sites (broken line).

From (3.31), (4.32), and (4.82)–(4.83), the density correlation functions are

$$\langle n_i^\alpha n_j^\alpha \rangle - \langle n_i^\alpha \rangle \langle n_j^\alpha \rangle$$

$$= \begin{cases} \left(\frac{e_2}{e_1}\right)^{-|i-j|} \frac{\lambda^4}{4c_1c_2} R_2^{(p)} L_2^{(p)} + \left(\frac{e_3}{e_1}\right)^{-|i-j|} \frac{\lambda^4}{4c_1c_3} R_3^{(p)} L_3^{(p)} \\ \qquad \text{for} \quad \alpha = p \\ \left(\frac{e_2}{e_1}\right)^{-|i-j|} \frac{1}{4c_1c_2} R_2^{(d)} L_2^{(d)} + \left(\frac{e_3}{e_1}\right)^{-|i-j|} \frac{1}{4c_1c_3} R_3^{(d)} L_3^{(d)} \\ \qquad \text{for} \quad \alpha = d \end{cases} \tag{4.85}$$

where

$$R_j^{(p)} = 4L_{11}R_{1j} + L_{12}R_{3j}$$

$$L_j^{(p)} = 4L_{j1}R_{21} + L_{j2}R_{31}$$

$$R_j^{(d)} = (2L_{11} - L_{12} + 2L_{13})\, R_{1j} + 2(L_{12} - 2L_{13})\, R_{2j} + 2L_{13}R_{3j}$$

$$L_j^{(d)} = L_{j1}(2R_{11}) + L_{j2}(-R_{11} + 2R_{21}) + 2L_{j3}(R_{11} - 2R_{21} + R_{31})$$

The density correlation functions take negative values and decay exponentially with distance. We show the results in Fig. 24b. For $|\lambda| \ll 1$ and $\lambda \gg 1$ the density correlations are suppressed.

We evaluate the spin correlation function. The transfer matrices are

$$\mathsf{S}_n = -2$$

$$\mathsf{S}_i^{R,(p)} = (\tfrac{1}{2}\lambda^2, \tfrac{5}{2}\lambda^2, 0), \qquad \mathsf{S}_j^{L,(p)} = \begin{pmatrix} 2\lambda^2 \\ 0 \\ 0 \end{pmatrix} \tag{4.86}$$

$$\mathsf{S}_i^{R,(d)} = (\tfrac{1}{2}\lambda^2, 0, 0), \qquad \mathsf{S}_j^{L,(d)} = \begin{pmatrix} -\lambda^4 \\ -\lambda^2 \\ -2 \end{pmatrix}$$

From (4.65), (4.81), and (4.86) we have

$$\langle S_i^z S_j^z \rangle = \left(-\frac{2}{e_1}\right)^{-|i-j|} \times \begin{cases} -\dfrac{\lambda^4}{2e_1 c_1}(L_{11}R_{11} + 5L_{12}R_{21}) & \text{for } \beta = p \text{ and } \alpha = p \\ -\dfrac{\lambda^2}{2e_1 c_1} L_{11}R_{11} & \text{for } \beta = p \text{ and } \alpha = d \\ -\dfrac{\lambda^2}{2e_1 c_1} L_{13}R_{11} & \text{for } \beta = d \text{ and } \alpha = d \end{cases} \tag{4.87}$$

The spin correlation functions decay exponentially with oscillating sign. We show the results in Figs. 25a–25c. For $|\lambda| \ll 1$ and $\lambda \gg 1$, the spin correlations are suppressed.

We evaluate the singlet-pair correlation function. For (4.55), case (iv), the correlation functions are vanishing for $|k-i| \geqslant 2$. We evaluate them for (4.55), cases (i) and (iii). The transfer matrices are

$$\mathsf{H}_n = 2, \qquad \mathsf{H}_i^{R,(\gamma)} = \lambda^2(1, 5, 0), \qquad \mathsf{H}_j^{L,(\gamma)} = \begin{pmatrix} -4\lambda^2 \\ 0 \\ 0 \end{pmatrix} \tag{4.88}$$

for $\gamma = p$ and dp. From (4.68), (4.81), and (4.88) we obtain

$$\langle b_{i,j}^\dagger b_{k,l} \rangle = -\left(\frac{2}{e_1}\right)^{-|i-k|} \frac{2\lambda^4}{e_1 c_1}(L_{11}R_{11} + 5L_{12}R_{21}) \qquad \text{for} \quad \alpha, \beta = p, dp \tag{4.89}$$

The singlet-pair correlation functions decay exponentially with distance. We show the results in Fig. 25d. For $|\lambda| \ll 1$ and $\lambda \gg 1$ the correlations are suppressed.

We evaluate the correlation function $\langle c_{i,\sigma} c_{j,\sigma}^\dagger \rangle$. The transfer matrices are

$$\mathsf{G}_n = -2\begin{pmatrix} 1+\lambda^2 & \lambda^2 \\ 1 & 1 \end{pmatrix}$$

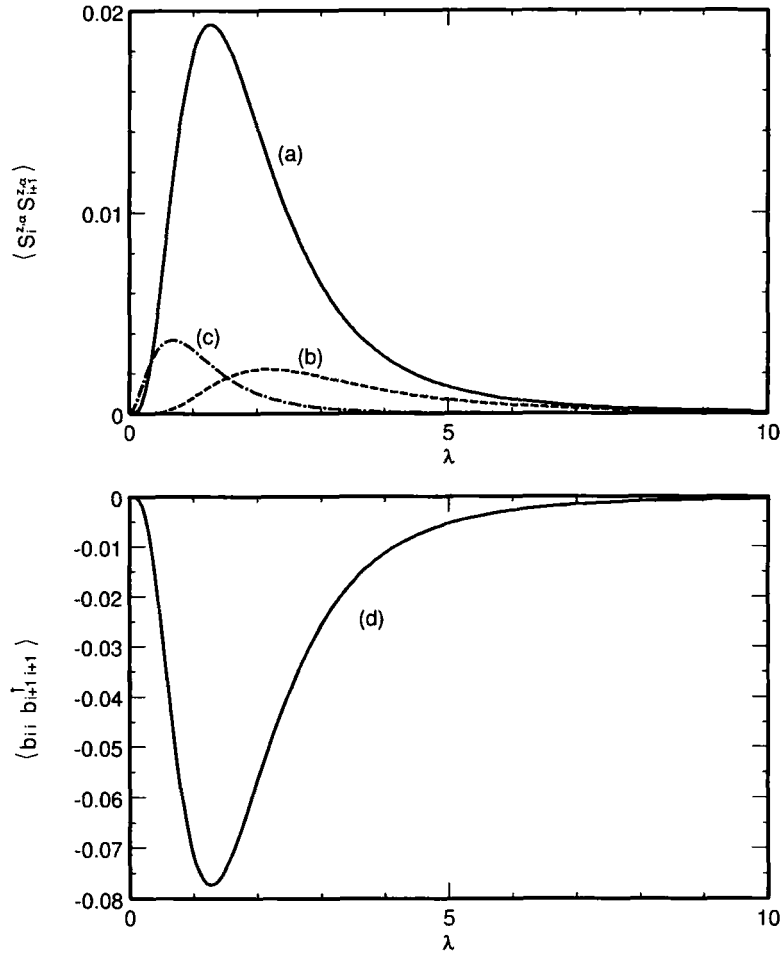

Fig. 25. Spin correlation function for (a) nearest neighbor p-sites, (b) p- and d-sites, and (c) d-sites. (d) Singlet-pair correlation function for the nearest neighbor p-sites.

$$G_i^{R,(p)} = -\lambda \begin{pmatrix} 2 & 2 & 0 \\ 1 & 4 & 1 \end{pmatrix}, \qquad G_j^{L,(p)} = -\lambda \begin{pmatrix} 2 & 0 \\ 1 & 1 \\ 0 & 0 \end{pmatrix}$$

$$G_i^{R,(d)} = -\begin{pmatrix} 1+\lambda^2 & \lambda^2 & 0 \\ 1 & 1 & 0 \end{pmatrix}, \qquad G_j^{L,(d)} = -\begin{pmatrix} \lambda^2+\lambda^4 & \lambda^4 \\ \frac{1}{2}+\lambda^2 & \lambda^2 \\ 2 & 2 \end{pmatrix} \quad (4.90)$$

The matrix G_n is diagonalized as

$$G_n = -2\tilde{R}\tilde{D}\tilde{L}\tilde{C}^{-1} \tag{4.91}$$

where the matrices are shown in (4.71). The corresponding quantities are $g_1 = (2+\lambda^2+\lambda\omega_3)/2$ and $g_2 = (2-\lambda^2+\lambda\omega_3)/2$ with $\omega_3 = (4+\lambda^2)^{1/2}$. They satisfy $g_1 > g_2 > 0$ for $\lambda \neq 0$. We choose the matrices $\tilde{L} = (\tilde{L}_{ij})$ and $\tilde{R} = (\tilde{R}_{ij})$ as we did in Section 4.3, where $\tilde{L}_{j1} = (g_j - 1)/\lambda^2$, $\tilde{L}_{j2} = 1$, $\tilde{R}_{1j} = g_j - 1$, and $\tilde{R}_{2j} = 1$. [See also (4.72).] From these matrices and (4.44) we obtain

$$\langle c_{i,\sigma} c^{\dagger}_{j,\sigma} \rangle = \left(-2\frac{g_1}{e_1}\right)^{-|i-j|} f_1^{(\alpha)} + \left(-2\frac{g_2}{e_1}\right)^{-|i-j|} f_2^{(\alpha)} \tag{4.92}$$

where

$$f_m^{(p)} = \frac{1}{2c_1\tilde{c}_m e_1 g_m}[2(g_m-1)L_{11} + g_m L_{12}]$$
$$\times [2(g_m-1)(R_{11}+R_{21}) + \lambda^2(R_{11}+4R_{21}+R_{31})] \tag{4.93}$$

$$f_m^{(d)} = \frac{2}{\lambda^2 c_1 \tilde{c}_m}[(g_m-1)L_{12} + 4L_{13}][(g_m-1)R_{11} + \lambda^2 R_{21}] \tag{4.94}$$

The correlation functions decay exponentially with oscillating sign.

By the Fourier transformation of the correlation function $\langle c_{i,\sigma} c^{\dagger}_{j,\sigma} \rangle$, we obtain the momentum distribution functions for $\alpha = p$ and d,

$$\langle n^{\alpha}_{k,\sigma} \rangle = f_1^{(\alpha)} F_1(k, r_1) + f_2^{(\alpha)} F_2(k, r_2) + f_0^{(\alpha)} \tag{4.95}$$

where $F_i(k, r_i)$ is defined by (4.77), $r_i = -g_i/e_1$, and $f_0^{(\alpha)} = \langle n^{\alpha}_{i,\sigma} \rangle$. The results are shown in Figs. 26a and 26b. There is no singularity in the momentum distribution functions. The momentum distribution for p-sites has a sharp peak at $k = \pi$ for $|\lambda| \ll 1$. It is almost flat for $\lambda \gg 1$. The momentum distribution for d-sites is expected to be flat for the complete limit $|\lambda| \ll 1$.

4.4.4. Discussion. All the correlation functions under consideration decay exponentially with distance. These results suggest the existence of a finite excitation gap. Therefore, it is expected that the state is insulating. Their correlation lengths are $\xi_{nn} = [\ln(e_2/e_1)]^{-1}$, $\xi_{ss} = \xi_{bb} = [\ln(2/e_1)]^{-1}$, and $\xi_{cc} = [\ln(2g_1/e_1)]^{-1}$ (Fig. 26c). (They satisfy the relation $\xi_{cc} > \xi_{nn} > \xi_{ss} = \xi_{bb}$.) We note that the spin correlation is antiferromagnetic.

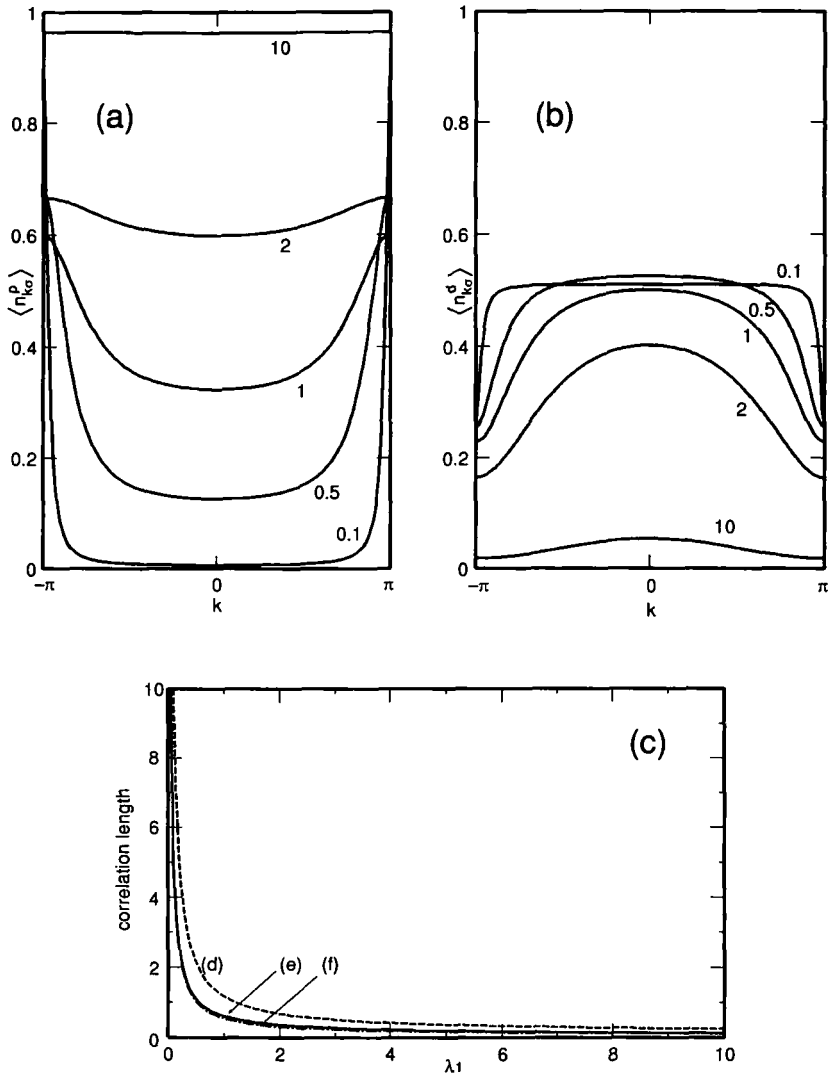

Fig. 26. Momentum distribution function for (a) the p-site and (b) the d-site for $\lambda = 0.1$, 0.5, 1, 2, and 10. (c) Correlation length of (d) the correlation function $\langle c_{i,\sigma} c^{\dagger}_{j,\sigma} \rangle$, (e) the density correlation function, and (f) the spin and the singlet-pair correlation functions.

We consider the region $|\lambda| \ll 1$. There is almost one electron per d-site. The p-sites are almost empty. The correlation lengths are large. However, the correlation functions for the nearest neighbor sites vanish.

For $\lambda \gg 1$ there are almost two electrons per p-site. The d-sites are almost empty. The correlation lengths and the correlation functions for the nearest neighbor sites vanish.

The ground state (4.79) is a 1/3-filling state. The filling factor corresponds to that of the band insulator in the noninteracting system for $\lambda > \sqrt{2}$. In the noninteracting system we have the metal–insulator transition at $\lambda = \sqrt{2}$ by the variation of λ. However, the ground state (4.79) is insulating for any λ. The properties of these states are completely different.

5. ABSENCE OF THE PERSISTENT CURRENT

In Section 4 we assumed the parameter λ_r to be real. Relaxing the condition, the effects of a magnetic field are included by taking hopping matrix elements to be complex. Thus the effects of the magnetic field are investigated exactly for the systems of strongly correlated electrons described in this paper. Let us calculate the persistent current. Considering the system in a ring geometry and putting a flux through the ring, we can measure the Aharonov–Bohm effect and the persistent current.[19–23] In the ring geometry, we include the effect of the flux Φ by changing the hopping matrix elements of the Nth cell. We first classify sites in the Nth cell into two classes as (i) sites which belong to the Nth unit cell and (ii) sites which are identified with sites in the cell C_1. We denote the sets of the sites (i) and (ii) by $C_{N;u}$ and $C_{N;e}$, respectively. The cell Hamiltonian (2.2) associated with the Nth cell is obtained by choosing

$$\alpha_{N,\sigma}(\Phi) = \sum_{r=1}^{|C_N|} \tilde{\lambda}_r^{(N)}(\Phi)\, c_{r,\sigma} \tag{5.1}$$

where

$$\tilde{\lambda}_r^{(N)}(\Phi) = \begin{cases} \lambda_r^{(N)} e^{i\Phi} & \text{for} \quad r \in C_{N;e} \\ \lambda_r^{(N)} & \text{for} \quad r \in C_{N;u} \end{cases} \tag{5.2}$$

with real $\lambda_r^{(N)}$. From (5.1) and (2.3) for $1 \leqslant n \leqslant N-1$, the Hamiltonian is

$$H_S(\Phi) = -\mathscr{P}\left\{ \sum_{\sigma=\uparrow,\downarrow} \sum_{x,y \in \Lambda_N} t_{x,y}(\Phi)\, c_{x,\sigma}^{\dagger} c_{y,\sigma} \right\} \mathscr{P} \tag{5.3}$$

where

$$t_{x,y}(\Phi)=\sum_{n=1}^{N-1} t_{r,s}^{(n)}+t_{r,s}^{(N)}(\Phi) \qquad \text{for} \quad x=f(n,r), \quad y=f(n,s) \tag{5.4}$$

with

$$t_{r,s}^{(n)}=\begin{cases}\lambda_r^{(n)}\lambda_s^{(m)}\delta_{n,m} & \text{for} \quad r\neq s \\ 2(\lambda_r^{(n)})^2 & \text{for} \quad r=s \text{ and } r\in C_{n;\,U=\infty} \\ (\lambda_r^{(n)})^2 & \text{for} \quad r=s \text{ and } r\in C_{n;\,U=\infty}\end{cases} \tag{5.5}$$

$(1\leqslant m\leqslant N-1,\ 1\leqslant n\leqslant N-1)$ and

$$t_{r,s}^{(N)}(\Phi)=\begin{cases}(\tilde{\lambda}_r^{(N)}(\Phi))^*\,\lambda_s^{(N)} & \text{for} \quad r\neq s \text{ and } r\in C_{N;e},\ s\in C_{N;u} \\ \lambda_r^{(N)}\tilde{\lambda}_s^{(N)}(\Phi) & \text{for} \quad r\neq s \text{ and } r\in C_{N;u},\ s\in C_{N;e} \\ \lambda_r^{(N)}\lambda_s^{(N)} & \text{for} \quad r\neq s \text{ and } r,s\in C_{N;u} \\ 2(\lambda_r^{(N)})^2 & \text{for} \quad r=s \text{ and } r\in C_{N;\,U=\infty} \\ (\lambda_r^{(N)})^2 & \text{for} \quad r=s \text{ and } r\in C_{N;\,U=0}\end{cases} \tag{5.6}$$

The ground state of $H_S(\Phi)$ is

$$|\Phi_{\text{G.S.}}(\Phi)\rangle=\mathscr{P}\prod_{\sigma=\uparrow,\downarrow}\left[\left(\prod_{n=1}^{N-1}\alpha_{n,\sigma}^{\dagger}\right)\alpha_{N,\sigma}^{\dagger}(\Phi)\right]|0\rangle \tag{5.7}$$

The ground-state energy is given explicitly by

$$\begin{aligned}E_0(\Phi)&=-\sum_{n=1}^{N-1}\sum_{r\in C_n}2\,|\lambda_r^{(n)}|^2-\sum_{r\in C_N}2\,|\tilde{\lambda}_r^{(N)}(\Phi)|^2 \\ &=-\sum_{n=1}^{N}\sum_{r\in C_n}2\,|\lambda_r^{(n)}|^2\end{aligned} \tag{5.8}$$

It is independent of the flux Φ. The persistent current I is evaluated by using the Byers–Yang relation.[19] We obtain

$$I\propto -\frac{\partial E_0(\Phi)}{\partial\Phi}=0 \tag{5.9}$$

The persistent current is vanishing for any of the solvable models discussed here. This is consistent with our conclusion that the ground state is insulating.

Extending the discussion here, the absence of the persistent current can be shown in any dimensions for the models discussed in this paper.

6. SUMMARY

We investigated three models with strongly correlated electrons which have the RVB state as an exact ground state. The number of electrons per unit cell is restricted to be 2. The correlation functions are evaluated exactly using the transfer matrix method for the geometric representations of the valence-bond states.[24] The two-point correlation functions for spin, density, and singlet-Cooper pairs are obtained for any distance. All the correlation functions decay exponentially with distance. The momentum distribution functions are also evaluated and there is no singularity. The results suggest that the ground states of the models are insulating. The persistent currents are also considered and turn out to be vanishing.

APPENDIX A

We describe the models used by several authors[1-5] and those investigated in this paper using the cell construction of Tasaki (see Table I). The lattice is constructed by the cell in the second column in Table I. The cell for the line graph is constructed as follows. We define a lattice $\mathscr{L} = (\Lambda, B)$, where Λ is the set of the sites (vertices) and B is the set of the bonds (edges). The line graph $L(\mathscr{L}) = (\Lambda^L, B^L)$ constructed from a lattice Λ has the bonds of $\mathscr{L}$ as sites ($\Lambda^L = B$), and two sites are connected by a bond in B^L if the corresponding bonds in B have a site in common. The cell is defined by sites ($\in \Lambda^L$) which are connected by a bond ($\in B$) to the same site ($\in \Lambda$).

APPENDIX B

We first note the equalities

$$c_{i,\sigma} b^{\dagger}_{i,j} = \mathrm{sgn}(\sigma)\, c^{\dagger}_{j,\sigma}(c_{i,\sigma} c^{\dagger}_{i,\sigma}) \tag{B.1}$$

and

$$b_{i,j} b^{\dagger}_{i,k} = \sum_{\sigma=\uparrow,\downarrow} (c_{i,\sigma} c^{\dagger}_{i,\sigma})(c_{j,-\sigma} c^{\dagger}_{k,-\sigma}) + \Delta_i \tag{B.2}$$

where $\Delta_i = -\sum_{\sigma=\uparrow,\downarrow} c^{\dagger}_{i,\sigma}(c^{\dagger}_{k,-\sigma} c_{j,\sigma})\, c_{i,-\sigma}$, which has the property $\Delta_i |0\rangle = \langle 0| \Delta_i = 0$.

We show an equality. Consider a connected graph $W \cup W'$ with $2n$ ($n \geqslant 1$) bonds. We set

$$W = \{\{2, 3\}, \{4, 5\}, \ldots, \{2n, 2n+1\}\}$$
$$W' = \{\{1, 2\}, \{3, 4\}, \ldots, \{2n-1, 2n\}\}$$

Table I. Cell Construction of Models in Refs. 1–5[a]

Authors	Cell	Dimension	Parameters[a] (a)	(b)	(c)	Uniqueness[b]
Brandt and Giesekus[1]		$d \geqslant 2$	(t)	$\lambda_j = \lambda$ $(j = 1, 2, 3, 4)$	$(-\lambda^2)$	O $(d \geqslant 3)$
		$d \geqslant 2$	V/t	$\lambda_j = (1/\sqrt{2})$ $(j = 1, 2, 3, 4)$, $\lambda_5 = \sqrt{2}\,\lambda$	-2λ	O, P
Mielke[2]	See text	$d \geqslant 1$	(t)	$\lambda_j = \lambda$	$(-\lambda^2)$	D
Strack[3]		$d = 1$	V/t	$\lambda_1 = \lambda_2 = 1$, $\lambda_3 = \lambda i$, $\lambda_4 = -\lambda i$	λ	O
		$d = 1$	V/t	$\lambda_1 = \lambda$, $\lambda_2 = -\lambda$, $\lambda_3 = 1$	$1/\lambda$	O
		$d = 2$	V/t	$\lambda_1 = \lambda$, $\lambda_2 = -\lambda$, $\lambda_3 = 1$	$1/\lambda$	O, P
Tasaki[4]	d-sites	$d \geqslant 1$	λ_j	λ_j	λ_j	D
Tasaki[5]	d- and p-sites	$d \geqslant 1$	λ_j	λ_j	λ_j	D
Present work						
Model A		$d = 1$		$\lambda_1, \lambda_2, \lambda_3 = 1$		O, P
Model B		$d = 1$		$\lambda_1, \lambda_2, \lambda_3 = 1$		O
Model C		$d = 1$		$\lambda_j = 1$ $(j = 1, 2, 3, 4)$, $\lambda_5 = \lambda$		O, P

[a] Parameters (a) are those of refs. 1–3. When we choose the λ_j defined in the cell as given in (b), the parameters (a) are given by those in column (c) in our parametrization.

[b] The models with the indicated conditions satisfy the uniqueness condition in ref. 5. Here O and P denote open and periodic boundary conditions, respectively. The symbol D denotes that the boundary condition depends on the model.

We define the quantity

$$L(n;\sigma,\rho)=\langle 0|\left(\prod_{k=1}^{n} b_{2k,2k+1}\right) c_{1,\sigma} c^{\dagger}_{2n+1,\rho} \prod_{k=1}^{n} b^{\dagger}_{2k-1,2k}\,|0\rangle \tag{B.3}$$

For $n=1$, from (B.1) we have

$$\begin{aligned} L(1;\sigma,\rho) &= \langle 0|\, b_{2,3} c_{1,\sigma} c^{\dagger}_{3,\rho} b^{\dagger}_{1,2}\,|0\rangle \\ &= -\langle 0|\, b_{2,3} c^{\dagger}_{3,\rho}(c_{1,\sigma} b^{\dagger}_{1,2})\,|0\rangle \\ &= -\operatorname{sgn}(\sigma)\langle 0|\, b_{2,3} c^{\dagger}_{3,\rho} c_{2,-\sigma}\,|0\rangle \\ &= \operatorname{sgn}(\sigma)\operatorname{sgn}(-\rho)\langle 0|\, c_{2,-\sigma} c^{\dagger}_{2,-\sigma} c_{3,\rho} c^{\dagger}_{3,\rho}\,|0\rangle \\ &= -\delta_{\sigma,\rho} \end{aligned} \tag{B.4}$$

From (B.1) we have

$$\begin{aligned} L(n;\sigma,\rho) &= \langle 0|\left(\prod_{k=1}^{n} b_{2k,2k+1}\right) c_{1,\sigma} c^{\dagger}_{2n+1,\rho} b^{\dagger}_{1,2} \prod_{k=2}^{n} b^{\dagger}_{2k-1,2k}\,|0\rangle \\ &= -\operatorname{sgn}(\sigma)\langle 0|\left(\prod_{k=1}^{n} b_{2k,2k+1}\right) c^{\dagger}_{2n+1,\rho} c^{\dagger}_{2,-\sigma} \prod_{k=2}^{n} b^{\dagger}_{2k-1,2k}\,|0\rangle \\ &= -\operatorname{sgn}(\sigma)\langle 0|\left(\prod_{k=2}^{n} b_{2k,2k+1}\right) b_{2,3} c^{\dagger}_{2n+1,\rho} c^{\dagger}_{2,-\sigma} \prod_{k=2}^{n} b^{\dagger}_{2k-1,2k}\,|0\rangle \\ &= -\operatorname{sgn}(\sigma)\operatorname{sgn}(-\sigma)\langle 0|\left(\prod_{k=2}^{n} b_{2k,2k+1}\right) \\ &\quad \times(-c_{3,\sigma})\, c^{\dagger}_{2n+1,\rho} \prod_{k=2}^{n} b^{\dagger}_{2k-1,2k}\,|0\rangle \\ &= -\langle 0|\left(\prod_{k=2}^{n} b_{2k,2k+1}\right) c_{3,\sigma} c^{\dagger}_{2n+1,\rho} \prod_{k=2}^{n} b^{\dagger}_{2k-1,2k}\,|0\rangle \end{aligned} \tag{B.5}$$

We change the labeling of the lattice sites by the rule $j \to j-2$ and obtain

$$\begin{aligned} L(n;\sigma,\rho) &= -\langle 0|\left(\prod_{k=1}^{n-1} b_{2k,2k+1}\right) c_{1,\sigma} c^{\dagger}_{2n-1,\rho} \prod_{k=1}^{n-1} b^{\dagger}_{2k-1,2k}\,|0\rangle \\ &= -L(n-1;\sigma,\rho) \\ &= \cdots \\ &= (-1)^{n-1} L(1;\sigma,\rho) \\ &= (-1)^{n}\,\delta_{\sigma,\rho} \end{aligned} \tag{B.6}$$

We show (3.10). For the self-closed bonds and degenerate graph we have $w_j=1$ and $w_j=2$, respectively. Consider the nondegenerate loop $W_j \cup W_j'$ with $l_j=2n$ $(n \geqslant 1)$ bonds. We set

$$W_j=\{\{2,3\},\{4,5\},\ldots,\{2n-2,2n-1\},\{2n,2n+1\,(=1)\}\}$$
$$W_j'=\{\{1,2\},\{3,4\},\ldots,\{2n-1,2n\}\}$$

From (B.2) and (B.6) the weight is

$$\begin{aligned}
w_j &= \langle 0| \prod_{k=1}^{n} b_{2k,2k+1} \prod_{k=1}^{n} b_{2k-1,2k}^{\dagger} |0\rangle \\
&= \langle 0| \left(\prod_{k=1}^{n-1} b_{2k,2k+1}\right) b_{2n,2n+1} b_{2n-1,2n}^{\dagger} \prod_{k=1}^{n-1} b_{2k-1,2k}^{\dagger} |0\rangle \\
&= \langle 0| \left(\prod_{k=1}^{n-1} b_{2k,2k+1}\right)\left(\sum_{\sigma=\uparrow,\downarrow} c_{2n,\sigma} c_{2n,\sigma}^{\dagger} c_{1,-\sigma} c_{2n-1,-\sigma}^{\dagger} + \Delta_{2n}\right) \\
&\quad \times \prod_{k=1}^{n-1} b_{2k-1,2k}^{\dagger} |0\rangle \\
&= \sum_{\sigma=\uparrow,\downarrow} \langle 0| \left(\prod_{k=1}^{n-1} b_{2k,2k+1}\right) c_{2n,\sigma} c_{2n,\sigma}^{\dagger} c_{1,-\sigma} c_{2n-1,-\sigma}^{\dagger} \prod_{k=1}^{n-1} b_{2k-1,2k}^{\dagger} |0\rangle \\
&= \sum_{\sigma=\uparrow,\downarrow} \langle 0| \left(\prod_{k=1}^{n-1} b_{2k,2k+1}\right) c_{1,-\sigma} c_{2(n-1)+1,-\sigma}^{\dagger} \prod_{k=1}^{n-1} b_{2k-1,2k}^{\dagger} |0\rangle \\
&= \sum_{\sigma=\uparrow,\downarrow} L(n-1;-\sigma,-\sigma) \\
&= \sum_{\sigma=\uparrow,\downarrow} (-1)^{n-1} \sigma_{-\sigma,-\sigma} \\
&= 2(-1)^{n-1} \\
&= 2(-1)^{l_j/2-1}
\end{aligned} \tag{B.7}$$

where we used the relation $l=2n$ in the last line.

APPENDIX C

We first note the equalities

$$\begin{aligned}
S_i^{-} b_{i,j}^{\dagger} &= \tfrac{1}{2} \tilde{b}_{i,j}^{\dagger} + \delta_{i,j} \\
S_i^{-} b_{i,j}^{\dagger} &= \tfrac{1}{2} b_{i,j}^{\dagger} - \tilde{\delta}_{j,i}
\end{aligned} \tag{C.1}$$

where

$$\tilde{b}^{\dagger}_{i,j} = c^{\dagger}_{i,\uparrow} c^{\dagger}_{j,\downarrow} + c^{\dagger}_{i,\downarrow} c^{\dagger}_{j,\uparrow} \tag{C.2}$$

is the creation operator of the triplet pair between sites i and j and satisfies the relation $\tilde{b}^{\dagger}_{i,j} = -\tilde{b}^{\dagger}_{j,i}$. Here

$$\begin{aligned} \delta_{i,j} &= -\frac{c^{\dagger}_{i,\uparrow} c^{\dagger}_{j,\downarrow} n_{i,\downarrow} - c^{\dagger}_{i,\downarrow} c^{\dagger}_{j,\uparrow} n_{i,\uparrow}}{2} \\ \tilde{\delta}_{i,j} &= -\frac{c^{\dagger}_{i,\uparrow} c^{\dagger}_{j,\downarrow} n_{i,\downarrow} + c^{\dagger}_{i,\downarrow} c^{\dagger}_{j,\uparrow} n_{i,\uparrow}}{2} \end{aligned} \tag{C.3}$$

which have the properties $\delta_i |0\rangle = \langle 0| \delta_i = 0$ and $\tilde{\delta}_i |0\rangle = \langle 0| \tilde{\delta}_i = 0$.

We show (3.17). Consider the connected graph $W^{(x,y)} \cup W'^{(x,y)}$ with $2n$ ($n \geqslant 1$) bonds. We set

$$\begin{aligned} W^{(x,y)} &= \{\{2,3\}, \{4,5\}, \ldots, \{2n, 2n+1\}\} \\ W'^{(x,y)} &= \{\{1,2\}, \{3,4\}, \ldots, \{2n-1, 2n\}\} \end{aligned}$$

We denote the right-hand side of (3.17) by $S(m)$,

$$S(m) = \langle 0| \left(\prod_{k=1}^{n} b_{2k,2k+1} \right) S^{z}_{1} S^{z}_{m} \prod_{k=1}^{n} b^{\dagger}_{2k-1,2k} |0\rangle \tag{C.4}$$

where we set $x = 1$ and $y = m$. From (C.1), we have

$$\begin{aligned} S(2m+1) &= \langle 0| \left(\prod_{k=1}^{n} b_{2k,2k+1} \right) S^{z}_{1} S^{z}_{2m+1} \prod_{k=1}^{n} b^{\dagger}_{2k-1,2k} |0\rangle \\ &= \langle 0| \left(\prod_{k=1}^{m-1} b_{2k,2k+1} \right) \left(\prod_{k=m+1}^{n} b_{2k,2k+1} \right) \\ &\quad \times b_{2m,2m+1} S^{z}_{2m+1} S^{z}_{1} \prod_{k=1}^{n} b^{\dagger}_{2k-1,2k} |0\rangle \\ &= \langle 0| \left(\prod_{k=1}^{m-1} b_{2k,2k+1} \right) \left(\prod_{k=m+1}^{n} b_{2k,2k+1} \right) \\ &\quad \times \left(\frac{1}{2} \tilde{b}_{2m+1,2m} + \delta_{2m+1,2m} \right) S^{z}_{1} \prod_{k=1}^{n} b^{\dagger}_{2k-1,2k} |0\rangle \end{aligned}$$

$$
\begin{aligned}
&= \langle 0| \left(\prod_{k=1}^{m-1} b_{2k,\,2k+1} \right) \left(\prod_{k=m+1}^{n} b_{2k,\,2k+1} \right) \\
&\quad \times \left(-\frac{1}{2} \tilde{b}_{2m,\,2m+1} \right) S_1^- \prod_{k=1}^{n} b_{2k-1,\,2k}^\dagger |0\rangle \\
&= -\langle 0| \left(\prod_{k=1}^{m-1} b_{2k,\,2k+1} \right) \left(\prod_{k=m+1}^{n} b_{2k,\,2k+1} \right) \\
&\quad \times b_{2m-1,\,2m} S_{2m}^- S_1^- \prod_{k=1}^{n} b_{2k-1,\,2k}^\dagger |0\rangle \\
&= \langle 0| \left(\prod_{k=1}^{n} b_{2k,\,2k+1} \right) S_1^- S_{2m}^- \prod_{k=1}^{n} b_{2k-1,\,2k}^\dagger |0\rangle \\
&= -\langle 0| \left(\prod_{k=1}^{n} b_{2k,\,2k+1} \right) S_1^- S_{2m}^- b_{2m-1,\,2m}^\dagger \\
&\quad \times \left(\prod_{k=1}^{m-1} b_{2k-1,\,2k}^\dagger \right) \prod_{k=m+1}^{n} b_{2k-1,\,2k}^\dagger |0\rangle \\
&= -\langle 0| \left(\prod_{k=1}^{n} b_{2k,\,2k+1} \right) S_1^- \left(\frac{1}{2} \tilde{b}_{2m,\,2m-1}^\dagger + \delta_{2m,\,2m-1} \right) \\
&\quad \times \left(\prod_{k=1}^{m-1} b_{2k-1,\,2k}^\dagger \right) \prod_{k=m+1}^{n} b_{2k-1,\,2k}^\dagger |0\rangle \\
&= -\langle 0| \left(\prod_{k=1}^{n} b_{2k,\,2k+1} \right) S_1^- \left(-\frac{1}{2} \tilde{b}_{2m-1,\,2m}^\dagger \right) \\
&\quad \times \left(\prod_{k=1}^{m-1} b_{2k-1,\,2k}^\dagger \right) \prod_{k=m+1}^{n} b_{2k-1,\,2k}^\dagger |0\rangle \\
&= (-1)^2 \langle 0| \left(\prod_{k=1}^{n} b_{2k,\,2k+1} \right) S_1^- S_{2m-1}^- b_{2m-1,\,2m}^\dagger \\
&\quad \times \left(\prod_{k=1}^{m-1} b_{2k-1,\,2k}^\dagger \right) \prod_{k=m+1}^{n} b_{2k-1,\,2k}^\dagger |0\rangle \\
&= (-1)^2 \langle 0| \left(\prod_{k=1}^{n} b_{2k,\,2k+1} \right) S_1^- S_{2m-1}^- \prod_{k=1}^{n} b_{2k-1,\,2k}^\dagger |0\rangle \\
&= (-)^2 S(2m-1) \\
&= \cdots
\end{aligned}
$$

$$
\begin{aligned}
&= (-1)^{2m} S(1) \\
&= (-1)^{2m} \langle 0 | \left(\prod_{k=1}^{n} b_{2k,\,2k+1} \right) S_1^- S_1^- \prod_{k=1}^{n} b_{2k-1,\,2k}^\dagger | 0 \rangle \\
&= \frac{(-1)^{2m}}{4} \langle 0 | \prod_{k=1}^{n} b_{2k,\,2k+1} \prod_{k=1}^{n} b_{2k-1,\,2k}^\dagger | 0 \rangle
\end{aligned} \tag{C.5}
$$

Similarly, we have

$$
S(2m) = (-1)^{2m-1} \tfrac{1}{4} \langle 0 | \prod_{k=1}^{n} b_{2k,\,2k+1} \prod_{k=1}^{n} b_{2k-1,\,2k}^\dagger | 0 \rangle \tag{C.6}
$$

Therefore, we obtain

$$
S(m) = \tfrac{1}{4} (-1)^{d(x,\,y)} w_j \tag{C.7}
$$

where we used the relation $d(x, y) = m - 1$ and the definition of w_j.

APPENDIX D

We show (3.22). Consider the line $W^{(x',\,y')} \cup W'^{(x',\,y')}$ with $2n$ $(n \geqslant 1)$ bonds. We set

$$
\begin{aligned}
W^{(x',\,y')} &= \{\{2, 3\}, \{4, 5\}, \ldots, \{2n, 2n+1\ (=y')\}\} \\
W'^{(x',\,y')} &= \{\{1\ (=x'), 2\}, \{3, 4\}, \ldots, \{2n-1, 2n\}\}
\end{aligned}
$$

From (B.3) the weight is

$$
\begin{aligned}
\langle 0 | \left(\prod_{k=1}^{n} b_{2k,\,2k+1} \right) c_{1,\,\sigma} c_{2n+1,\,\rho}^\dagger \prod_{k=1}^{n} b_{2k-1,\,2k}^\dagger | 0 \rangle &= L(n; \sigma, \sigma) \\
&= (-1)^n \\
&= (-1)^{l(x',\,y')/2}
\end{aligned} \tag{D.1}
$$

where we used the relation $l(x', y') = 2n$.

APPENDIX E

We show (3.28). Consider the graph $W^{(x)} \cup W'^{(x)}$; we set

$$
\begin{aligned}
W^{(x)} &= \{\{1\ (=x), 2\}, \{3, 4\}, \ldots, \{2n-1, 2n\}\} \\
W'^{(x)} &= \{\{2, 3\}, \{4, 5\}, \ldots, \{2n, 1\}\}
\end{aligned}
$$

We have

$$\langle 0|\left(\prod_{k=1}^{n} b_{2k-1,2k}\right) n_{1,\sigma} \prod_{k=1}^{n} b^{\dagger}_{2k,2k+1}|0\rangle$$
$$= \langle 0|\left(\prod_{k=2}^{n} b_{2k-1,2k}\right) b_{1,2}(1-c_{1,\sigma}c^{\dagger}_{1,\sigma})\, b^{\dagger}_{2n,1} \prod_{k=1}^{n-1} b^{\dagger}_{2k,2k+1}|0\rangle$$
$$= \langle 0|\prod_{k=1}^{n} b_{2k-1,2k} \prod_{k=1}^{n} b^{\dagger}_{2k,2k+1}|0\rangle$$
$$- \langle 0|\left(\prod_{k=1}^{n} b_{2k-1,2k}\right) c_{1,\sigma}c^{\dagger}_{1,\sigma} \prod_{k=1}^{n} b^{\dagger}_{2k,2k+1}|0\rangle \qquad \text{(E.1)}$$

From (B.3), the second term is

$$\langle 0|\left(\prod_{k=1}^{n} b_{2k-1,2k}\right) c_{1,\sigma}c^{\dagger}_{1,\sigma} \prod_{k=1}^{n} b^{\dagger}_{2k,2k+1}|0\rangle$$
$$= \langle 0|\left(\prod_{k=2}^{n} b_{2k-1,2k}\right) b_{1,2}c_{1,\sigma}c^{\dagger}_{1,\sigma}b^{\dagger}_{2n,1} \prod_{k=1}^{n-1} b^{\dagger}_{2k,2k+1}|0\rangle$$
$$= \langle 0|\left(\prod_{k=2}^{n} b_{2k-1,2k}\right)(-b_{1,1}c_{2,\sigma})(-c^{\dagger}_{2n,\sigma}b^{\dagger}_{1,1}) \prod_{k=1}^{n-1} b^{\dagger}_{2k,2k+1}|0\rangle$$
$$= \langle 0|\left(\prod_{k=2}^{n} b_{2k-1,2k}\right) c_{2,\sigma}c^{\dagger}_{2n,\sigma} \prod_{k=1}^{n-1} b^{\dagger}_{2k,2k+1}|0\rangle$$
$$= \langle 0|\left(\prod_{k=1}^{n-1} b_{2k,2k+1}\right) c_{1,\sigma}c^{\dagger}_{2n-1,\sigma} \prod_{k=1}^{n-1} b^{\dagger}_{2k-1,2k}|0\rangle$$
$$= L(n-1;\sigma,0)$$
$$= (-1)^{n-1}$$
$$= (-1)^{l(x)/2-1} \qquad \text{(E.2)}$$

The fourth line is obtained by renaming the site j as $j-1$. We used the relation $l(x)=2(n-1)$. From (B.7) and (E.2) we have

$$\langle 0|\prod_{k=1}^{n} b_{2k-1,2k}n_{1,\sigma} \prod_{k=1}^{n} b^{\dagger}_{2k,2k+1}|0\rangle = 2(-1)^{l(x)/2-1} - (-1)^{l(x)/2-1}$$
$$= (-1)^{l(x)/2-1} \qquad \text{(E.3)}$$

APPENDIX F

We show (3.35). For (i), the sets $W^{(x,y)}$ and $W'^{(x,y)}$ are empty. The right-hand side of (3.34) is

$$w_j(x, y; \sigma) = \tfrac{1}{2}\{\langle 0|\, c_{x,\sigma} c_{y,\sigma} c^\dagger_{y,\sigma} c^\dagger_{x,\sigma}\, |0\rangle + \langle 0|\, c_{x,\sigma} c_{y,-\sigma} c^\dagger_{y,-\sigma} c^\dagger_{x,\sigma}\, |0\rangle\} = 1 \tag{F.1}$$

where we used the equality $\langle 0|\, c_{x,\sigma} c_{y,\sigma} c^\dagger_{y,\sigma} c^\dagger_{x,\sigma}\, |0\rangle = \langle 0|\, c_{x,\sigma} c_{y,-\sigma} c^\dagger_{y,-\sigma} c^\dagger_{x,\sigma}\, |0\rangle = 1$.

For (ii) we suppose that the site x belongs to the graph. From (3.28), the right-hand side of (3.34) is

$$\begin{aligned} w_j(x, y; \sigma) = \tfrac{1}{2}\Bigg\{ & \langle 0|\, c_{y,\sigma} c^\dagger_{y,\sigma}\, |0\rangle \langle 0| \Bigg(\prod_{\{u',v'\} \in W'^{(x)}} b_{u',v'} \Bigg) \\ & \times c_{x,\sigma} c^\dagger_{x,\sigma} \prod_{\{u,v\} \in W^{(x)}} b^\dagger_{u,v}\, |0\rangle \\ & + \langle 0|\, c_{y,-\sigma} c^\dagger_{y,-\sigma}\, |0\rangle \langle 0| \Bigg(\prod_{\{u',v'\} \in W'^{(x)}} \Bigg) \\ & \times b_{u',v'} c_{x,\sigma} c^\dagger_{x,\sigma} \prod_{\{u,v\} \in W^{(x)}} b^\dagger_{u,v}\, |0\rangle \Bigg\} \\ = {} & (-1)^{l(x)/2 - 1} \end{aligned} \tag{F.2}$$

where we used the equality $\langle 0|\, c_{y,\sigma} c^\dagger_{y,\sigma}\, |0\rangle = \langle 0|\, c_{y,-\sigma} c^\dagger_{y,-\sigma}\, |0\rangle = 1$.

For (iii) the right-hand side of (3.34) is

$$\begin{aligned} w_j(x, y; \sigma) = \tfrac{1}{2}\Bigg\{ & \langle 0| \Bigg(\prod_{\{u',v'\} \in W'^{(x,y)}} b_{u',v'} \Bigg) c_{y,\sigma} c^\dagger_{y,\sigma} \prod_{\{u,v\} \in W^{(x,y)}} b^\dagger_{u,v}\, |0\rangle \\ & \times \langle 0| \Bigg(\prod_{\{u',v'\} \in W'^{(x,y)}} b_{u',v'} \Bigg) c_{x,\sigma} c^\dagger_{x,\sigma} \prod_{\{u,v\} \in W^{(x,y)}} b^\dagger_{u,v}\, |0\rangle \\ & + \langle 0| \Bigg(\prod_{\{u',v'\} \in W'^{(x,y)}} b_{u',v'} \Bigg) c_{y,-\sigma} c^\dagger_{y,-\sigma} \prod_{\{u,v\} \in W^{(x,y)}} b^\dagger_{u,v}\, |0\rangle \\ & \times \langle 0| \Bigg(\prod_{\{u',v'\} \in W'^{(x,y)}} b_{u',v'} \Bigg) c_{x,\sigma} c^\dagger_{x,\sigma} \prod_{\{u,v\} \in W^{(x,y)}} b^\dagger_{u,v}\, |0\rangle \Bigg\} \\ = {} & (-1)^{l(x)/2 - 1} (-1)^{l(y)/2 - 1} \end{aligned} \tag{F.3}$$

where we used (3.28).

For (iv) consider the graph $W^{(x,y)} \cup W'^{(x,y)}$. We set

$$W^{(x,y)} = \{\{1\ (=x), 2\}, \{3, 4\}, \ldots, \{2n-1, 2n\}\}$$
$$W'^{(x,y)} = \{\{2, 3\}, \{4, 5\}, \ldots, \{2n, 1\}\}$$

We denote one of the terms in the right-hand side of (3.34) by $G(n, j; \sigma, \tau)$,

$$G(n, j; \sigma, \tau) = \langle 0| \left(\prod_{k=1}^{n} b_{2k-1,2k} \right) c_{1,\sigma} c_{j,\tau} c^{\dagger}_{j,\tau} c^{\dagger}_{1,\sigma} \prod_{k=1}^{n} b^{\dagger}_{2k,2k+1} |0\rangle \qquad \text{(F.4)}$$

From (B.1) we have

$$\begin{aligned}
&G(n, j; \sigma, \tau) \\
&= \langle 0| \left(\prod_{k=2}^{n} b_{2k-1,2k} \right) b_{1,2} c_{1,\sigma} c_{j,\tau} c^{\dagger}_{j,\tau} c^{\dagger}_{1,\sigma} b^{\dagger}_{2n,1} \prod_{k=1}^{n-1} b^{\dagger}_{2k,2k+1} |0\rangle \\
&= \langle 0| \left(\prod_{k=2}^{n} b_{2k-1,2k} \right) (-b_{1,1} c_{2,\sigma})\, c_{j,\tau} c^{\dagger}_{j,\tau} (-c^{\dagger}_{2n,\sigma} b^{\dagger}_{1,1}) \prod_{k=1}^{n-1} b^{\dagger}_{2k,2k+1} |0\rangle \\
&= \langle 0| \left(\prod_{k=2}^{n} b_{2k-1,2k} \right) c_{2,\sigma} c_{j,\tau} c^{\dagger}_{j,\tau} c^{\dagger}_{2n,\sigma} \prod_{k=1}^{n-1} b^{\dagger}_{2k,2k+1} |0\rangle \\
&= \langle 0| \left(\prod_{k=1}^{n-1} b_{2k,2k+1} \right) c_{1,\sigma} c_{j-1,\tau} c^{\dagger}_{j-1,\tau} c^{\dagger}_{2n-1,\sigma} \prod_{k=1}^{n-1} b^{\dagger}_{2k-1,2k} |0\rangle \qquad \text{(F.5)}
\end{aligned}$$

The last line is obtained by renaming the lattice sites by the rule $k \to k-1$. For $j = 2m$ we have

$$\begin{aligned}
&G(n-1, 2m; \sigma, \tau) \\
&= \langle 0| \left(\prod_{k=1}^{n-1} b_{2k,2k+1} \right) c_{1,\sigma} c_{2m-1,\tau} c^{\dagger}_{2m-1,\tau} c^{\dagger}_{2(n-1)+1,\sigma} \prod_{k=1}^{n-1} b^{\dagger}_{2k-1,2k} |0\rangle \\
&= \langle 0| \left(\prod_{k=1}^{n-1} b_{2k,2k+1} \right) c_{2m-1,\tau} c^{\dagger}_{2m-1,\tau} c^{\dagger}_{2(n-1)+1,\sigma} (-c_{1,\sigma} b^{\dagger}_{1,2}) \\
&\quad \times \prod_{k=2}^{n-1} b^{\dagger}_{2k-1,2k} |0\rangle \\
&= -\operatorname{sgn}(\sigma) \langle 0| \left(\prod_{k=1}^{n-1} b_{2k,2k+1} \right) c_{2m-1,\tau} c^{\dagger}_{2m-1,\tau} c^{\dagger}_{2(n-1)+1,\sigma} c_{2,-\sigma} \\
&\quad \times \prod_{k=2}^{n-1} b^{\dagger}_{2k-1,2k} |0\rangle
\end{aligned}$$

$$= -\operatorname{sgn}(\sigma) \langle 0| \left(\prod_{k=2}^{n-1} b_{2k,\,2k+1} \right) (b_{2,3} c_{2,-\sigma})\, c_{2m-1,\tau} c^{\dagger}_{2m-1,\tau} c^{\dagger}_{2(n-1)+1,\sigma}$$

$$\times \prod_{k=2}^{n-1} b^{\dagger}_{2k-1,\,2k} |0\rangle$$

$$= -\langle 0| \left(\prod_{k=2}^{n-1} b_{2k,\,2k+1} \right) c_{3,\sigma} c_{2m-1,\tau} c^{\dagger}_{2m-1,\tau} c^{\dagger}_{2(n-1)+1,\sigma}$$

$$\times \prod_{k=2}^{n-1} b^{\dagger}_{2k-1,\,2k} |0\rangle \tag{F.6}$$

We change the labeling of the lattice sites by the rule $j \to j-2$ and obtain

$$G(n-1, 2m; \sigma, \tau)$$

$$= -\langle 0| \left(\prod_{k=1}^{n-2} b_{2k,\,2k+1} \right) c_{1,\sigma} c_{2(m-1)-1,\tau} c^{\dagger}_{2(m-1)-1,\tau} c^{\dagger}_{2(n-2)+1,\sigma}$$

$$\times \prod_{k=1}^{n-2} b^{\dagger}_{2k-1,\,2k} |0\rangle$$

$$= -G(n-1, 2(m-1); \sigma, \tau)$$

$$= \cdots$$

$$= (-1)^m G(n-m-1, 2; \sigma, \tau)$$

$$= (-1)^m \langle 0| \left(\prod_{k=1}^{n-m-1} b_{2k,\,2k+1} \right) c_{1,\sigma} c_{1,\tau} c^{\dagger}_{1,\tau} c^{\dagger}_{2(n-m-1)+1,\sigma}$$

$$\times \prod_{k=1}^{n-m-1} b^{\dagger}_{2k-1,\,2k} |0\rangle$$

$$= (-1)^m \langle 0| \left(\prod_{k=1}^{n-m-1} b_{2k,\,2k+1} \right) c_{1,\sigma} c_{1,\tau} c^{\dagger}_{2(n-m-1)+1,\sigma} (-c^{\dagger}_{1,\tau} b^{\dagger}_{1,2})$$

$$\times \prod_{k=2}^{n-m-1} b^{\dagger}_{2k-1,\,2k} |0\rangle$$

$$= (-1)^m \langle 0| \left(\prod_{k=1}^{n-m-1} b_{2k,2k+1} \right) c_{1,\sigma} c_{1,\tau} b^\dagger_{1,1} c^\dagger_{2(n-m-1)+1,\sigma} c^\dagger_{2,\tau}$$
$$\times \prod_{k=2}^{n-m-1} b^\dagger_{2k-1,2k} |0\rangle$$
$$= (-1)^m \operatorname{sgn}(\tau)\, \delta_{\sigma,-\tau} \langle 0| \left(\prod_{k=1}^{n-m-1} b_{2k,2k+1} \right) c^\dagger_{2(n-m-1)+1,\sigma} c^\dagger_{2,\tau}$$
$$\times \prod_{k=2}^{n-m-1} b^\dagger_{2k-1,2k} |0\rangle$$
$$= (-1)^m \delta_{\sigma,-\tau} \langle 0| \left(\prod_{k=2}^{n-m-1} b_{2k,2k+1} \right) c^\dagger_{3,-\tau} c^\dagger_{2(n-m-1)+1,\sigma}$$
$$\times \prod_{k=2}^{n-m-1} b^\dagger_{2k-1,2k} |0\rangle \tag{F.7}$$

We change the labeling of the lattice sites by the rule $k \to k-2$ and obtain

$$G(n-1, 2m; \sigma, \tau)$$
$$= (-1)^m \delta_{\sigma,-\tau} \langle 0| \left(\prod_{k=1}^{n-m-2} b_{2k,2k+1} \right) c^\dagger_{1,-\tau} c^\dagger_{2(n-m-2)+1,\sigma}$$
$$\times \prod_{k=1}^{n-m-2} b^\dagger_{2k-1,2k} |0\rangle$$
$$= (-1)^m \delta_{\sigma,-\tau} L(n-m-2; \sigma, -\tau)$$
$$= (-1)^m \delta_{\sigma,-\tau} \times (-1)^{n-m-2} \delta_{\sigma,-\tau}$$
$$= (-1)^{n-1} \delta_{\sigma,-\tau} \tag{F.8}$$

where we used (B.6). For $j = 2m-1$ a similar calculation leads to

$$G(2m-1; \sigma, \tau) = (-1)^{n-1} \delta_{\sigma,\tau} \tag{F.9}$$

Combining (F.8) and (F.9), we find for (F.5)

$$\langle 0| \left(\prod_{k=1}^{n} b_{2k,2k+1} \right) c_{1,\sigma} c_{y,\tau} c^\dagger_{y,\tau} c^\dagger_{1,\sigma} \prod_{k=1}^{n} b^\dagger_{2k-1,2k} |0\rangle = (-1)^{n-1} \delta_{\sigma,(-1)^{d(x,y)}\tau} \tag{F.10}$$

We obtain the weight

$$w_j(x, y; \sigma) = \frac{1}{2}[G(n, y; \sigma, \sigma) + G(n, y; \sigma, -\sigma)]$$

$$= (-1)^{l(x,y)/2-1} \frac{\delta_{\sigma,(-1)^{d(x,y)}\sigma} + \delta_{\sigma,(-1)^{d(x,y)+1}\sigma}}{2}$$

$$= \frac{(-1)^{l(x,y)/2-1}}{2} \tag{F.11}$$

where we used the relation $n = l(x, y)/2$.

ACKNOWLEDGMENTS

We are grateful to H. Tasaki for valuable discussions. The methods used in this work were developed by him. We would like to thank P.-A. Bares and P.-A. Lee for useful discussions and sending their article prior to publication. This work is supported in part by a grant for Priority Area from the Ministry of Education, Science, and Culture, Japan.

REFERENCES

1. U. Brandt and A. Giesekus, *Phys. Rev. Lett.* **68**:2648 (1992).
2. A. Mielke, *J. Phys. A* **25**:6507 (1992).
3. R. Strack, *Phys. Rev. Lett.* **70**:833 (1993).
4. H. Tasaki, *Phys. Rev. Lett.* **70**:3303 (1993).
5. H. Tasaki, *Phys. Rev. B* **49**:7763 (1993).
6. P.-A. Bares and P. A. Lee, *Phys. Rev. B* **49**:8882 (1993).
7. L. Pauling, *Proc. R. Soc. Lond. A* **196**:343 (1949).
8. P. W. Anderson, *Phil. Mag.* **30**:423 (1974).
9. H. Tasaki and M. Kohmoto, *Phys. Rev. B* **42**:2547 (1992).
10. P. W. Anderson, *Science* **235**:1196 (1987).
11. P. W. Anderson, G. Baskaran, Z. Zou, and T. Hsu, *Phys. Rev. Lett.* **58**:2790 (1987).
12. P. L. Iske and W. J. Casper, *Physica* **142A**:360 (1987).
13. B. Sutherland, *Phys. Rev. B* **37**:3786 (1988).
14. S. Liang, B. Doucot, and P. W. Anderson, *Phys. Rev. Lett.* **61**:365 (1988).
15. D. S. Rokhsar and S. A. Kivelson, *Phys. Rev. Lett.* **61**:2376 (1988).
16. M. Kohmoto, *Phys. Rev. B* **37**:3812 (1988); M. Kohmoto and Y. Shapir, *Phys. Rev. B* **37**:9439 (1988); M. Kohmoto and J. Friedel, *Phys. Rev. B* **38**:5811 (1988); Y. Shapir and M. Kohmoto, *Phys. Rev. B* **39**:4524 (1989).
17. D. J. Klein, T. G. Shmalz, G. E. Hite, A. Metropoulos, and A. Seitz, *Chem. Phys. Lett.* **120**:367 (1985).
18. Y. Fan and M. Ma, *Phys. Rev. B* **37**:1820 (1988).
19. N. Byers and C. N. Yang, *Phys. Rev. Lett.* 7:46 (1961).

20. M. Buttiker, Y. Imry, and R. Landauer, *Phys. Lett.* **96A**:365 (1983).
21. L. P. Levy, G. Dolan, J. Dunsmuir, and H. Bouchiat, *Phys. Rev. Lett.* **64**:2074 (1990).
22. V. Chandrasekhar, R. A. Webb, M. J. Brady, M. B. Ketchen, W. J. Gallagher, and A. Kleinsasser, *Phys. Rev. Lett.* **67**:3573 (1991).
23. D. Mailly, C. Chapelier, and A. Benoit, *Phys. Rev. Lett.* **70**:2020 (1993).
24. H. Tasaki, Private communication.
25. H. Tasaki, Unpublished.
26. G. Runner, *Nachr. Ges. Wiss. Göttingen Math. Phys. Kl.* **1932**:337 (1932).
27. L. Pauling, *J. Chem. Phys.* **1**:280 (1933).
28. K. Kimura, Y. Hatsugai, and M. Kohmoto, Unpublished.